Review

Journal of the Brazilian Chemical Society

https://dx.doi.org/10.21577/0103-5053.20260042

J. Braz. Chem. Soc. **2026**, *37*, e-20260042, 1-53

The 2025 FDA Small-Molecule Portfolio: Clinical Applications, Synthetic Approaches, Challenges, and Solutions

Felipe L. N. da Silva,[a,b] *Raquel A. C. Leão,*[a] *Edgar Schaeffer,*[c,d] *Samir F. A. Cavalcante*[d,e] *and Rodrigo O. M. A. de Souza*[*,a,b]

[a]*Grupo de Biocatalálise e Síntese Orgânica, Instituto de Química, Universidade Federal do Rio de Janeiro, 21941-909 Rio de Janeiro-RJ, Brazil*

[b]*Novasynth Tecnologia, Incubadora de Empresas da Coppe, Cidade Universitária, Ilha do Fundão, 21941-914 Rio de Janeiro-RJ, Brazil*

[c]*Instituto de Pesquissas de Produtos Naturais Walter Mors, Universidade Federal do Rio de Janeiro, 21941-902 Rio de Janeiro-RJ, Brazil*

[d]*Asymmetra Científica, Centro, 20080-070 Rio de Janeiro-RJ, Brazil*

[e]*Instituto de Defesa Química, Biológica, Radiológica e Nuclear, Centro Tecnológico do Exército, Guaratiba, 23020-470 Rio de Janeiro-RJ, Brazil*

In 2025, the U.S. Food and Drug Administration (FDA) approved 46 new drugs comprising 31 small-molecule entities. These approvals represent significant milestones in the evolution of privileged structures and novel mechanisms of action, serving as invaluable leads for the development of next-generation therapeutics with enhanced efficacy. This article reviews the synthetic routes and clinical indications of these newly marketed drugs, highlighting their significance in the current pharmaceutical landscape.

Keywords: new drugs, chemical synthesis, clinical applications

1. Introduction

The pharmaceutical and biotechnology industries play an essential role in medical innovation and improving global health outcomes. Within this sector, approvals by the United States Food and Drug Administration (FDA) represent a key milestone for introducing new therapies to the market, influencing both patient access to innovative treatments and the financial performance of the companies involved. Over the past 15 years, the global pharmaceutical market has experienced remarkable growth, driven by scientific innovation, demographic changes, and evolving healthcare demands. In 2010, the market was valued at approximately $800 billion, and by 2024, it had surpassed $2.5 trillion. This expansion has been largely fueled by the increasing prevalence of chronic diseases such as diabetes, cardiovascular disorders, and cancer, alongside an aging global population that has heightened the demand for prescription drugs. North America, particularly the United States, has remained the dominant market, accounting for nearly 45% of global pharmaceutical sales, while Europe has held its position as the second-largest region. However, the Asia-Pacific region has emerged as the fastest-growing market, with China and India playing pivotal roles in drug manufacturing and consumption.[1,2]

A major shift in the industry has been the rise of biopharmaceuticals, including monoclonal antibodies, messenger ribonucleic acid (mRNA) therapies, and gene-editing technologies, which have driven innovation and changed the landscape of drug development. The expiration of patents for blockbuster drugs has also led to a surge in generics and biosimilars, making medications more accessible while increasing competition among manufacturers.[3,4] Simultaneously, large pharmaceutical companies have pursued aggressive mergers and acquisitions to strengthen their portfolios, with landmark deals such as Pfizer's acquisition of Wyeth and Bristol-Myers Squibb's purchase of Celgene reshaping the industry. The integration of artificial intelligence, big data analytics, and digital

*e-mail: rodrigosouza@iq.ufrj.br
Editor handled this article: Brenno A. D. Neto (Editor-in-Chief)

tools has further accelerated drug discovery, clinical trials, and personalized medicine, making pharmaceutical development more efficient. The coronavirus disease 2019 (COVID-19) pandemic significantly impacted the pharmaceutical sector, accelerating vaccine development through groundbreaking mRNA technology and reshaping healthcare systems with the rise of telemedicine and digital health solutions. However, challenges persist, particularly in the form of increasing regulatory scrutiny and pricing pressures. Governments worldwide have imposed stricter oversight on drug approvals and pricing policies, especially in the United States, where concerns over affordability have led to policy changes.[5]

Industry has also faced revenue losses due to major patent expirations, often referred to as the "patent cliff," which has intensified competition among both established companies and generic drug manufacturers. Looking ahead, the future of the pharmaceutical industry appears to be shaped by precision medicine, artificial intelligence (AI)-driven drug discovery, and the expansion of market access in low-income regions.[6,7] Sustainability is becoming a key focus, with companies adopting environmentally friendly production practices. As the demand for innovative therapies continues to grow, the industry is expected to maintain its upward trajectory, with biologics, digital health, and targeted treatments driving the next phase of pharmaceutical advancement. Last year, the FDA approved a total of 46 new molecular entities (NMEs), a number slightly above the ten-year average (Figure 1).[8]

Despite the increase in the number of approvals, there has been a decline in sales projections for new drugs. The total projected annual sales for new therapeutic drugs (NTDs) approved in 2024 is approximately US$ 60 billion, significantly lower than the ten-year average of US$ 88 billion. This decline can be attributed to the absence of "mega-blockbusters" with projected sales exceeding US$ 10 billion, as seen between 2021 and 2023, driven by vaccines and treatments for COVID-19 and glucagon-like peptide-1 (GLP-1) receptor agonists.

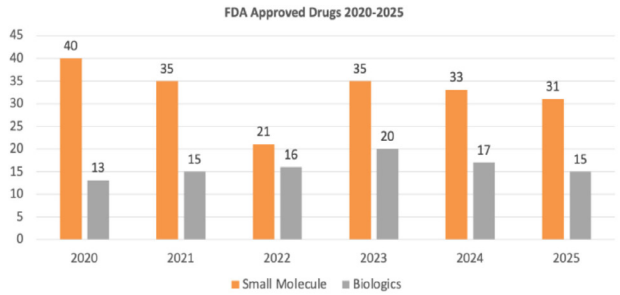

Figure 1. FDA approved drugs from 2020 to 2025 distinguished between small molecules and biologics (following the definition made by the FDA), public data available at FDA website.[9]

Additionally, there is a growing trend of approvals targeting therapeutic niches, aimed at smaller patient populations, which directly impacts the market potential of these new drugs. It is also important to note that 2025 sales figures have not yet been consolidated, and the final results are expected in the first quarter of 2026.[10]

Cancer remained the dominant area of innovation, with 16 new oncology drugs approved, accounting for 34% of all approvals. Other notable therapeutic areas included dermatology and non-malignant hematology, receiving a total of six approvals, while cardiology followed with 5 new agents. However, fewer neurology and infectious disease treatments were approved compared to previous years. Among the new approvals, 73% were small molecules, above the five-year average for this modality. Biologics comprised 27% of approvals, including 11 new monoclonal antibodies. (Figure 2).[9]

In the following sections, this review delves into the synthetic strategies behind the small molecules approved by the FDA in 2025, offering a comprehensive examination of the chemical innovations that have shaped modern drug development. Each section provides a detailed analysis of the synthetic approaches employed in the creation of these molecules, highlighting the breakthroughs, challenges, and optimizations that have influenced their design and production. Beyond the chemistry, this review tries explores the historical context behind each molecule, tracing its

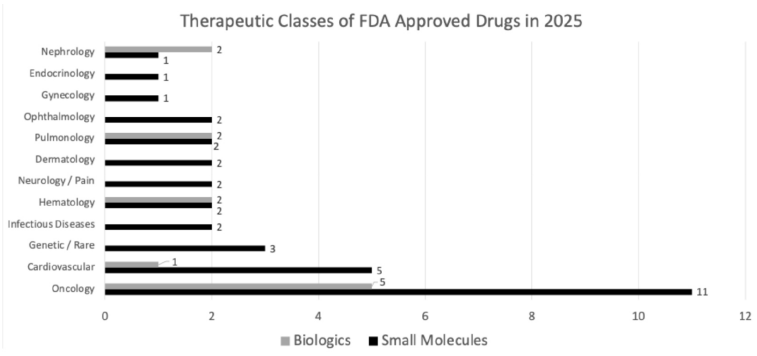

Figure 2. Therapeutic classes (based on FDA classification) of biologics and small molecules approved by the FDA in 2025.[8]

journey from initial discovery to clinical application. By merging scientific insights with historical perspectives, the review aims to provide a deep understanding of how these compounds emerged as key therapeutic advancements. Whether you are a researcher, a chemist, or simply an enthusiast of pharmaceutical science, these insights will shed light on the evolving landscape of drug synthesis and the impact of modern medicinal chemistry on global healthcare.

The following sections were structured to enable a comparative reading of the small molecules approved in 2025 through the lens of mechanism of action, molecular complexity, and synthetic strategy. Schemes were adapted or created based on the evidence of patents and research literature. First, we group the drugs by therapeutic classes and/or mechanistic families, briefly outlining their clinical relevance. Next, for each selected compound, we summarize the reported synthetic route (patent and/or primary literature), highlighting key retrosynthetic decisions, transformations that most strongly influence overall yield, and steps that may limit scalability (e.g., cross-couplings, selective oxidations, stereocontrolled constructions, and telescoped sequences). Finally, we consolidate cross-cutting trends and reporting gaps (isolated yields/conversions), providing a critical perspective on opportunities for innovation in process development.

2. FDA Approved Drugs 2025

2.1. Oncology

2.1.1. Sevabertinib

Sevabertinib, marketed under the trade name Hyrnuo, is an oral kinase inhibitor that received approval from the FDA in November 2025 for use in adult patients with locally advanced or metastatic non-squamous non-small cell lung cancer (NSCLC) that possesses HER2 (ERBB2) tyrosine kinase domain activating mutations following previous systemic treatment.[11,12] This agent exhibits selective activity against HER2 mutations, notably including exon 20 insertions, functioning as a reversible dual inhibitor of EGFR and HER2 while sparing wild-type EGFR to reduce adverse effects.[13] Sevabertinib exerts its effect through reversible association with these kinases, leading to the inhibition of HER2 phosphorylation and consequently preventing the activation of downstream signaling cascades essential for tumor proliferation and viability. *In vitro* experiments indicate that this mechanism effectively reduces the growth of cancer cells that either over-express wild-type HER2 or possess particular HER2 mutations.[14,15] In the SOHO-01 clinical trial (NCT05099172), which enrolled 70 participants, sevabertinib demonstrated an objective response rate of 71%, with substantial tumor reduction and disease stabilization extending beyond nine months in numerous cases.[14]

Starting from 3-chloro-2-methoxyaniline (**1**), the aniline functionality was first transformed into the corresponding aryl isothiocyanate via reaction with thiophosgene in a biphasic dichloromethane (DCM) / saturated aqueous $NaHCO_3$ system. The mixture was stirred at 0 °C for 2 h, promoting conversion of the aniline into 1-chloro-3-isothiocyanato-2-methoxybenzene (**2**) in > 99% yield, which was used directly in the next step. In the subsequent transformation, aryl isothiocyanate **2** was coupled with *tert*-butyl 2,4-dioxopiperidine-1-carboxylate (**3**) in acetonitrile using 1,8-diazabicycloundec-7-ene (DBU). In this step, DBU serves to generate a nucleophilic/enolized form of the cyclic 1,3-dicarbonyl partner, enabling C–C/C–N bond formation at the electrophilic isothiocyanate carbon and installation of the carbamothioyl motif on the heterocyclic scaffold. The reaction mixture was stirred at room temperature overnight giving intermediate **4** in 71% yield (Scheme 1).[16]

Next, intermediate *tert*-butyl 5-[(3-chloro-2-methoxyphenyl)carbamothioyl]-4-hydroxy-6-oxo-3,6-dihydropyridine-1(2*H*)-carboxylate (**4**) underwent acidic deprotection with trifluoroacetic acid (TFA) in dichloromethane, for 1.5 h at room temperature. This operation removes the *tert*-butyl carbamate (Boc-type) protecting group at the ring nitrogen, thereby unveiling the corresponding free N–H lactam/heterocycle while retaining the aryl-carbamothioyl substituent. After purification intermediate **5** was isolated in 78% yield. *N*-(3-Chloro-2-methoxyphenyl)-4-hydroxy-2-oxo-1,2,5,6-tetrahydropyridine-3-carbothioamide (**5**) was reacted with 1-{3-[(1,4-dioxan-2-yl)methoxy]pyridin-4-yl}methanamine (**6**) by heating the mixture at 80 °C for 4 h, delivering the product of this step in 81% yield. The aminomethylpyridine partner **6** can be prepared from the corresponding nitrile precursor 3-[(1,4-dioxan-2-yl)methoxy]pyridine-4-carbonitrile (**8**) by catalytic hydrogenation. An autoclave is charged with nitrile **8**, and Raney nickel, and the mixture is stirred under 25 bar H_2 at room temperature for 22 h in 94% yield. In this transformation, the nitrile (–C≡N) is reduced to the corresponding primary amine ($–CH_2NH_2$), with ammonia helping to suppress over-alkylation/secondary amine formation.

Finally, compound **7** was converted to sevabertinib through an oxidative cyclization promoted by TFA and aqueous hydrogen peroxide in MeOH. Thus, treatment of a suspension of *N*-(3-chloro-2-methoxyphenyl)-4-[({3-[(1,4-dioxan-2-yl)methoxy]pyridin-4-yl}

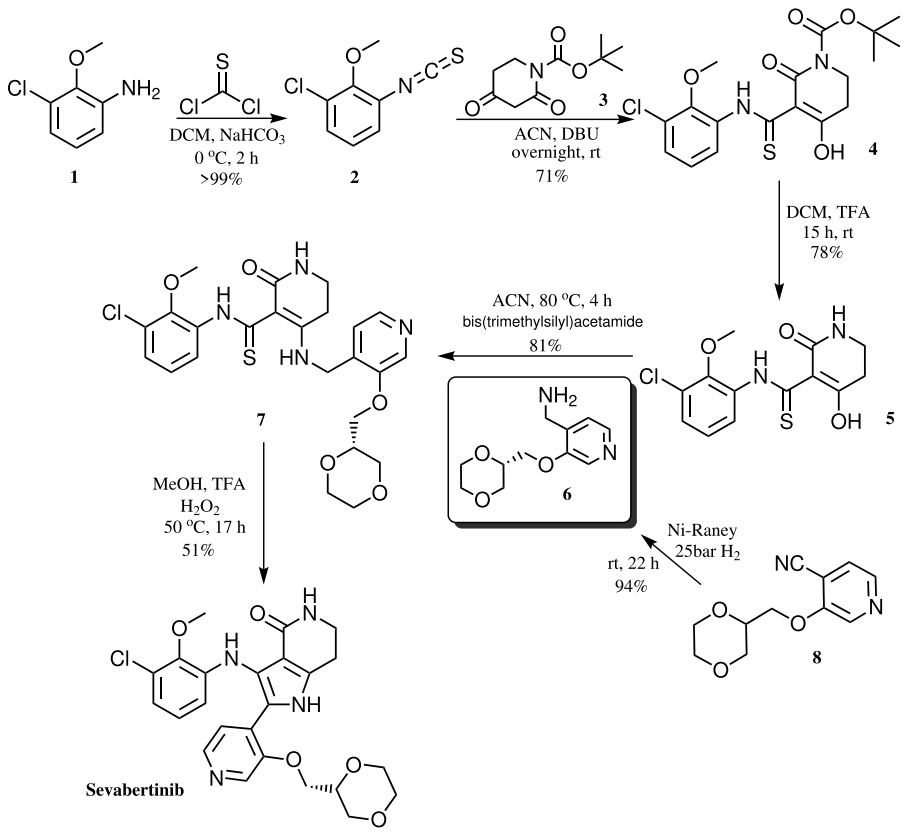

Scheme 1. Sevabertinib synthesis.

methyl)amino]-2-oxo-1,2,5,6-tetrahydropyridine-3-carbothioamide (**7**) with TFA followed by 35% H_2O_2, and heating at 50 °C for 17 h, afforded the corresponding pyrrolo[3,2-*c*]pyridin-4-one core in 51% yield.

Considering the isolated yields for each of the five consecutive transformations, the overall yield for the sevabertinib synthesis is 22.6%. This global yield indicates that, while the early-stage conversions proceed efficiently, the overall material throughput is predominantly governed by the later-stage steps-particularly the terminal transformation-highlighting where further optimization would have the greatest impact on the end-to-end efficiency of the route.[16] It is important to note that, the reliance on hazardous reagents (thiophosgene) and energy-intensive operations, such as high-pressure hydrogenation (25 bar), presents clear flags for industrial scale-up. Furthermore, the use of problematic halogenated solvents (DCM) increases the overall waste risk, suggesting that while the route is chemically robust, it remains sensitive to the qualitative sustainability indicators increasingly prioritized in modern process development.

2.1.2. Ziftomenib

Ziftomenib, marketed under the trade name Komzifti, is an orally administered inhibitor of menin that received FDA approval on November 13, 2025. It is indicated for the treatment of adult patients with relapsed or refractory acute myeloid leukemia (AML) characterized by a susceptible NPM1 mutation and lacking alternative effective therapies.[17,18] The mechanism of action involves disrupting the interaction between menin (MEN1) and KMT2A proteins, thereby inhibiting oncogenic processes in NPM1-mutated AML cells and encouraging differentiation of leukemia blasts.[19-21] In the phase I/II KOMET-001 clinical trial involving 112 participants, ziftomenib demonstrated a combined complete remission (CR) and CR with partial hematologic recovery (CRh) rate of 21.4%, with a median duration of five months; notably, 21.2% of transfusion-dependent patients achieved independence from transfusions.[22,23]

A representative convergent approach to ziftomenib relies on the independent preparation of two advanced fragments-namely the piperidinyl thienopyrimidine partner **16** and an indole-2-carbonitrile aldehyde fragment **23**, followed by late-stage union via reductive amination. In the first branch (Scheme 2), 4,4,4-trifluorobutanal (**9**) is converted into 2-amino-5-(2,2,2-trifluoroethyl)thiophene-3-carboxamide (**10**) through a Gewald-type thiophene synthesis with 2-cyanoacetamide and sulfur, typically conducted in the presence of Et_3N in 65% yield. Subsequent

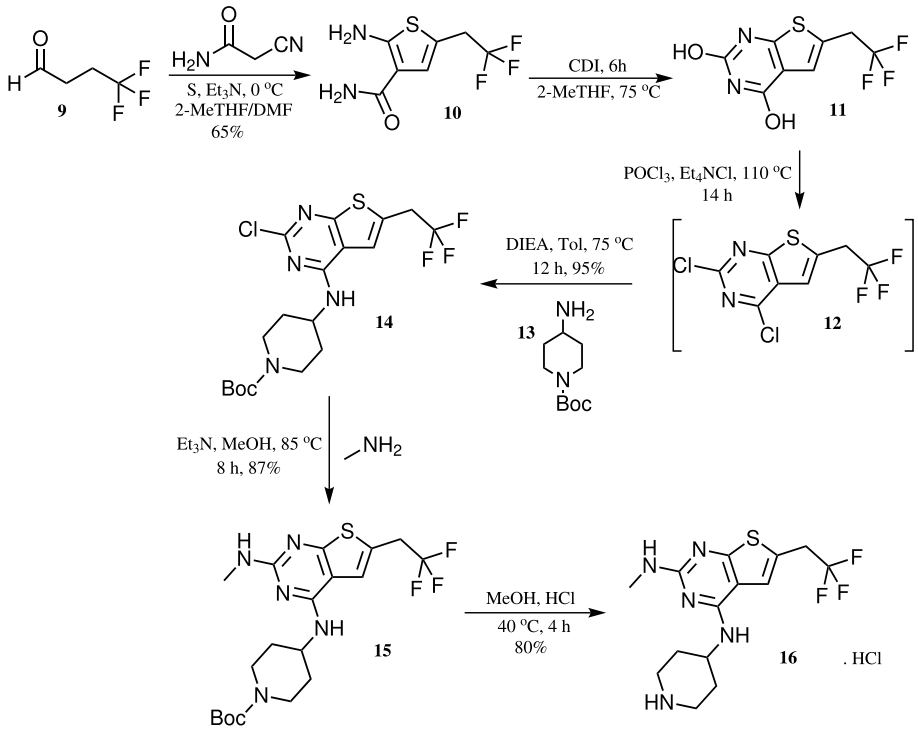

Scheme 2. Synthesis of intermediate **16**.

annulation of **10** with 1,1'-carbonyldiimidazole (CDI) in 2-methyl tetrahydrofuran (2-MeTHF) at 75 °C furnishes the heterobicyclic core 6-(2,2,2-trifluoroethyl)thieno[2,3-*d*] pyrimidine-2,4-diol (**11**). Activation of the diol motif via dehydrative chlorination (commonly using $POCl_3$ in the presence of Et_4NCl) provides the electrophilic dichloro intermediate **12**, which is leveraged in sequential regioselective SN_{Ar} substitutions: first, coupling with *tert*-butyl 4-aminopiperidine-1-carboxylate (**13**) under *N*,*N*-diisopropylethylamine (DIEA) in toluene at 75 °C affords (**14**, 94%), followed by displacement with methylamine in the presence of Et_3N in MeOH at 85 °C to deliver (**15**, 87%). Final *N*-Boc deprotection using HCl in MeOH at 40 °C for 4 h resulted in the formation of the corresponding free piperidine **16** in 80% yield.[24]

In the second branch (Scheme 3), the indole-derived amide fragment **19** is assembled from 3-nitro-*o*-xylene (**13**) via sequential acylation/condensation with diethyl oxalate under basic conditions in THF at 25 °C for 30 h, followed by reduction of the nitro group with $Na_2S_2O_4$ provides the corresponding aniline, which upon ester hydrolysis and intramolecular cyclocondensation under $NaOH/H_2O$ at 5 °C forms 4-methyl-1*H*-indole-2-carboxylic acid (**18**, 76%). Conversion to the acid chloride with $(COCl)_2$/DMF in CH_2Cl_2 at 50 °C, followed by amidation with 25% aq. NH_3, affords the carboxamide **19** in 80% yield. $POCl_3$-mediated dehydration in refluxing toluene then furnishes the indole-2-carbonitrile (**20**, 84%). Introduction of the (2*S*)-piperazinylpropyl side chain is achieved via a Mitsunobu substitution of the primary alcohol **21** (using diisopropyl azodicarboxylate (DIAD)/PPh_3 in tetrahydrofuran (THF)) to give (**22**, 75%), which is subsequently converted to aldehyde **23** by Rieche formylation in low isolated yields ca. 40%.[24]

The convergent endgame involves reductive amination of aldehyde **23** with the free base of amine **16**, generated by basification of its dihydrochloride salt with Et_3N in CH_2Cl_2, followed by reduction with $NaBH_4$ in the presence of isobutyric acid in CH_2Cl_2, providing the target ziftomenib in 90% isolated yield (Scheme 4).

Considering the convergent nature of the route toward ziftomenib, the overall yield was assessed by combining the cumulative yields of the two independently prepared advanced intermediates with the final coupling efficiency. The reliance on $POCl_3$ and oxalyl chloride requires rigorous moisture control and specialized waste handling. Additionally, the use of a Mitsunobu substitution and the low-yielding Rieche formylation (ca. 40% yield) represent significant efficiency bottlenecks. The sequence leading to intermediate **16** proceeds in 32.2% cumulative yield, whereas the route to intermediate **23** delivers the partner fragment in 15.1% cumulative yield. When these streams are merged under the convergent coupling conditions (90% yield, 1:1.05 stoichiometry), the calculated end-to-end efficiency of the overall synthetic plan corresponds to a global yield of ca. 4.39% from the respective starting

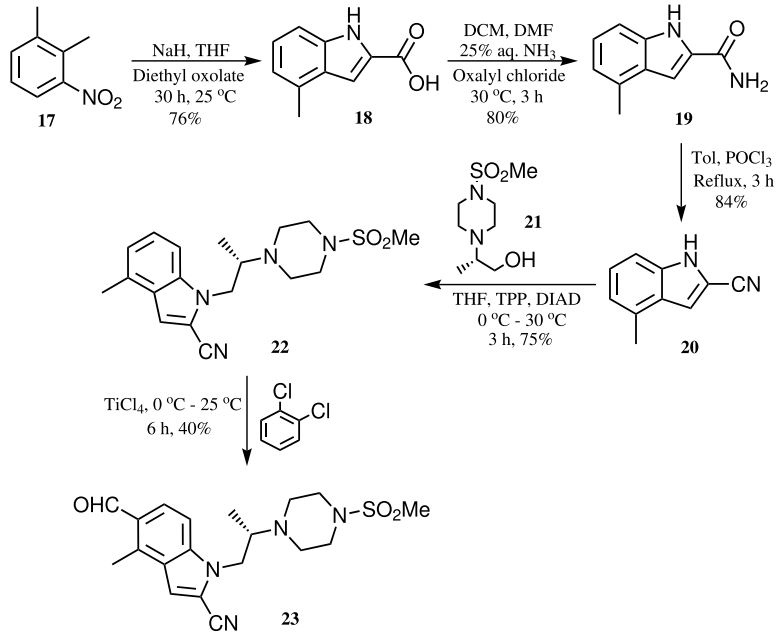

Scheme 3. Synthesis of intermediate **23**.

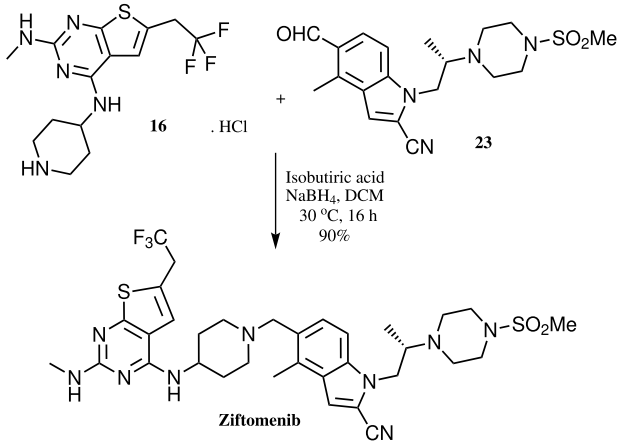

Scheme 4. Final coupling of intermediates **23** and **16** towards ziftomenib.

materials through to the final Active Pharmaceutical Ingredient (API).[24]

2.1.3. Imlunestrant

Imlunestrant, marketed under the name Inluriyo, is an oral chemotherapeutic agent developed by Eli Lilly and Company for the treatment of certain breast cancer subtypes.[25,26] Specifically, it is indicated for use in adult patients with estrogen receptor (ER)-positive, human epidermal growth factor receptor 2 (HER2)-negative, ESR1-mutated advanced or metastatic breast cancer that has shown progression following at least one prior endocrine therapy regimen.[27,28] Results from EMBER clinical studies demonstrate that imlunestrant extends progression-free survival relative to conventional therapies, with a median duration of 5.5 months compared to 3.8 months observed in patients harboring ESR1 mutations.[29-31] As a selective estrogen receptor degrader (SERD) and antagonist, imlunestrant binds to estrogen receptors on neoplastic cells, thereby inhibiting estrogen-mediated proliferative signals and promoting receptor degradation.[32,33] It offers advantages over injectables like fulvestrant due to its oral form and ability to penetrate the blood-brain barrier.[27] Regulatory approval was granted by the U.S. Food and Drug Administration in September 2025, and similar authorization has been obtained within European markets.[25,34]

A concise synthetic sequence toward imlunestrant has been described starting from 7-methoxyquinolin-4-ol (**24**) (Scheme 5). Initial electrophilic chlorination with *N*-chlorosuccinimide (NCS) in dimethylformamide (DMF) at 45 °C affords 3-chloro-7-methoxyquinolin-4-ol (**25**) in 83% yield. Subsequent halogenation under brominating conditions (using PBr_3 in toluene, 40-100 °C) provides the complementary dihalogenated quinoline 4-bromo-3-chloro-7-methoxyquinoline (**26**) in 87% yield, establishing a versatile platform for further chemoselective functionalization.[35,36]

Installation of the benzylic side chain is achieved via magnesium-halogen exchange of **26** with i-PrMgCl in THF at −20 °C under inert atmosphere, followed by nucleophilic addition to 4-fluorobenzaldehyde to give the corresponding secondary benzylic alcohol. Without isolation, this intermediate is oxidized under 2,2,6,6-tetramethylpiperidin-1-oxyl (TEMPO)/NaOCl conditions to furnish the ketone **27** in 68% yield.[35]

Demethylation with BBr_3 in DCM then delivers the free phenolic analogue **28** in 85% yield (Scheme 5),

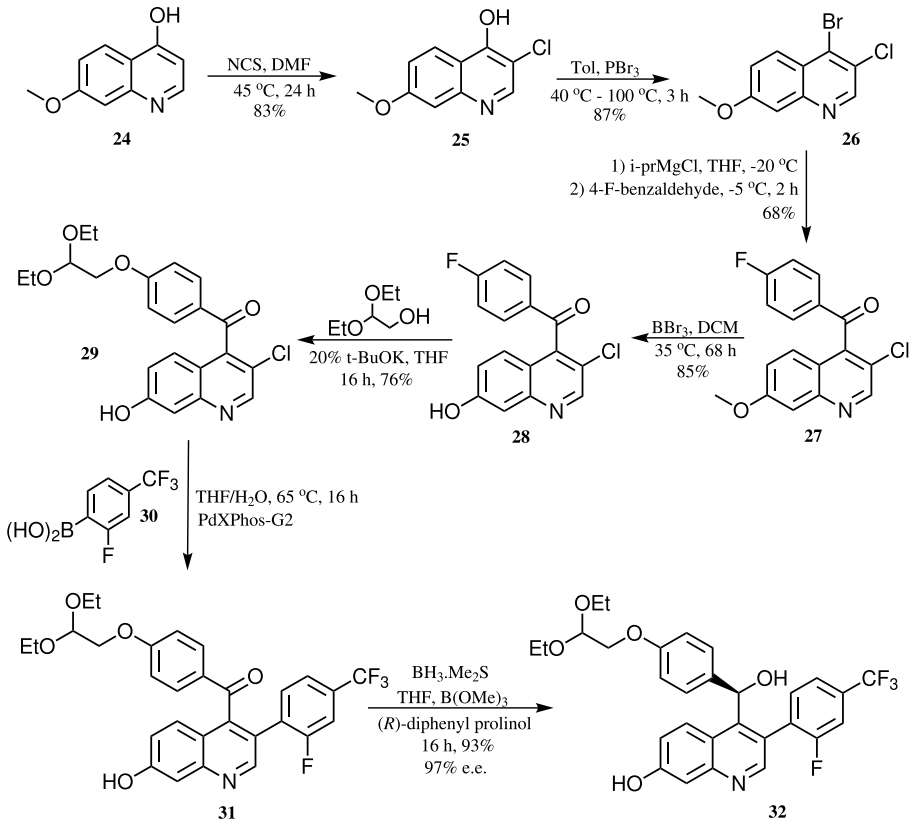

Scheme 5. Synthetic approach to intermediate **32**.

which is *O*-alkylated with 2,2-diethoxyethanol using 20% t-BuOK in THF to provide ether **29** in 76% yield. The aryl substituent is introduced by Suzuki-Miyaura cross-coupling of **29** with 2-fluoro-4-(trifluoromethyl) phenylboronic acid (**30**) employing XPhos-Pd-G2, giving 3-[2-fluoro-4-(trifluoromethyl)phenyl]quinolin-7-ol (**31**). Enantioselective reduction of ketone **31** under Corey-Bakshi-Shibata catalyst (CBS) conditions (using $BH_3{\cdot}Me_2S$, $B(OMe)_3$, and (*R*)-diphenylprolinol in THF) affords the target (*R*)-alcohol **32** in 93% yield and 97% enantiomeric excess (ee).[36]

Downstream, base-promoted intramolecular cyclization of (Scheme 6, **32**) with Cs_2CO_2 in MeCN at 85 °C furnishes the polycyclic acetal **33** in 86% yield while largely preserving stereochemical integrity (95% ee). Acidic cleavage of the diethyl acetal using HCl in MeCN/H_2O at 60 °C provides the corresponding acetaldehyde **34** in good yield. Final assembly is achieved through reductive amination of **34** with 3-(fluoromethyl) azetidine (**35**) using $NaBH(OAc)_3$ and Et_3N in EtOH at 0 °C, delivering imlunestrant in 99% yield and 99.5% ee (Scheme 6).

The linear sequence toward imlunestrant demonstrates high stereochemical control but faces sustainability challenges due to its ten-step length and reliance on hazardous reagents such as PBr_3 and BBr_3. The requirement for cryogenic temperatures (–20 °C) during the magnesium-halogen exchange step further increases the energy footprint of the process. While the 17.5% overall yield is supported by highly enantioselective transformations like the CBS reduction, the accumulation of moderate losses in the mid-sequence remains a primary driver of the final material throughput and waste profile.[35]

2.1.4. Zongertinib

Zongertinib, marketed under the trade name Hernexeos, is an orally administered kinase inhibitor that specifically targets HER2 (human epidermal growth factor receptor 2, or Erb-B2 Receptor Tyrosine Kinase 2 (ERBB2)) mutations associated with non-small cell lung cancer (NSCLC).[37] Its acrylamide group establishes a covalent linkage with the cysteine 805 residue of the HER2 receptor, leading to the suppression of HER2 phosphorylation and subsequent activation of downstream signaling cascades such as extracellular signal-regulated kinase (ERK), mitogen-activated protein kinases (MAPK), and PI3K/Akt pathways, and, consequently, a reduction in the proliferation rate of lung cancer cells.[38] In August 2025, the U.S. Food and Drug Administration authorized its use for adult patients with unresectable or metastatic non-squamous NSCLC

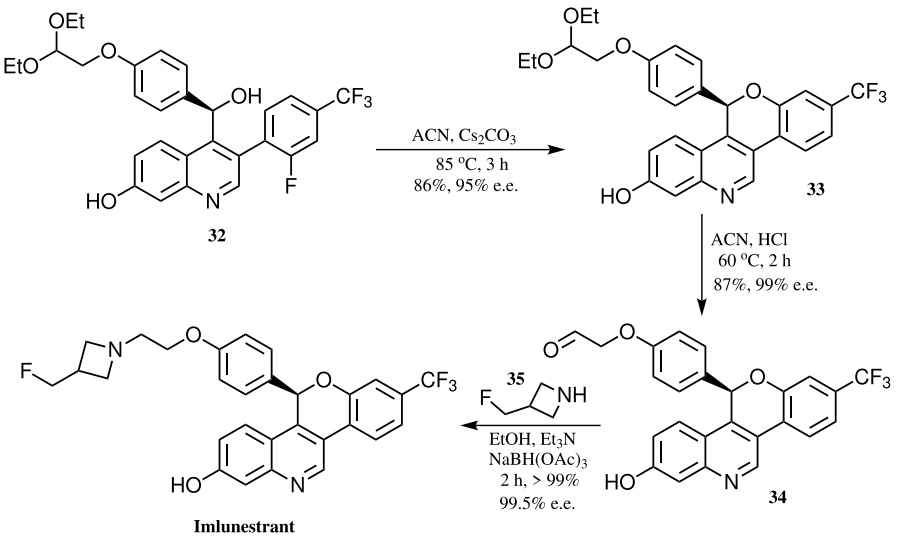

Scheme 6. Final approach to imlunestrant.

possessing activating mutations in the HER2 tyrosine kinase domain following previous systemic therapy.[39] Data derived from the Beamion LUNG-1 clinical trial (NCT04886804)-evaluated through blinded independent central review using RECIST v1.1 criteria-demonstrated an objective response rate indicative of treatment efficacy.[38,40] As an irreversible, HER2-selective tyrosine kinase inhibitor, Zongertinib minimizes inhibition of EGFR (ERBB1), thereby diminishing adverse effects like rash and diarrhea observed with earlier treatments.[41,42] Phase 1 trial outcomes revealed a confirmed objective response rate of 71%, along with a median progression-free survival period of approximately 12.4 months in patients with pretreated HER2-mutant NSCLC.[38]

Zongertinib has been accessed via a linear sequence (Scheme 7) starting from 8-chloro-2-(methylthio) pyrimido[5,4-*d*]pyrimidine (**36**) which is first elaborated through nucleophilic aromatic substitution with 3-methyl-4-[(1-methyl-1*H*-benzimidazol-5-yl)oxy]aniline (**37**). This amination, performed in an i-PrOH/toluene mixture at 43 °C for 30 min, delivers the corresponding secondary aniline adduct **38** in 93% yield. Although the preparation of coupling partner **37** is described elsewhere, it is noteworthy that it is accessed in 15% overall yield from its respective precursors.[43-47]

Oxidation of the thioether substituent in **38** to the corresponding sulfone is achieved using 30% aqueous solution H_2O_2 in the presence of catalytic Na_2MoO_2 in EtOH/H_2O, affording intermediate **39** in 94% yield. The resulting activated heteroaryl system then undergoes a second SN_{Ar} substitution with *tert*-butyl piperidin-4-ylcarbamate (**40**) in THF at 60 °C, providing the 6-(piperidin-1-yl)pyrimido[5,4-*d*]pyrimidin-4-amine derivative (**41**) in 87% yield.[44]

Subsequent *N*-Boc deprotection (acetyl chloride (AcCl) in isopropyl alcohol (IPA), 65 °C) furnishes the corresponding amine trihydrochloride **48** in 99% yield (Scheme 8). This intermediate is then *N*-acylated with 3-chloropropanoyl chloride in the presence of K_3PO_4 in THF to give carboxamide **49** in 69% yield, and final base-mediated dehydrochlorination using KOH in THF/H_2O delivers the target zongertinib with 91% of yield.[46]

The synthetic route toward zongertinib is characterized by a high global efficiency of ca. 46.1%, outperforming many contemporary linear sequences for complex APIs. This performance is supported by a sustainable catalytic oxidation step utilizing H_2O_2, which significantly reduces the environmental footprint of the heteroaryl activation. However, the process remains limited by the *N*-acylation step, which serves as a yield bottleneck at 69%. Furthermore, the requirement for 3-chloropropanoyl chloride represents a qualitative sustainability flag due to its hazardous nature and the need for specialized handling, suggesting that further optimization of this acylation-dehydrochlorination sequence could enhance both the safety and atom economy of the overall process.[37]

2.1.5. Dordaviprone

Dordaviprone, marketed under the trade name Modeyso, is indicated for the treatment of diffuse midline glioma characterized by an H3 K27M mutation in patients experiencing disease progression following previous therapeutic interventions. On August 6, 2025, the Food and Drug Administration granted expedited approval for this medication, representing the inaugural systemic therapy for this highly malignant brain tumor variant that affects both adult and pediatric populations.[48,49] The pharmacological action of Dordaviprone involves serving

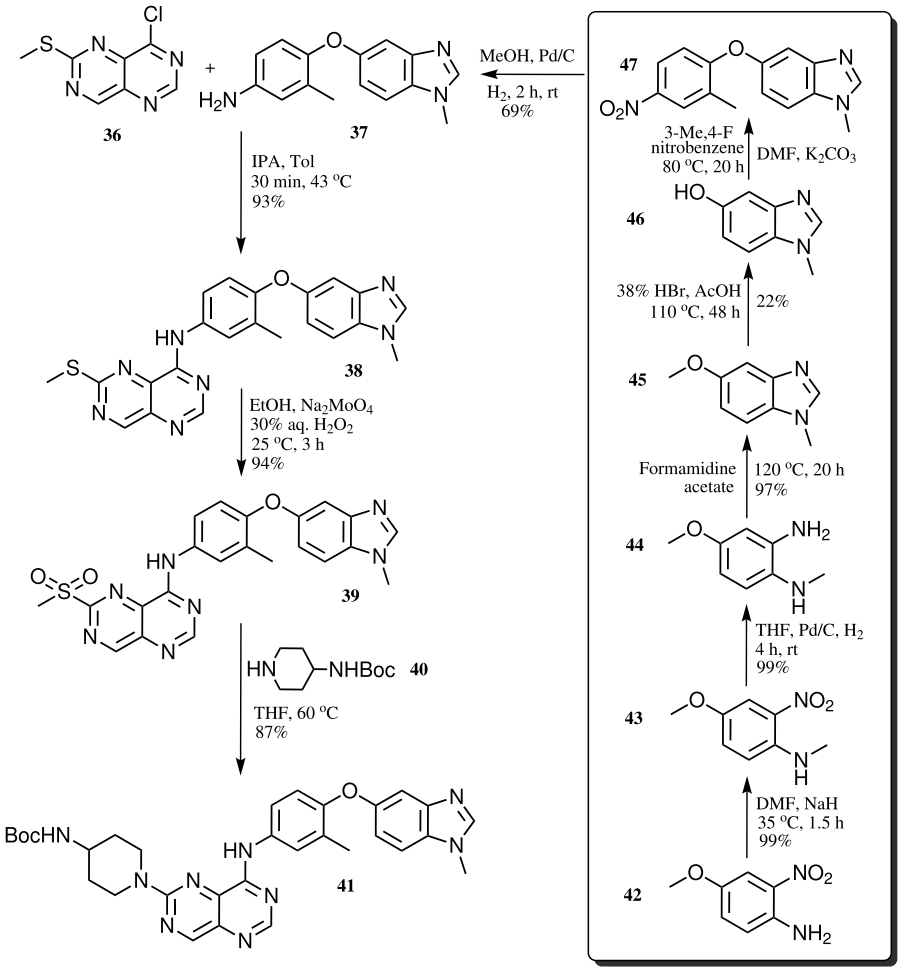

Scheme 7. Synthesis of intermediate **41**.

as a protease activator of mitochondrial caseinolytic protease P (ClpP) as well as functioning as an antagonist of dopamine receptor D2; these mechanisms facilitate apoptosis in cancer cells and suppress signals that promote tumor proliferation.[50,51] This agent specifically targets recurrent cases of H3 K27M-mutant diffuse midline glioma, but does not extend its indication to conditions such as diffuse intrinsic pontine glioma or primary spinal tumors. Clinical evaluation has demonstrated a response rate of approximately 22%, with some patients experiencing sustained clinical benefits exceeding one year.[52-54]

A reported preparation of dordaviprone hydrochloride (Scheme 9) begins with 2-methylthio-2-imidazoline hydroiodide (**50**), which undergoes *N*-methoxycarbonylation with *tert*-butyl bromoformate (BrCOO-*t*Bu, **51**) in EtOH to afford methyl 2-methylsulfanyl-4,5-dihydroimidazole-1-carboxylate (**52**) in 94% yield. Intermediate **52** is then converted to the corresponding secondary amine **54** via nucleophilic substitution/amination with 2-methylbenzylamine (**53**) in refluxing THF, albeit in a more modest 61% yield. The key scaffold-forming step involves base-mediated cyclocondensation of **54** with methyl 1-benzyl-4-oxopiperidine-3-carboxylate hydrochloride (**55**) using NaOMe in refluxing MeOH, providing dordaviprone in 86% yield. Final conversion to the clinically relevant salt is achieved by acidification with HCl in dioxane/methyl *tert*-butyl ether (MTBE), furnishing dordaviprone hydrochloride.[55,56]

The synthetic strategy toward dordaviprone hydrochloride underscores a concise and high-yielding assembly, delivering a remarkable 49% global yield. Despite this efficiency, the route is delineated by specific process hazards, notably the liberation of methanethiol during the formation of intermediate **54**. The generation of such volatile sulfurous byproducts presents substantial containment challenges during scale-up. Furthermore, the employment of *tert*-butyl bromoformate and the reliance on dioxane for salt formation serve as qualitative indicators of a process that remains contingent on high-risk reagents and problematic solvents. Addressing the 61% yield limitation in the amination stage through alternative leaving group strategies could potentially mitigate the environmental

footprint while further enhancing the cumulative mass intensity of this clinical-stage tricyclic scaffold.

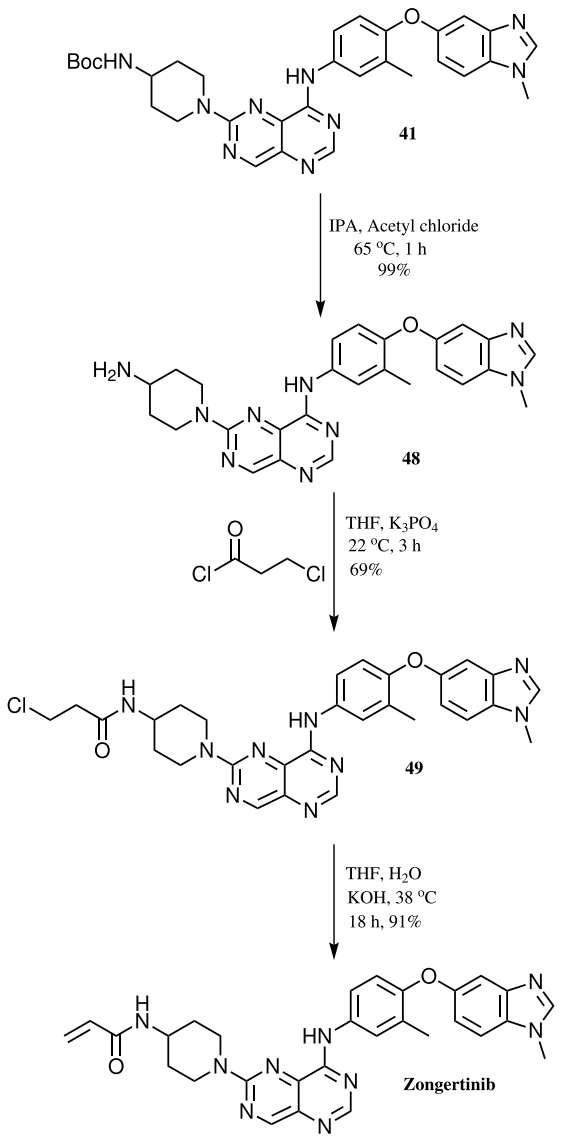

Scheme 8. Synthesis of final product zongretinib.

2.1.6. Sunvorzetinib

Sunvozertinib (DZD9008) is an oral inhibitor of tyrosine kinase activity, specifically targeting mutations in the epidermal growth factor receptor (EGFR), and is predominantly indicated for the treatment of non-small cell lung cancer (NSCLC).[57] This medication is prescribed for adult patients with locally advanced or metastatic NSCLC characterized by EGFR exon 20 insertion mutations, identified through FDA-approved diagnostic tests, after disease progression following platinum-based chemotherapy.[58-60] It received accelerated approval from the U.S. Food and Drug Administration in July 2025 under the commercial name Zegfrovy, along with conditional approval in China achieved in 2023.[61,62] The WU-KONG1B clinical trial (NCT03974022) demonstrated that a daily dose of 200 mg of sunvozertinib elicited marked antitumor responses among 85 pretreated individuals, with notable objective response rates and an acceptable profile of manageable adverse effects. Additionally, a phase 2 investigation (WU-KONG15) involving treatment-naïve patients reported sustained progression-free survival and a median overall survival of approximately 23.1 months as of early 2025.[63-65]

Sunvozertinib has been synthesized starting from methyl 2-amino-4-chloro-5-fluorobenzoate (Scheme 10, **56**), which is converted to the corresponding tertiary benzylic alcohol **57** via Grignard addition of methylmagnesium bromide in THF (78% yield). Subsequent nucleophilic aromatic substitution with 2,4-dichloropyrimidine (**58**) under basic conditions (DIEA, 90 °C, 27 h) installs the aminopyrimidine fragment to give intermediate **59**, albeit in low yield (14%). Further elaboration through acid-promoted condensation of **59** with 4-fluoro-2-methoxy-5-nitroaniline (**60**, TFA in BuOH, 50 °C) affords the corresponding triarylamine intermediate **61**, which is then advanced to the tetracyclic framework **63** by coupling with *N*,*N*-dimethylpyrrolidin-3-(*R*)-amine (**62**) in the

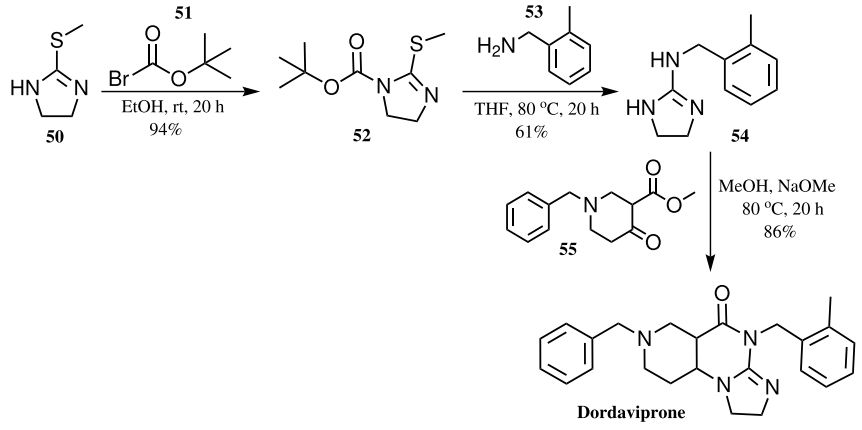

Scheme 9. Synthesis of dordaviprone.

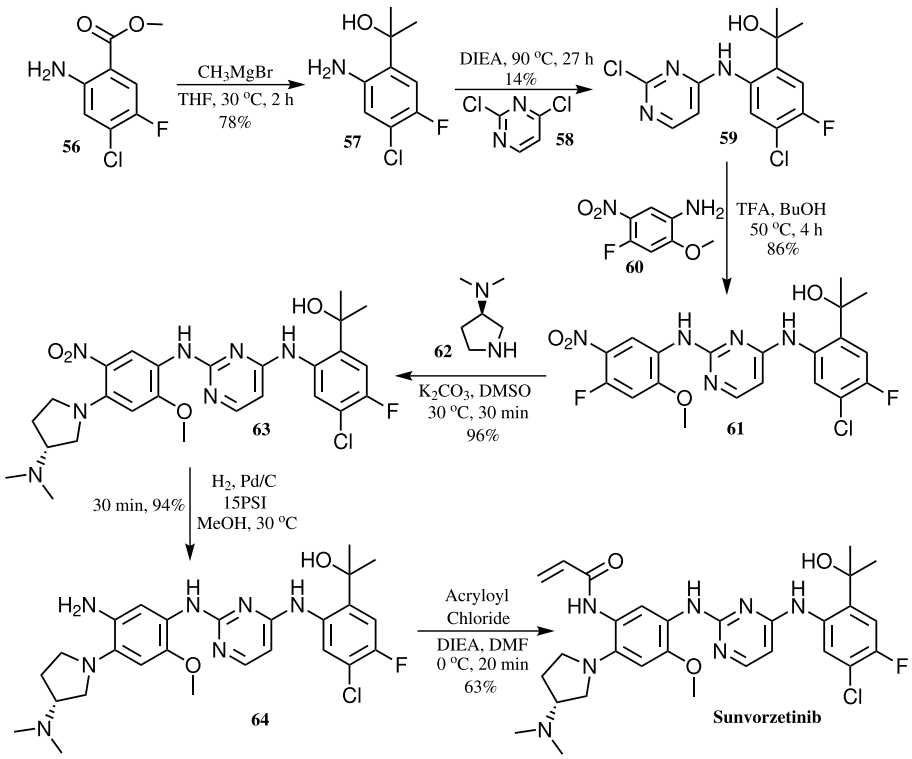

Scheme 10. Verticalized approach to sunvorzetinib.

presence of K_2CO_3 in dimethyl sulfoxide (DMSO, 96% yield). The nitro group is subsequently reduced under H_2/Pd-C in MeOH to provide aniline **64** in 94% yield, and the sequence is completed by acylation with acryloyl chloride in DMF using DIEA to furnish sunvozertinib (63% yield in the final step).[66-68]

The synthetic architecture for sunvozertinib serves as a definitive case study in how an early-stage transformational bottleneck can compromise the viability of a multi-step sequence, resulting in a restrained ca. 5.3% overall yield. This inefficiency is fundamentally anchored in the 14% yield obtained during the base-mediated coupling of the pyrimidine fragment-a step that severely erodes the end-to-end material throughput. Although the route benefits from a highly efficient catalytic nitro reduction and a robust late-stage cyclization (> 90% yields), the process is delineated by substantial safety and operational hurdles, including the employment of air-sensitive Grignard reagents and the final incorporation of the hazardous acryloyl chloride. These factors suggest that a strategic redesign of the heterocyclic coupling phase is essential to improve the atom economy and environmental profile of the current manufacturing paradigm.

2.1.7. Taletrectinib

Taletrectinib, marketed under the brand name Ibtrozi, is an orally administered kinase inhibitor that received approval from the FDA in June 2025 for use in adults with either locally advanced or metastatic ROS1-positive non-small cell lung cancer (NSCLC).[69,70] This agent specifically inhibits ROS1 tyrosine kinase activity, including mutations conferring resistance such as G2032R, and exhibits activity against tropomyosin receptor kinases (TRK) receptor subtypes (TRKA/B/C). By interfering with fusion proteins that drive oncogenic signaling pathways, taletrectinib impedes mechanisms underpinning tumor proliferation.[71] Results from clinical trials such as TRUST-II have demonstrated elevated response rates, sustained therapeutic responses, significant intracranial efficacy, and extended progression-free survival among both tyrosine kinase inhibitor (TKI)-naïve and previously treated patient populations.[72-74]

A convergent strategy toward taletrectinib has been described (Scheme 11) in which a functionalized aryl boronate and a heteroaryl amine fragment are assembled and merged via cross-coupling. In this context, *p*-bromophenol (**65**) can be converted to *N*-Boc-1-(4-bromophenoxy)-2(*R*)-propanamine (**66**) through a Mitsunobu *O*-alkylation with *N*-Boc-*D*-alaninol (PPh_3/DIAD); notably, this specific preparation is not explicitly detailed in the originating patent. The aryl bromide **66** is subsequently transformed into the corresponding pinacol boronate ester **67** via Miyaura borylation employing bis(pinacolato)diboron, $Pd(OAc)_2/PPh_3$, and KOAc in DMAc at 100 °C, providing **67** in 88% yield.[75]

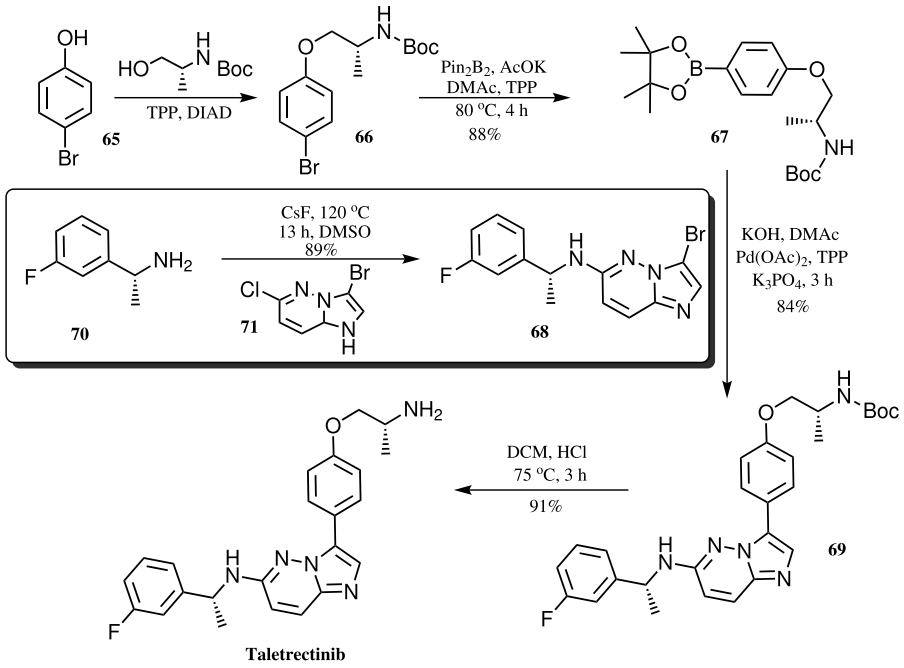

Scheme 11. Synthesis of taletrectinib.

In parallel, the heteroaryl coupling partner **68** is assembled by reacting 1(*R*)-(3-fluorophenyl) ethanamine (**70**) with 3-bromo-6-chloroimidazo[1,2-*b*] pyridazine (**71**) under CsF in DMSO at 120 °C for 13 h. This intermediate is then combined with boronate **67** in a Suzuki-Miyaura coupling ($Pd(OAc)_2/PPh_3$, K_3PO_4, DMAc/H_2O, 90 °C) to deliver *N*-Boc-taletrectinib (**69**) in 84% yield. Final carbamate deprotection using HCl in DCM at 75 °C provides taletrectinib in 91% yield, and subsequent salt formation with adipic acid furnishes taletrectinib adipate in 91% yield.[76]

The preparative route toward taletrectinib leverages a convergent endgame that effectively streamlines the assembly of the polycyclic scaffold, resulting in a commendable partial overall yield of ca. 63.4%. Central to this strategy is a robust Suzuki-Miyaura coupling (84% yield) that merges advanced intermediates under standard palladium catalysis. Nevertheless, the qualitative sustainability profile is tempered by the early-stage Mitsunobu transformation, which introduces substantial mass intensity through the stoichiometric generation of phosphine oxide waste. Furthermore, the requirement for energy-intensive heating in high-boiling solvents like DMSO and *N*,*N*-dimethylacetamide (DMAc) underscores a typical scalability hurdle for these medicinal chemistry-derived routes. While individual downstream steps exhibit high efficiency, the lack of full disclosure for the initial *O*-alkylation emphasizes the complexity of determining the absolute environmental footprint and total mass intensity for this clinical candidate.

2.1.8. Vimseltinib

Vimseltinib is an orally administered, targeted pharmacological agent utilized in the treatment of a rare joint tumor known as tenosynovial giant cell tumor (TGCT). It is commercially available under the brand name Romvimza. As a small molecule kinase inhibitor taken orally, vimseltinib specifically antagonizes the colony stimulating factor 1 receptor (CSF1R), a receptor tyrosine kinase expressed on macrophages and related cell types.[77,78] This antineoplastic drug has received approval from FDA for use in adult patients presenting with symptomatic TGCT when surgical intervention is likely to impair function or result in significant morbidity.[79] The tumor's pathogenesis frequently involves overexpression of CSF1, which attracts CSF1R-expressing macrophages that constitute most of the tumor mass; vimseltinib mitigates this process by inhibiting CSF1R signaling pathways.[80] Employing a novel "switch control" mechanism, the drug stabilizes CSF1R in its inactive conformation with high selectivity-exceeding 500-fold-over other kinases, thereby minimizing off-target effects relative to earlier inhibitors like pexidartinib.[78] Clinical data from the phase 3 MOTION trial demonstrated that vimseltinib significantly enhanced objective response rates and patient-reported physical functioning compared to placebo in cases of symptomatically inoperable TGCT. Patients also experienced notable improvements in joint mobility and reduction of stiffness, with responses intensifying over time and many achieving sustained decreases in tumor volume as confirmed through imaging studies.[81,82]

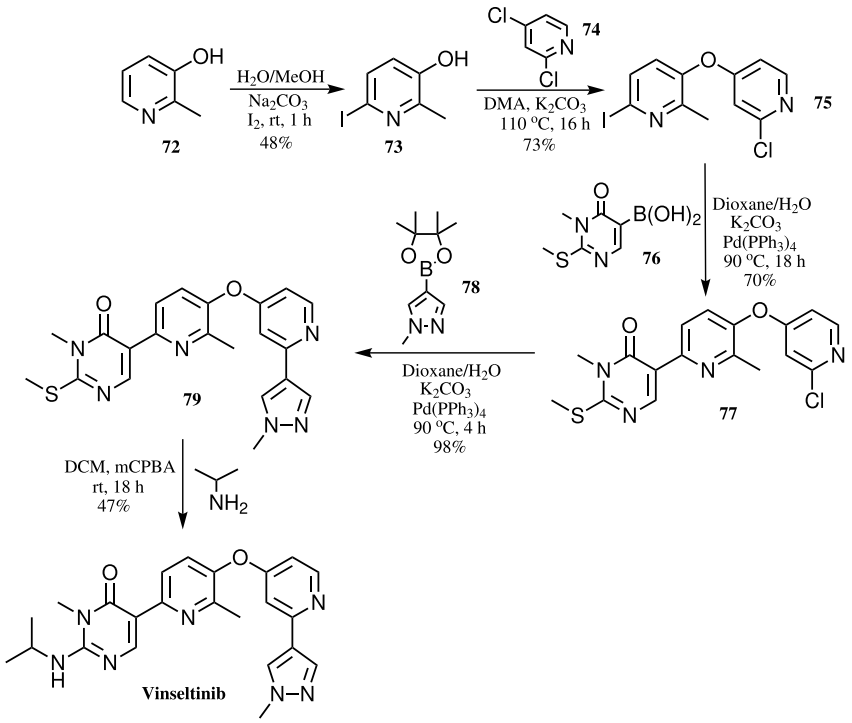

Scheme 12. Vinseltinib synthesis starting from 2-methyl-3-pyridinol (**57**).

The originator patent route (Scheme 12) to vimseltinib has been disclosed starting from 2-methyl-3-pyridinol (**72**), which is first converted to the corresponding iodinated derivative 6-iodo-2-methyl-3-pyridinol (**73**) via electrophilic aromatic substitution using I_2 in the presence of Na_2CO_3 in MeOH/H_2O; notably, this transformation is reported to proceed in low yield (48%). The aromatic intermediate (**73**) is subsequently advanced through *O*-arylation with 2,4-dichloropyridine (**74**) under basic conditions (K_2CO_3, DMAc, 110 °C), affording 3-[(2-chloro-4-pyridinyl) oxy]-6-iodo-2-methylpyridine (**75**). Installation of the heteroaryl fragment is then achieved via a regioselective Suzuki-Miyaura cross-coupling of the aryl iodide (**75**) with (1-methyl-2-(methylthio)-6-oxo-1,6-dihydropyrimidin-5-yl)boronic acid (**76**) using $Pd(PPh_3)_4$ and Na_2CO_3 in refluxing dioxane/H_2O, delivering diaryl intermediate **77** in 70% yield. A second Suzuki-Miyaura coupling of **77** with 1-methylpyrazole-4-boronic acid pinacol ester (**78**) ($Pd(PPh_3)_4$, K_2CO_3, dioxane/H_2O, 90 °C) provides intermediate **79** in 98% yield. Finally, conversion to the target is accomplished by nucleophilic amination of the thioether-containing heterocycle with isopropylamine, furnishing vimseltinib in 47% yield.[83-85]

The chemical approach toward vimseltinib is characterized by a reliance on dual palladium-catalyzed cross-couplings, culminating in a restrained global yield of ca. 11.4%. The overall throughput is predominantly throttled by the 47% yield achieved in the final nucleophilic amination, which serves as the primary transformational bottleneck. From a sustainability perspective, the process is delineated by the extensive use of problematic solvents like dioxane and high-temperature operations in DMAc (110 °C), both of which introduce substantial energy and waste-management burdens. These findings suggest that transitioning toward a more atom-economical assembly-perhaps by refining the low-yielding initial iodination (48%) or adopting more sustainable catalytic systems-could significantly enhance the commercial scalability and environmental profile of this clinical candidate.

2.1.9. Mirdametinib

Mirdametinib, marketed under the trade name Gomekli, is an orally administered inhibitor of kinases that specifically targets the MEK1 and MEK2 enzymes. The United States Food and Drug Administration granted approval for this medication on February 11, 2025, for the treatment of symptomatic plexiform neurofibromas in patients with neurofibromatosis type 1 (NF1) who are at least two years of age and for whom surgical intervention is not suitable.[86,87] Mirdametinib functions as a selective inhibitor that does not compete with adenosine triphosphate (ATP) binding sites on MEK1/2, thereby preventing the phosphorylation of ERK1/2 kinases downstream in the MAPK signaling pathway. This mechanism interferes with tumor cell proliferation in models harboring B-Raf proto-oncogene, serine/threonine kinase (BRAF) or

Rat Sarcoma vírus (RAS) mutations, resulting in tumor reduction observed during preclinical evaluations.[88,89] The regulatory approval was based on findings from the ReNeu phase IIb clinical trial, which demonstrated a confirmed overall response rate determined by magnetic resonance imaging (MRI) assessments indicating at least a 20% decrease in plexiform neurofibroma volume-encompassing partial and complete responses. Additionally, the drug has been shown to alleviate pain and enhance quality of life, with its capacity to penetrate the central nervous system aiding in addressing neurofibromatosis-related complications.[90,91] Developed by SpringWorks Therapeutics, mirdametinib is taken orally and is effective against inoperable plexiform neurofibromas associated with NF1-a genetic disorder characterized by nerve tumors. Its use has been extensively studied across adult and pediatric populations; however, issues such as resistance development and adverse effects remain significant challenges.[92,93]

A concise preparation of mirdametinib (Scheme 13) has been described via assembly of a benzohydroxamate precursor from 3,4-difluoro-2-(2-fluoro-4-iodophenylamino)benzoic acid (**82**). Activation of the carboxylic acid **80** and subsequent coupling with *O*-(2,2-dimethyl[1,3]dioxolan-4-ylmethyl) hydroxylamine (**81**)-typically using diphenylphosphinyl chloride and *N*-methylmorpholine (NMM) in THF-affords the corresponding benzohydroxamate **82**, which upon TsOH-mediated deprotection/hydrolysis in MeOH/H_2O provides mirdametinib.

Notably, the patent disclosure does not report isolated yields for these transformations, precluding a quantitative assessment of the efficiency of the end-to-end sequence from the available data. The protected hydroxylamine coupling partner **81** can be prepared from 1,2,4-butanetriol (**83**) through dioxolane protection (**84**), followed by a standard Gabriel-based sequence, delivering **81** in 75% yield.[94,95]

The chemical protocol described for mirdametinib centers on the amidation of a highly functionalized benzoic acid core with a protected hydroxylamine side chain. The broader preparative framework is characterized by a lack of quantitative transparency, as the patent disclosure omits isolated yields for the key coupling and subsequent TsOH-mediated deprotection. Qualitatively, the reliance on diphenylphosphinyl chloride for carboxylic acid activation and the requirement for a final hydrolysis step to cleave the dioxolane moiety represent standard yet atom-inefficient transformations. The absence of specific yield data prevents a rigorous evaluation of the end-to-end efficiency, highlighting a common challenge in assessing the commercial scalability of clinical candidates solely through early-stage patent disclosures.

2.1.10. Treosulfan

Treosulfan is a bifunctional alkylating agent predominantly employed in conditioning protocols preceding allogeneic hematopoietic stem cell transplantation (HSCT). It is frequently administered in combination with fludarabine for individuals diagnosed with acute myeloid leukemia (AML), myelodysplastic syndromes (MDS), or other high-risk hematologic malignancies.[96,97] As a prodrug, treosulfan undergoes non-enzymatic activation within the body to generate epoxy derivatives that facilitate deoxyribonucleic acid (DNA) cross-linking, thereby promoting apoptosis predominantly in rapidly dividing malignant cells. Chemically akin to busulfan, treosulfan provides a more consistent pharmacokinetic profile and exhibits decreased toxicity to select organs.[98,99] The FDA has authorized the use of treosulfan-marketed under the names Grafapex and Trecondi-in conjunction with fludarabine as a preparative treatment for allogeneic HSCT in both adult and pediatric populations aged one month and older suffering from AML or MDS. Evidence

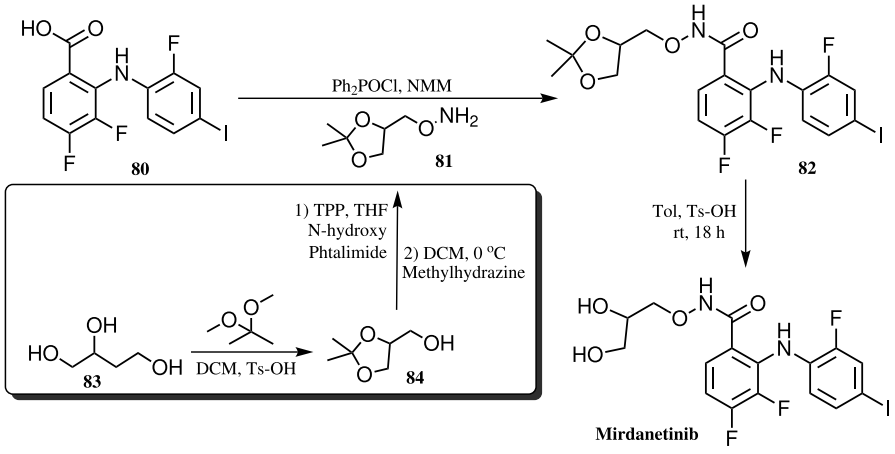

Scheme 13. Concise synthesis of mirdanetinib.

suggests that this regimen results in lower incidences of relapse-related mortality as well as reduced rates of chronic graft-*versus*-host disease (GVHD) when contrasted with busulfan-based alternatives. The drug is administered via intravenous infusion.[100,101]

A representative synthesis of treosulfan (Scheme 14) proceeds from dimethyl L-tartrate (**85**) through formation of a protected dioxolane framework and subsequent functional group interconversions. Under *p*-TsOH catalysis in toluene at 110 °C, condensation with *p*-anisaldehyde dimethylacetal (**86**) furnishes dimethyl 2-phenyl-1,3-dioxolane-4(*R*),5(*R*)-dicarboxylate (**87**) in 92% yield after 2 h. The diester **87** is then reduced using $NaBH_4/I_2$ in THF/H_2O to provide the corresponding diol, [5(*S*)-(hydroxymethyl)-2-phenyl-4(S)-dioxolanyl] methanol (**88**), in 84% yield. Conversion of **88** to the activated leaving-group derivative is achieved by bis-sulfonylation with methanesulfonyl chloride in the presence of pyridine in DCM, affording disulfonate **89**. Final ketal hydrolysis under acidic conditions (aqueous HCl in MeOH) releases the target treosulfan in 68% yield.[102]

The synthetic evolution of treosulfan highlights a classical approach to converting chiral pool precursors into functionalized alkylating agents. The sequence outlined above follows an efficient protection-functionalization-deprotection logic, where a global yield of 41% is achieved on the basis of the reported isolated yields, leaving room for further optimization, particularly in the final two steps. Starting from dimethyl L-tartrate, the preparative sequence is anchored by a high-yielding acetalization (92%) and a subsequent reduction using the $NaBH_4/I_2$ protocol-a system that, while effective, necessitates careful management of molecular iodine's corrosive properties on an industrial scale. The qualitative sustainability of the route is further influenced by the requirement for stoichiometric bis-sulfonylation and a concluding ketal deprotection. This final hydrolysis step (68% yield) serves as the primary efficiency constraint, suggesting that while the route is chemically straightforward, its overall atom economy and mass intensity remain tied to traditional protection-deprotection strategies and the generation of significant sulfonate-related byproducts.

2.1.11. Avutometinib/defacitinib

Avmapki Fakzynja is a combined prescription medication consisting of two kinase inhibitors: avutometinib (Avmapki) and defactinib (Fakzynja). In 2025, the FDA granted accelerated approval for this therapy to treat adult patients with recurrent low-grade serous ovarian cancer (LGSOC) characterized by KRAS mutations, following previous systemic treatments. The continuation of regulatory approval is contingent upon results from ongoing confirmatory trials demonstrating tangible clinical benefits.[103,104] This medication specifically targets certain tumor mutations such as G12D, G12V, among others identified in responsive case.[105] Avutometinib functions by inhibiting MEK1, thereby disrupting Rapidly Accelerated Fibrosarcoma kinase (RAF)/ Mitogen-Activated Protein Kinase Kinase (MEK) complexes and consequently impeding MAPK pathway signaling that promotes tumor growth.[106,107] Conversely, defactinib acts on auxiliary pathways to intensify the blockade against cancer cell survival and proliferation.[108-110]

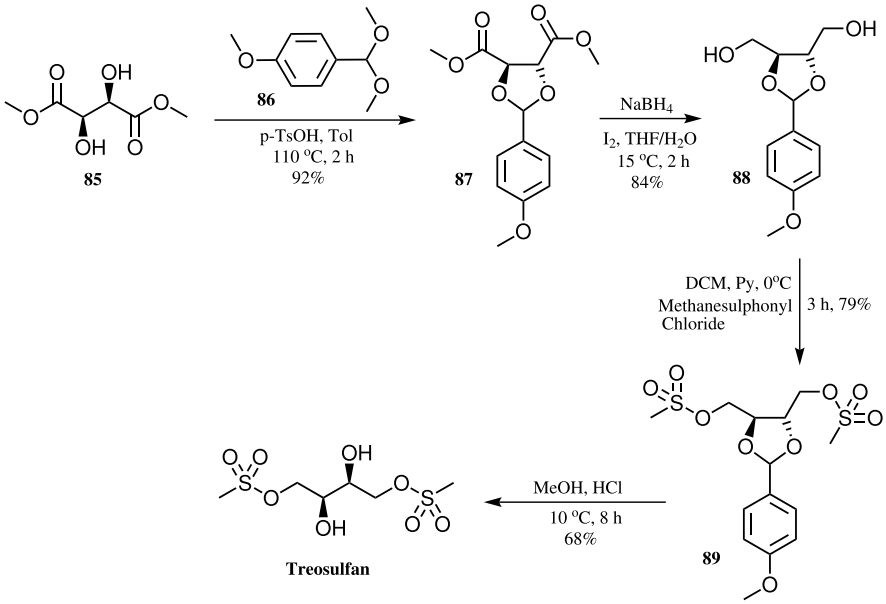

Scheme 14. Four step synthesis of treosulfan.

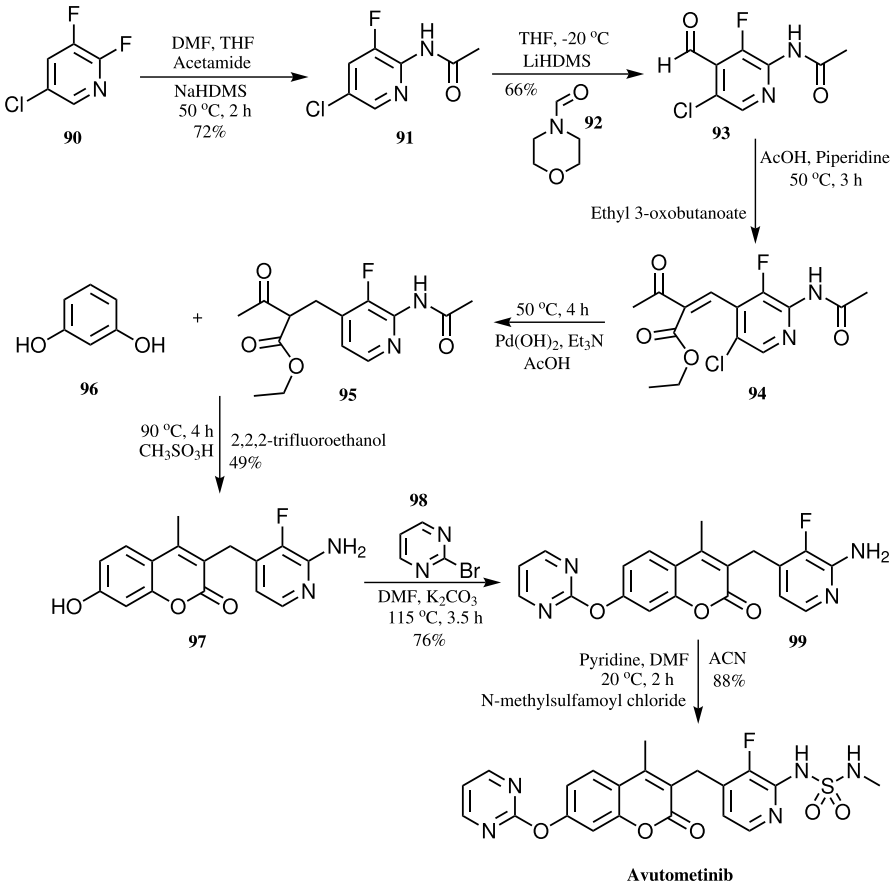

Scheme 15. Avutomectinib synthesis.

A disclosed route to avutometinib (Scheme 15) proceeds through stepwise functionalization of a difluorochloropyridine, construction of a chromenone core, and late-stage *O*-arylation followed by sulfamoylation. Thus, 5-chloro-2,3-difluoropyridine (**90**) is converted to the corresponding amide via condensation with acetamide under sodium hexamethyldisilazide (NaHMDS) in DMF/THF (50 °C, 2 h) to give *N*-(5-chloro-3-fluoropyridin-2-yl)acetamide (**91**, 72%). Directed formylation using *N*-formylmorpholine (**92**) with LiHMDS in THF furnishes *N*-(5-chloro-3-fluoro-4-formylpyridin-2-yl)acetamide (**93**) in 66% yield. Knoevenagel-type condensation of **93** with ethyl 3-oxobutanoate under piperidine/AcOH catalysis (50 °C) provides the corresponding alkylidene 3-oxobutanoate intermediate **94**. Subsequent reductive transformation with formic acid over $Pd(OH)_2$/C delivers ethyl 2-[2-acetamido-3-fluoropyridin-4-ylmethyl]-3-oxobutyrate (**95**). Treatment of **95** with resorcinol (**96**) under strongly acidic conditions (MsOH, 2,2,2-trifluoroethanol, 90 °C) effects chromenone formation concomitant with *N*-deprotection to afford 2-chromenone mesylate (**97**, 49%). *O*-Arylation of **97** with 2-bromopyrimidine (**98**) using K_2CO_3 in DMF (115 °C, 3.5 h) furnishes the chromenyl-pyrimidinyl ether (**99**, 76%). Final installation of the methylsulfamoyl group with methylsulfamoyl chloride in the presence of pyridine (DMF/MeCN) provides avutometinib with 88% yield.[111,112]

Central to this sequence is a directed formylation and a subsequent Knoevenagel-type condensation, though the overall material throughput is primarily hampered by the 49% yield achieved during the strongly acidic chromenone cyclization. Qualitatively, the synthetic trajectory is delineated by the employment of high-energy bases (LiHMDS/NaHMDS) and the requirement for elevated thermal conditions (115 °C) in problematic solvents like DMF. Although the route effectively employs a safer reductive protocol using formic acid over palladium hydroxide, the reliance on corrosive sulfamoylating agents and the accumulation of yield losses in the mid-sequence highlight significant opportunities for streamlining the process to enhance its industrial scalability and atom economy.

In a separate sequence leading to defactinib (Scheme 16), 3-chloropyrazine-2-carbonitrile (**100**) undergoes sulfonamide substitution with *N*-methylmethanesulfonamide in the presence of Cs_2CO_3 (MeCN, 80 °C) to give *N*-(3-cyano-2-pyrazinyl)-*N*-methylmethanesulfonamide (**101**, 73%). Catalytic hydrogenation of the nitrile (H_2, Pd/C) in methanolic ammonia, followed by treatment with AcOH

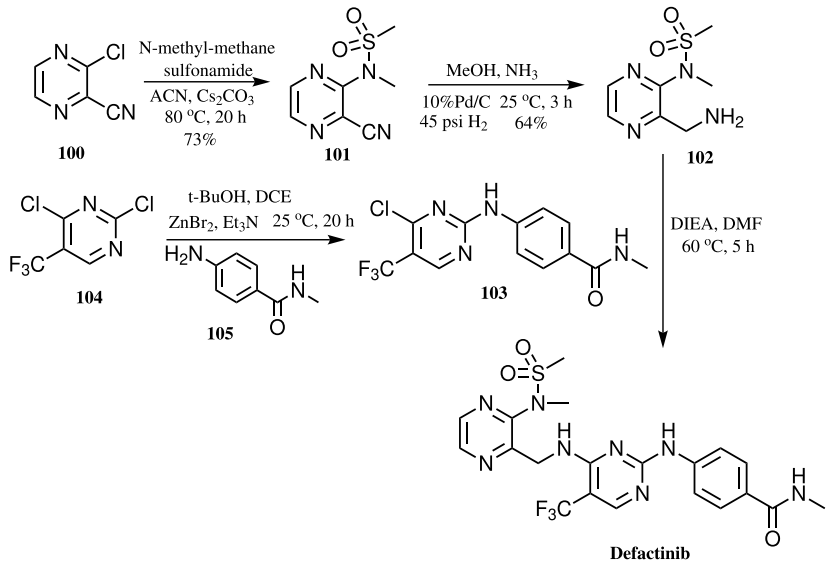

Scheme 16. Defactinib synthesis.

in EtOAc, affords the corresponding primary amine acetate salt (**102**, 64%). In parallel, 2,4-dichloro-5-(trifluoromethyl)pyrimidine (**104**) is coupled with 4-amino-*N*-methylbenzamide (**105**) in the presence of $ZnBr_2$ and Et_3N (1,2-dichloroethane (DCE)/t-BuOH) to furnish the aryl amine intermediate **103**. Subsequent substitution of the remaining chloropyrimidine with aminomethylpyrazine **102** (DIPEA, DMF, 60 °C) then delivers defactinib.[113]

On the other hand, defactinib utilizes a modular assembly that independently elaborates pyrazine and pyrimidine building blocks before their late-stage unification. A notable feature of this sequence is the Lewis-acid mediated coupling of fragment **104** using $ZnBr_2$, a strategy that enables regioselective functionalization but introduces metal-related mass intensity. Qualitatively, the process is delineated by the employment of problematic solvents such as DCE and DMF, alongside the requirement for catalytic hydrogenation to access the aminomethylpyrazine partner. Although the initial stages exhibit moderate efficiency (64-73% yields), the absence of disclosed yields for the final coupling phase limits a comprehensive evaluation of the global yield of the route and industrial throughput. This lack of transparency highlights a recurring challenge in benchmarking the scalability of complex heterocycles from early-stage patent disclosures.

2.2. Cardiovascular

2.2.1. Aficamten

Aficamten is a selective inhibitor of cardiac myosin employed in the management of symptomatic obstructive hypertrophic cardiomyopathy (oHCM) in adult patients.[114-117] It interacts with the motor domain of cardiac myosin, promoting stabilization of a conformational state characterized by weak actin binding, thereby diminishing exaggerated myocardial contractility. This mechanism leads to improved hemodynamics and alleviation of clinical symptoms such as dyspnea.[118,119] The FDA granted approval for aficamten, marketed under the name Myqorzo, in December 2025 for adult individuals with symptomatic oHCM aimed at enhancing their functional capacity.[120] Clinical evidence indicates that aficamten effectively reduces obstruction within the left ventricular outflow tract and demonstrates superior performance compared to metoprolol in enhancing peak oxygen consumption among patients with ongoing symptoms.[121-123]

A patent route to aficamten (Scheme 17) starts from 1-(*R*)-amino-5-bromoindane hydrochloride (**106**), which is first converted to the corresponding Boc-protected intermediate by treatment with Boc_2O and Et_3N in DCM, affording **107** in 92% yield. The aryl bromide **107** is then transformed into 1(*R*)-*N*-Boc-aminoindane-5-carbonitrile **108** via a Pd-catalyzed cyanation using $K_4Fe(CN)_6{\cdot}3H_2O$ (XPhos-Pd-G2/XPhos, KOAc) in dioxane/H_2O at 100 °C. Conversion of nitrile **108** to the corresponding amidoxime is achieved by reaction with hydroxylamine hydrochloride, providing 1(*R*)-*N*-Boc-amino-*N*-hydroxyindane-5-carboximidamide (**109**), which serves as the immediate precursor to the oxadiazole intermediate **110**. Subsequent Boc deprotection with TFA in DCM furnishes the free amine **111**, and final amide bond formation with 1-methylpyrazole-4-carboxylic acid under EDC/HOAt/DIEA conditions in DMF delivers aficamten in 88% yield.[124,125]

The strategy presented here leverages a robust functionalization of a chiral indane core, anchored by a

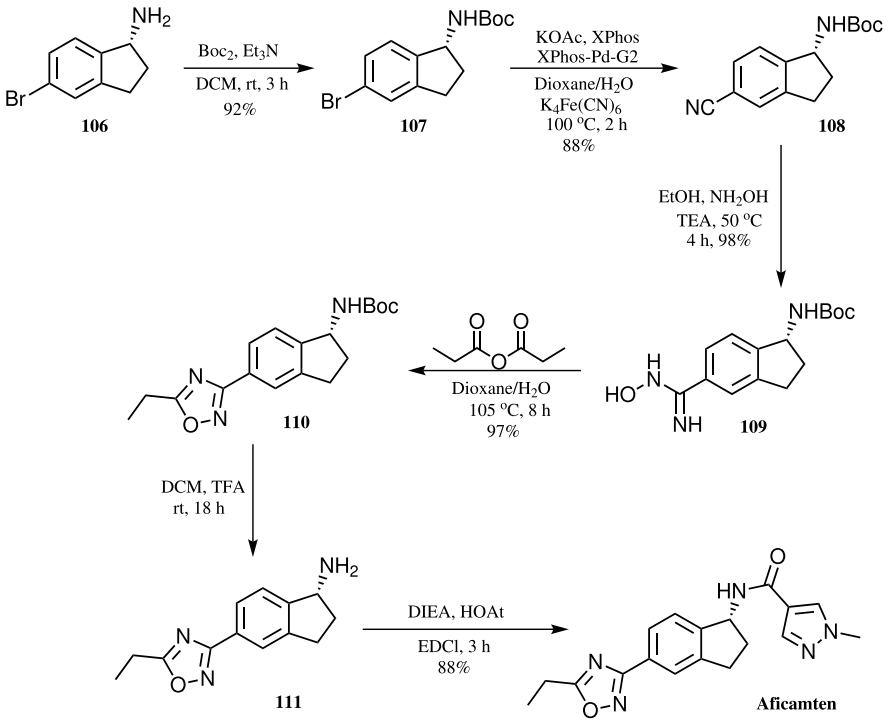

Scheme 17. Original route to aficamten.

high-yielding Boc-protection (92%) and a final amide coupling reaching 88% efficiency. A key strategic element is the employment of a surrogate-based Pd-catalyzed cyanation using potassium ferrocyanide, which significantly mitigates the safety risks associated with traditional cyanide salts. Qualitatively, however, the route is characterized by a reliance on halogenated solvents (DCM) and problematic high-boiling media such as dioxane and DMF. Furthermore, the requirement for a protection-deprotection sequence and the use of specialized coupling additives like HOAt highlight typical medicinal chemistry trade-offs where high step-wise yields are prioritized over total atom economy. While the disclosed steps demonstrate a chemically robust trajectory, the absolute material throughput remains sensitive to the undisclosed efficiencies of the intermediate oxadiazole cyclization.

2.2.2. Etripamil

Etripamil is a pharmaceutical agent classified as a calcium channel antagonist that received approval from the FDA in December 2025 for the management of acute episodes of paroxysmal supraventricular tachycardia (PSVT) in adult patients. Marketed under the name Cardamyst as a nasal spray, this medication facilitates patient self-administration, enabling prompt conversion of PSVT episodes to normal sinus rhythm outside clinical environments.[126,127] The drug specifically targets symptomatic PSVT by inhibiting L-type calcium channels within atrioventricular (AV) nodal cells, thereby disrupting reentrant conduction pathways. Data from clinical investigations such as the Randomized Phase II study (RAPID) trial demonstrated that individuals utilizing etripamil were twice as likely to achieve faster normalization of sinus rhythm compared to placebo controls. If symptoms persist, a second dose may be administered after an interval of 10-15 min from the initial dose.[128-132] In addition to its application for PSVT, etripamil is currently undergoing Phase 3 clinical trials for atrial fibrillation characterized by rapid ventricular response and Phase 2 trials for pediatric PSVT cases. The medication presents an alternative treatment modality to intravenous agents such as adenosine and has the potential to decrease hospital admissions.[133]

A disclosed route to etripamil proceeds through sequential functional-group interconversions on a substituted benzylic scaffold (Scheme 18). Thus, methyl 3-(bromomethyl)benzoate (**112**) undergoes cyanide displacement with KCN in refluxing MeOH to afford methyl 3-(cyanomethyl)benzoate (**113**). Chemoselective reduction of the nitrile in the presence of TFA using $NaBH_4$ in THF then provides methyl 3-(2-aminoethyl) benzoate (**114**). Protection of the resulting amine with Boc_2O in THF furnishes carbamate **115**, which is subsequently *N*-methylated (dimethyl sulfate, NaHMDS, THF) to give the tertiary Boc-protected derivative **116**. Removal of the Boc group with TFA in DCM yields the corresponding secondary amine **117**, which is finally

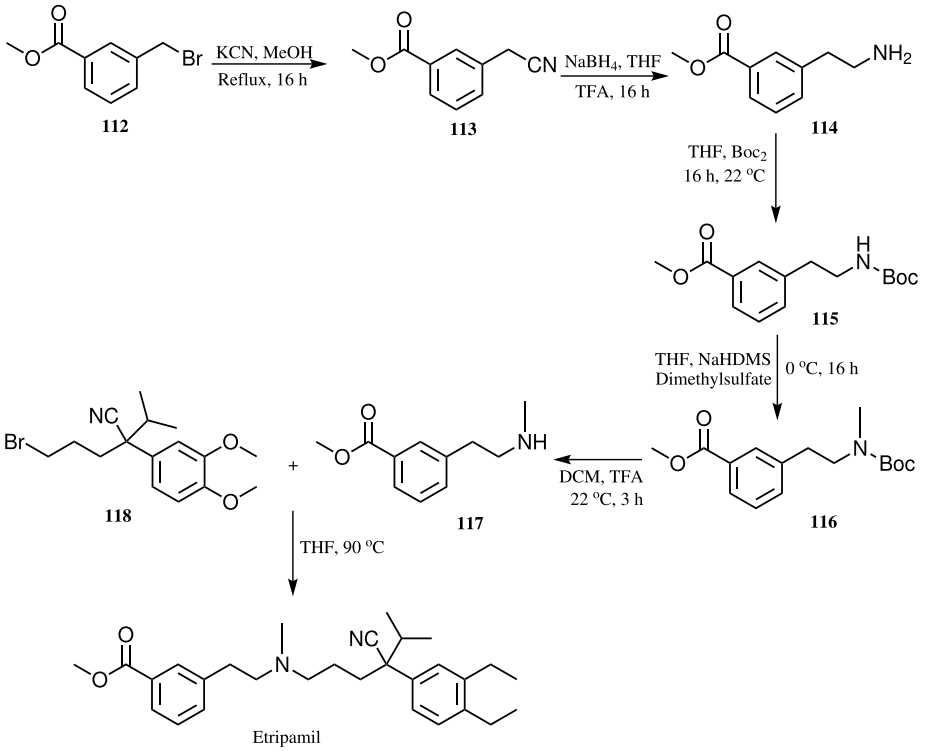

Scheme 18. Etripamil original synthesis.

N-alkylated with 5-bromo-2-(3,4-dimethoxyphenyl)-2-(propan-2-yl)pentanenitrile (**118**) in THF at 90 °C to deliver etripamil.[134,135]

The preparation of etripamil is marked by significant transparency constraints and operational risks. The synthetic assembly relies on highly hazardous reagents, including potassium cyanide and the mutagenic alkylating agent dimethyl sulfate, both of which introduce substantial safety liabilities into the manufacturing paradigm. Furthermore, the process is currently limited to the production of a racemate, with no disclosed methodology for asymmetric induction or chiral resolution-a critical gap for a modern pharmaceutical candidate. In the absence of reported isolated yields, it is impossible to evaluate the route's mass intensity or cumulative efficiency. Consequently, this itinerary likely represents a preliminary discovery-scale approach that requires extensive process intensification, specifically targeting the replacement of high-risk reagents and the implementation of a stereoselective endgame to be industrially viable.

2.2.3.Sebaltralstat

Sebetralstat is an oral agent that functions as a plasma kallikrein inhibitor, indicated for the management of acute hereditary angioedema (HAE) attacks in individuals aged 12 years and older, including adults. Marketed under the trade name Ekterly by KalVista Pharmaceuticals, it received its initial approval in the United States in July 2025 and subsequently in the European Union in September 2025.[136-138] Its mechanism of action involves the competitive and reversible inhibition of plasma kallikrein, a serine protease responsible for cleaving high-molecular-weight kininogen to generate bradykinin. By decreasing bradykinin levels, sebetralstat effectively mitigates increased vascular permeability and edema associated with HAE episodes and interrupts positive feedback within the kallikrein-kinin system. This medication offers an on-demand treatment option for acute HAE attacks via oral administration, providing a convenient alternative to injectable therapies.[139,140] Phase 3 clinical trials such as KONFIDENT reported faster symptom resolution and decreased attack severity relative to placebo. After oral dosing, sebetralstat achieves peak plasma concentration approximately one hour post-administration and exhibits 77% protein binding.[141,142]

Sebetralstat was prepared via a concise (Scheme 19), modular sequence in which 4-(chloromethyl)benzyl alcohol (**119**) is first converted to the *N*-benzylpyridone alcohol **120** by alkylation of 2-hydroxypyridine (K_2CO_3, acetone, 50 °C) in 78% yield. The benzylic alcohol is then activated (via mesylation) to the corresponding chloride **121** (93%), followed by *N*-alkylation with methyl 3-(methoxymethyl)-1*H*-pyrazole-4-carboxylate (**122**) to furnish the key pyrazole ester intermediate **123**

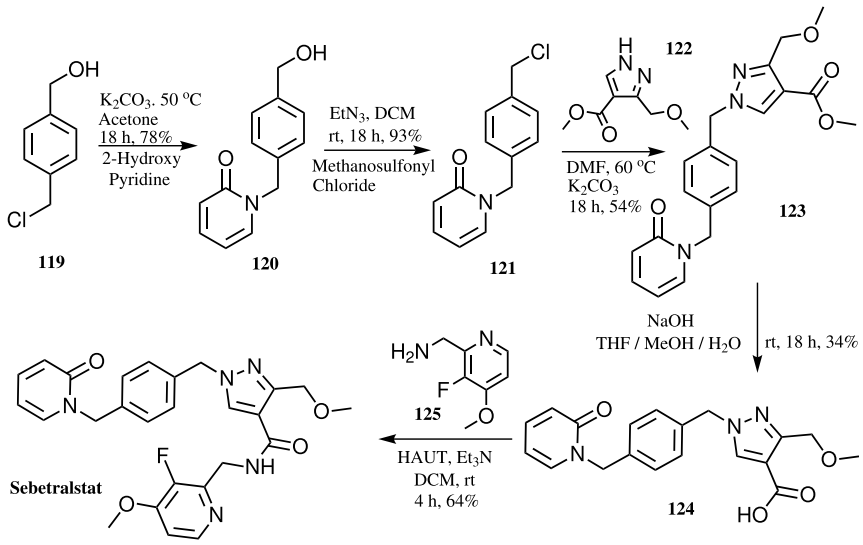

Scheme 19. Synthesis of sebetralstat.

(54%). Saponification to the acid **124** (34%), and final 1-[bis(dimethylamino)methylene]-1*H*-1,2,3-triazolo[4,5-b] pyridinium 3-oxid hexafluorophosphate (HAUT)-mediated amidation with C-(3-fluoro-4-methoxypyridin-2-yl) methylamine (**125**) delivers sebetralstat in 64% yield.[143]

The preparative itinerary for sebetralstat is designed as a modular five-step sequence, yet its industrial potential is currently constrained by a restrained global yield of ca. 7.4%. Although the initial construction of the *N*-benzylpyridone core proceeds with reasonable efficiency, the route faces substantial material attrition during the regioselective installation of the pyrazole ester **123** (54% yield) and a subsequent, highly inefficient saponification/isolation phase (34% yield). From a sustainability perspective, the reliance on high-mass coupling reagents like HATU for the final amidation further limits the atom economy of the endgame. These findings suggest that while the modular nature of the synthesis allows for rapid scaffold assembly, significant process intensification-specifically regarding regiochemical control and late-stage purification-is required to mitigate the environmental footprint and improve the cumulative throughput of this clinical candidate.

2.3. Genetic and rare diseases

2.3.1. Doxecitine and doxribtimine

Doxecitine and doxribtimine (Kygevvi, dC and dT), developed by UCB, represents the first-in-class substrate replacement therapy approved by the FDA in November 2025[144] for Thymidine Kinase 2 deficiency (TK2d), an ultra-rare autosomal recessive mitochondrial DNA (mtDNA) depletion syndrome due to mutations in the nuclear TK2 gene, which severely impairs the mitochondrial salvage pathway for pyrimidine nucleosides, leading to insufficient deoxynucleotide pools (dTTP and dCTP) and subsequent failure of mtDNA replication.[145-147] Kygevvi's represents a valuable example of a new combination drug which containing two previously disclosed, classical pyrimidine nucleosides, deoxycytidine (dC) and deoxythymidine (dT), whose clinical efficacy was established by clinical trials and retrospective natural history comparisons involving 82 patients with symptom onset started at 12 years-old or younger.[148-150] Kygevvi demonstrated a profound survival benefit, with an approximately 86% reduction in the risk of mortality compared to untreated historical controls.[151,152] Its mechanism of action is to provide dC and dT, which are phosphorylated by cytosolic enzymes and transported into the mitochondria, effectively bypassing the enzymatic defect and avoiding failure of mtDNA replication.[153,154] Since this small molecules have already their synthesis disclosed many years ago we are not going to discuss the process in this review.

2.3.2. Elamipretide

Elamipretide (Forzinity), first therapy indicated to improve muscle strength in adult and pediatric patients with Barth syndrome, an ultra-rare and life-limiting X-linked genetic disorder. Developed by Stealth BioTherapeutics[155] and approved by FDA in September 2025,[156] this tetrapeptide targets pathogenic variants in the TAZ gene, which lead to a deficiency in mature cardiolipin, a critical phospholipid located in the inner mitochondrial membrane (IMM). This deficiency results in severe mitochondrial dysfunction, clinically manifesting as cardiomyopathy, skeletal myopathy, cyclic neutropenia, and growth delay.[157-159]

Clinical evidence supporting its accelerated approval demonstrated a measurable improvement in knee extensor muscle strength, an intermediate clinical endpoint. Patients who received elamipretide showed significant gains in functional assessments like the 6-Minute Walk Test (6MWT) and improvements in cardiac remodeling over long-term extension studies.[160-162] Its mechanism of action centers on its ability to selectively bind to cardiolipin in the inner mitochondrial membrane, stabilizing the mitochondrial cristae structure and modulates membrane electrostatic potentials, ultimately enhancing the efficiency of the electron transport system, simultaneously increasing ATP production and reducing the generation of damaging reactive oxygen species (ROS), counteracting the lipid abnormalities seen in Barth syndrome.[162-164]

Selective *O*-benzyl protection of N-Boc-DMT-OH (Scheme 20, **126**), followed by Boc removal with HCl in DCM, afforded DMT-OBn·HCl (**127**) in 90% yield over the two-step sequence. Subsequent coupling with Boc-D-Arg-OH·HCl (**128**) using T3P/DIEA in DMF furnished Boc-D-Arg-DMT-OBn (**129**) in 90% yield. Debenzylation by hydrogenation over Pd/C in MeOH provided Boc-D-Arg-DMT-OH (**130**), which, upon coupling with Lys(Boc)-Phe-$CONH_2$ (**131**) under T3P/DIEA conditions in DMF, delivered the Boc-protected elamipretide (**132**) in only 22% yield. This low-yielding step is clearly the bottleneck of the route and has a strong negative impact on the overall efficiency: with an overall yield from **126** to elamipretide limited to ca. 13%. Final deprotection with AcCl in i-PrOH then provided elamipretide in 88% yield.[165,166]

The synthetic design for elamipretide utilizes a liquid-phase assembly strategy anchored by T3P-mediated couplings, though it is marked by a substantial efficiency drain during the fragment condensation phase. Specifically, the union of the dipeptide fragments to form intermediate **132** proceeds in only 22% yield, serving as the primary bottleneck that restricts the global yield to ca. 13%. Qualitatively, the route benefits from a clean Pd/C-catalyzed debenzylation, yet the heavy reliance on DMF and the requirement for acidic Boc-cleavage in DCM underscore the persistent challenges of solvent intensity in peptide synthesis. This sequence illustrates the typical trade-offs in liquid-phase methods, where the advantages of

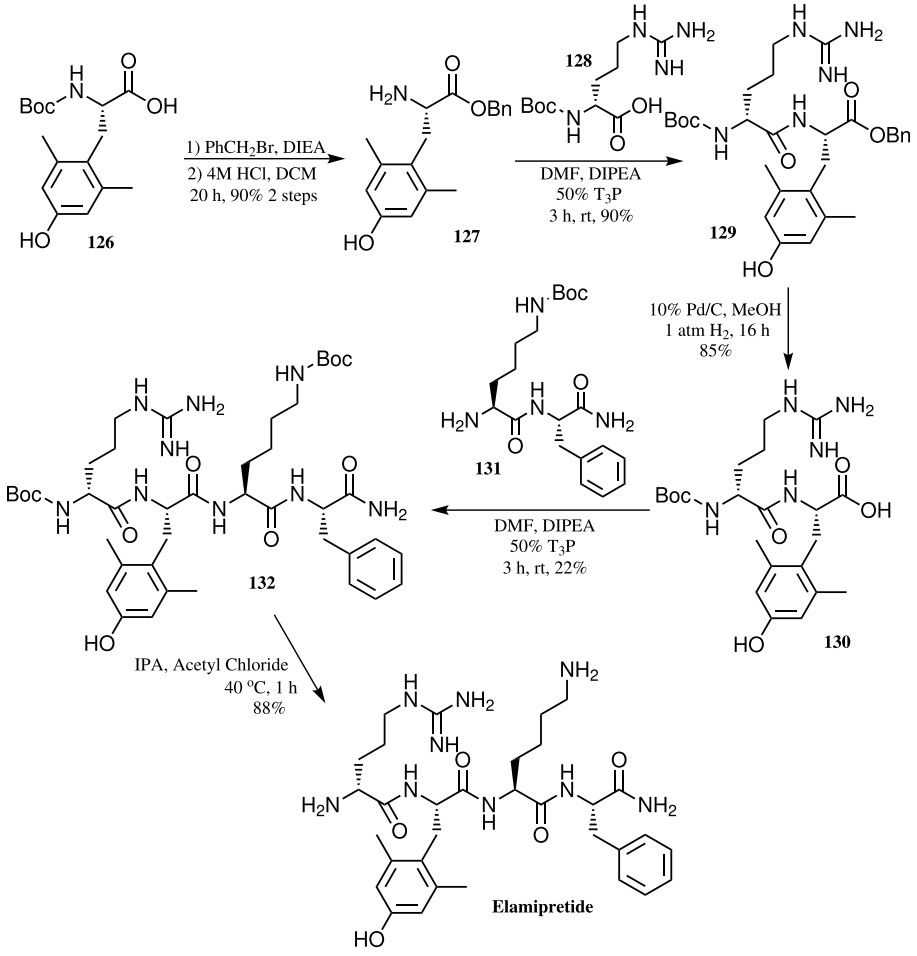

Scheme 20. Sequential peptide couplings to elamipretide synthesis.

fragment-based assembly are offset by the low yields often encountered during the coupling of sterically demanding or poorly soluble peptide segments.

2.3.3. Sepiapterin

Sepiapterin (Sephience), developed by PTC Therapeutics, is regarded as a pharmacological advancement in the treatment of hyperphenylalaninemia (HPA), having received European Medicines Agency (EMA) and FDA approval in June 2025 and July 2025, respectively, as a breakthrough therapy for adult and pediatric patients from one month of age diagnosed with phenylketonuria (PKU).[167,168] Sephience was granted to orphan drug designation for both agencies, as PKU is a critical unmet medical condition, being able of addressing a broader range of disease phenotypes, including those who do not respond adequately to sapropterin, current therapy standard.[169,170] In the APHENITY Phase 3 trial, drug achieved robust results, with a mean reduction of 63% in blood phenylalanine (Phe) levels after six weeks of treatment, compared to a negligible 1% reduction in the placebo group. Notably, 84% of participants achieved therapeutic Phe targets and, surprisingly, 97% of patients were able to significantly increase protein intake, while maintaining metabolic control.[170-172] Its mechanism of action is distinct from previous therapies as it serves as a natural precursor to tetrahydrobiopterin, the essential cofactor for the enzyme phenylalanine hydroxylase (PAH). Unlike direct supplementation, sepiapterin is a more stable molecule that crosses cellular membranes and the blood-brain barrier with higher efficiency. Once inside the cell, it is converted into tetrahydrobiopterin by sepiapterin reductase through an intracellular salvage pathway. This restores cofactor levels and stabilizes misfolded PAH enzyme variants, thereby enhancing catalytic activity and facilitating the conversion of Phe into tyrosine.[173-176]

The patent route published to sepiapterin (Scheme 21) starts from the condensation reaction between (2*R*,3*S*)-epoxy-4*S*-methoxymethoxypentanal (**133**) and 2,5,6-triamino-4-cyclohexyloxypyrimidine (**134**) using acetonitrile (ACN) as solvent. After, iodine and hydrogen peroxide were added to this reaction to oxidize the intermediate **135**, affording the pteridine (**136**) in 62% yield. Oxidation of the hydroxyl moiety of **136** to carbonyl was achieve using tetrapropylammonium perruthenate and 4-methylmorpholine *N*-oxide (NMMO). Compound **137** was then deprotected with HCl acidified methanolic solution furnishing the product **138** in 94% yield. The last step involves the selective hydrogenation of **138** with catalytic palladium, yielding sepiapterin in 59% yield.[177]

The linear functionalization of sepiapterin is anchored by a strategic condensation-oxidation sequence that constructs the pteridine core in 62% yield. This pivotal transformation is facilitated by an oxidative protocol that presents distinct industrial challenges regarding reagent toxicity and equipment corrosion. The route further incorporates a catalytic TPAP/NMMO oxidation to install the necessary carbonyl functionality, reflecting a robust but reagent-intensive methodology typical of complex heterocyclic assembly. While the acidic deprotection of the MOM ether is highly efficient (94%), the end-to-end material throughput is restricted by the selective catalytic hydrogenation endgame, which delivers the final product in 59% yield. Consequently, the current synthetic campaign is delineated by its reliance on multiple redox manipulations and noble metal catalysis, highlighting clear opportunities for optimization in atom economy and solvent sustainability.

2.4. Infectious diseases

2.4.1. Zoliflodacin

Zoliflodacin (Nuzolvence), developed through a public-private partnership between Innoviva Specialty Therapeutics (previsouly Entasis Therapeutics) and the Global Antibiotic Research & Development Partnership (GARDP), received U.S. FDA approval in late 2025.[178-181] It is a breakthrough antimicrobial therapy towards multidrug-resistant *Neisseria gonorrhoeae*, a designated as a pathogen of concern by World Health Organization (WHO) and Centers for Disease Control and Prevention (CDC).[178] The clinical efficacy was established through a rigorous developmental program, including a pivotal Phase 3 that compared a single oral dose of zoliflodacin *versus* the combination of intramuscular ceftriaxone and oral azithromycin, with cure rates of over 90%.[182,183] It is indicated as a single-dose oral treatment for uncomplicated urogenital gonorrhea in adults and adolescents, as oral alternative to injectable ceftriaxone.[184-186] As the first member of the spiropyrimidinetrione class, its mechanism of action is distinct from existing antibiotics, targeting bacterial Type II topoisomerases (DNA gyrase and topoisomerase IV) in a novel manner. Unlike fluoroquinolones, which bind to the enzyme-DNA complex at sites prone to resistance-conferring mutations, zoliflodacin binds to a conserved pocket within the DNA gyrase B (GyrB) subunit, stabilizing a pre-translocational cleavage complex, effectively arresting bacterial DNA synthesis and, ultimately leading to bacterial cell death.[187] Additionally, zoliflodacin's mechanism of action avoids cross-resistance with quinolones, macrolides, and cephalosporins, ensuring its potency against highly resistant strains.

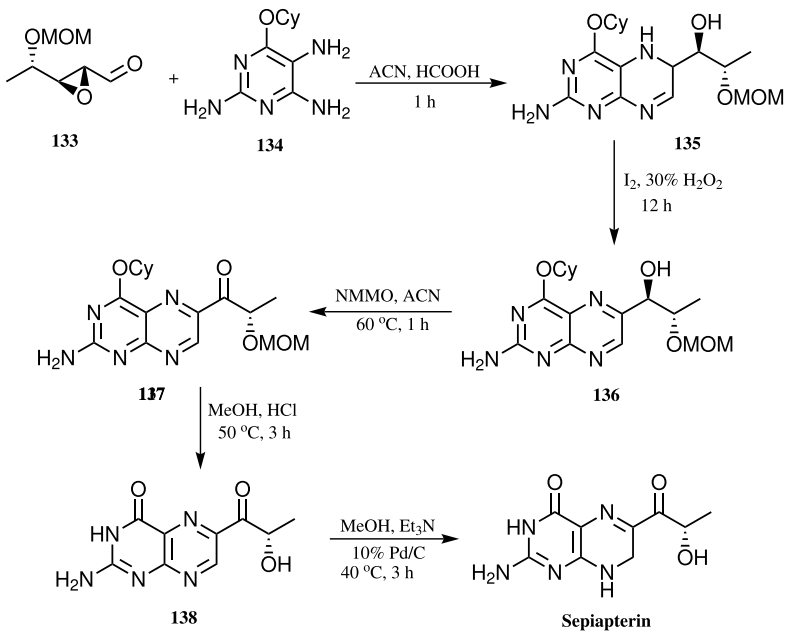

Scheme 21. Sepiapterin short synthesis.

Methyl 3,4-difluoro-2-hydroxybenzoate (**139**) was converted to the corresponding hydroxamic acid 3,4-difluoro-*N*,2-dihydroxybenzamide (**140**) by treatment with hydroxylamine in MeOH under basic conditions (Scheme 22, 94%). Cyclization of **140** with CDI in refluxing THF (2 h) delivered 6,7-difluoro-1,2-benzisoxazol-3-one (**141**), which was chlorodehydrated with $POCl_3/Et_3N$ under microwave heating (140 °C) to give 3-chloro-6,7-difluoro-1,2-benzisoxazole (**142**, 62%). Regioselective lithiation of **142** with BuLi in the presence of TMP in THF, followed by trapping with DMF, furnished the aldehyde 3-chloro-6,7-difluoro-1,2-benzisoxazole-5-carbaldehyde (**143**, 76%). Subsequent condensation of **143** with 2(*R*),6(*R*)-dimethylmorpholine (**144**) using diisopropylamine (DIPA) in ACN at 85 °C afforded the corresponding morpholine-substituted benzisoxazole intermediate **145**. The aldehyde of **145** was then protected as the ethylene glycol acetal (*p*-TsOH, toluene, reflux) to provide dioxolane **146**, which underwent condensation with 4(*S*)-methyloxazolidin-2-one (**147**) in DMF at 80 °C to yield 3-(oxazolidin-3-yl)-1,2-benzisoxazole derivative (**148**). Finally, cyclocondensation of **148** with barbituric acid (**149**) in AcOH at 110 °C, followed by separation of the resulting diastereomers by supercritical fluid chromatography (SFC), afforded zoliflodacin.[188]

The chemical itinerary toward zoliflodacin leverages a multi-component assembly of a benzisoxazole core, but is delineated by high-energy operations and significant transparency gaps in its endgame. Notable technical flags include the use of microwave-assisted chlorodehydration at 140 °C and a regioselective lithiation sequence requiring hazardous organolithium reagents. While the initial functionalization of the hydroxamic acid precursor is highly efficient (94%), the cumulative throughput is obscured by the lack of disclosed yields for the final barbituric acid cyclization and the subsequent SFC resolution. The requirement for diastereomeric separation via chromatography underscores a critical opportunity for process intensification, as achieving a stereoselective assembly would significantly reduce the energy footprint and mass intensity currently associated with the final purification of this novel antibiotic candidate.

2.4.2. Gepotidacin

Gepotidacin (Blujepa), is a first-in-class antibiotic developed by GSK to address the critical global challenge of antimicrobial resistance, representing the first new oral antibiotic class for urinary tract infections (UTI) in nearly three decades. In March 2025, the FDA granted initial approval for gepotidacin as an oral treatment for female adult and pediatric patients (12 years and older) with uncomplicated UTI.[189-191] Its clinical development was supported by robust Phase III clinical trials, where a dosage regimen of 1,500 mg twice a day (b. i. d.) *per* 5 days proved to be similar to reference drug nitrofurantoin in patients with UTI. Gepotidacin has also shown positive outcomes in Phase III trials for uncomplicated urogenital gonorrhea, showing non-inferiority to reference treatment (ceftriaxone plus azithromycin). This diverse clinical profile positions gepotidacin as an alternative against prevalent Gram-negative and Gram-positive uropathogens, including *Escherichia coli* and *Staphylococcus saprophyticus*.[192-195] As the first

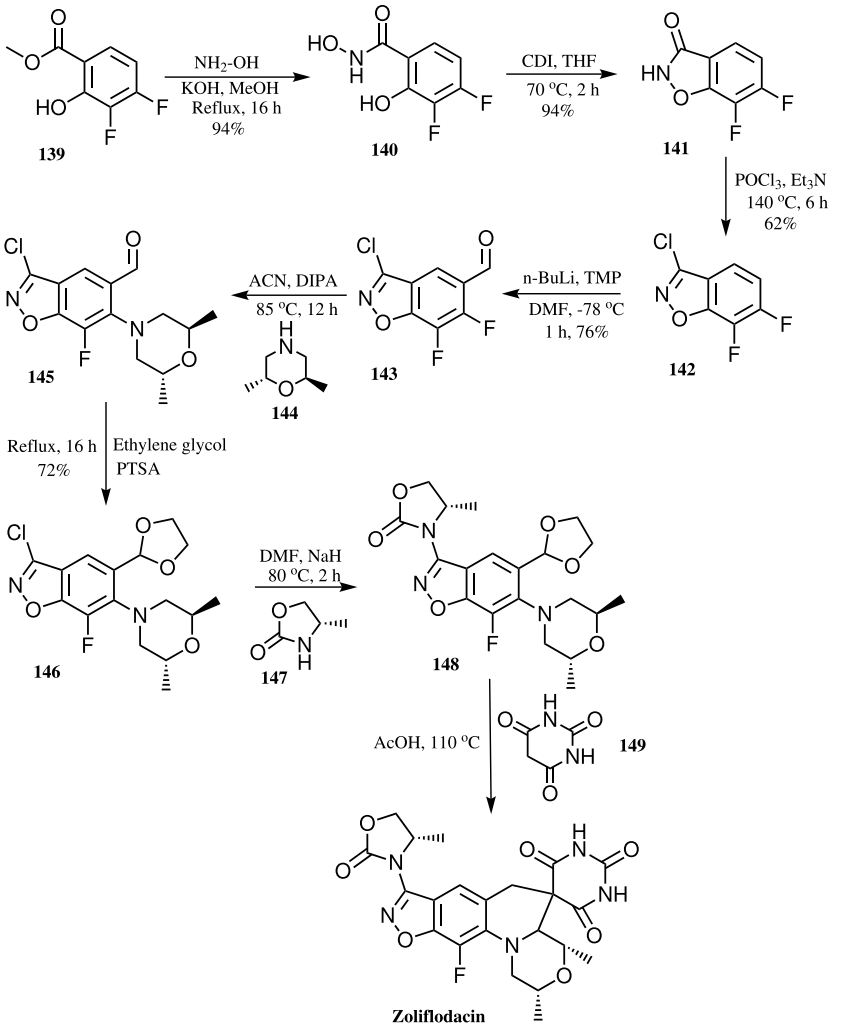

Scheme 22. Patented route to zoliflodacin.

member of the triazaacenaphthylene class, it was specifically engineered to overcome existing resistance mechanisms that have rendered traditional therapies less effective. Its mechanism of action is distinct from that of existing antibiotics, such as fluoroquinolones, acting as a bacterial type II topoisomerase inhibitor by selectively interacting with the GyrA subunit of DNA gyrase and the ParC subunit of topoisomerase IV.[196] Unlike fluoroquinolones, which require two drug molecules to bind at the DNA cleavage site, a single gepotidacin molecule achieves a well-balanced, dual-targeting, by binding at a unique site between the two scissile DNA bonds. This novel binding motif requires concurrent mutations in both enzymes for resistance to develop, resulting in a low propensity for target-mediated resistance and allowing it to remain effective against pathogens already resistant to older antibiotic classes.[197-200]

The synthesis of gepotidacin from 2-chloro-6-methoxy-3-nitropyridine (**150**), as disclosed in the patent, proceeds through *N*-alkylation, diol protection, nitro reduction, *N*-alkylation with ethyl bromoacetate, cyclization/oxidation, acetal deprotection, intramolecular ring closure, coupling with a Boc-protected aminopiperidine, *N*-deprotection followed by chiral resolution, and a final reductive amination (Scheme 23).[201]

Condensation of **150** with 2-aminopropane-1,3-diol (**151**) in refluxing EtOH affords 2-(6-methoxy-3-nitropyridin-2-ylamino)propane-1,3-diol (**152**). The diol is protected as the corresponding acetonide **153** using 2,2-dimethoxypropane and *p*-TsOH. Catalytic hydrogenation (H_2, Pd/C, MeOH) reduces the nitro group to give primary amine **154**, which is alkylated with ethyl bromoacetate (K_2CO_3) to furnish secondary amine **155**. Treatment with NaH in DMF promotes cyclization to the 1,4-dihydropyrido[2,3-*b*]pyrazine derivative **156**, and oxidation with MnO_2 in toluene provides intermediate **157**. Acidic cleavage of the acetonide (HCl, MeOH) gives diol **158**, which undergoes cyclization in the presence of MsOH and Et_3N at room temperature to form the fused tricyclic intermediate **159**.

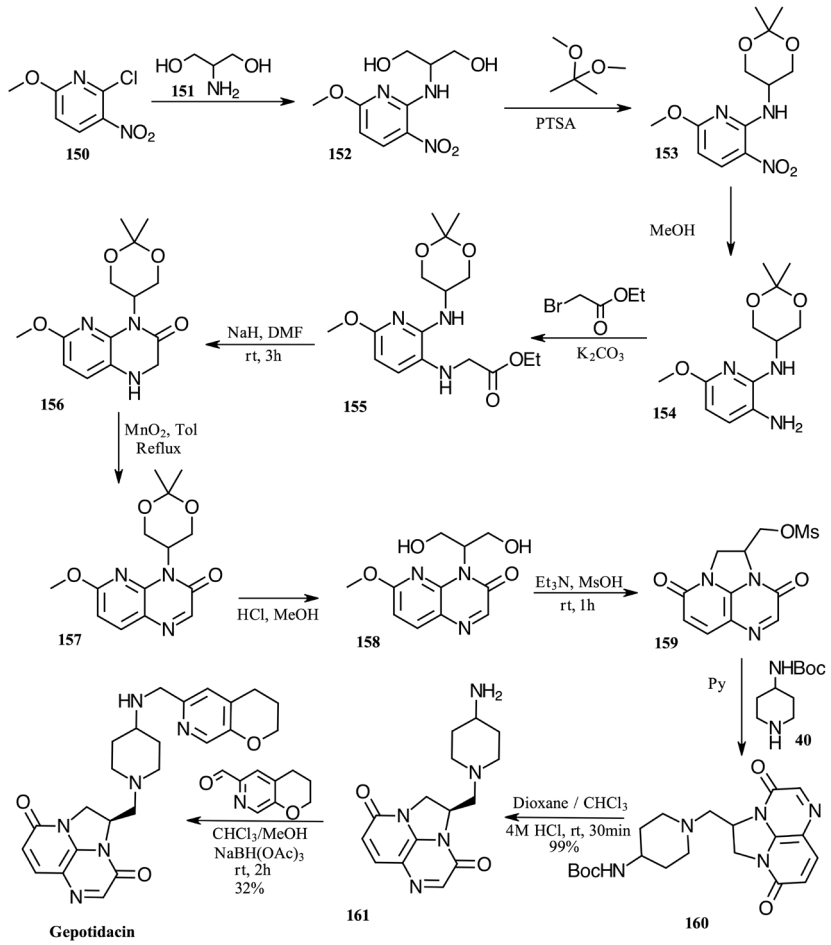

Scheme 23. Reported synthesis of gepotidacin.

Subsequent substitution/condensation with 4-*N*-Boc-aminopiperidine (**40**) in refluxing ACN with pyridine affords tertiary amine **160**. Boc deprotection with HCl in dioxane/$CHCl_3$, followed by preparative chiral HPLC of the resulting amine dihydrochloride, delivers enantioenriched intermediate **161**. Finally, reductive amination of aldehyde **162** with amine **161** using $NaBH(OAc)_{3}$[3] in $CHCl_3$/MeOH furnishes gepotidacin.[202]

Notably, the patent reports isolated yields only for the final two operations (the chiral resolution leading to **161** and the terminal reductive amination), with the last step affording gepotidacin in 32% yield; isolated yields for the earlier transformations are not disclosed, preventing a reliable calculation of the overall yield and identification of the true yield-limiting steps upstream.

The chemical approach toward gepotidacin is delineated by an intricate construction of a fused tricyclic framework, characterized by substantial operational hazards and persistent transparency gaps. The synthetic assembly involves a demanding series of redox and cyclization manipulations, relying on high-energy reagents like sodium hydride and stoichiometric MnO_2. Qualitatively, the process is further burdened by the employment of problematic halogenated solvents ($CHCl_3$) and the requirement for preparative chiral HPLC to resolve the final core intermediate-a strategy that significantly compromises the total mass intensity and throughput. With the concluding reductive amination proceeding in a restrained 32% yield, the currently disclosed route highlights the clear need for process intensification, specifically regarding the development of an enantioselective core assembly and the replacement of high-risk reagents to ensure industrial viability.

2.5. Hematology

2.5.1. Rilzabrutinib

Rilzabrutinib (Wayrilz) is a first-in-class, oral, reversible covalent inhibitor of Bruton's tyrosine kinase (BTK), developed by Sanofi and approved by FDA in August 2025, to address the unmet needs in immune thrombocytopenia (ITP) management. It is indicated to individuals who have had an insufficient response to previous treatments for chronic or persistent ITP.[203-205] Unlike traditional covalent BTK inhibitors used in oncology, which can lead to irreversible

inhibition and increased bleeding risks, rilzabrutinib was molecularly engineered for high selectivity and a reversible binding mode, allowing the drug to effectively suppress autoimmune pathways while preserving essential physiological functions, such as collagen-induced platelet aggregation, thereby maintaining a critical balance between immune modulation and hemostatic safety, representing an advancement in targeted therapy for refractory ITP patients, offering a durable and well-tolerated oral treatment option.[206-208] The therapeutic efficacy of rilzabrutinib is driven by a dual mechanism of action that targets the core pathophysiology of ITP, namely, inhibition of the B-cell receptor signaling to reduce the production of pathogenic autoantibodies and modulation of the Fcγ receptor signaling to interrupt macrophage-mediated platelet destruction in the spleen and liver.[209-211] This comprehensive approach was validated in the Phase 3 LUNA3 trial, with rilzabrutinib achieving rapid and durable platelet responses in adult patients with persistent or chronic ITP who had failed multiple prior therapies.[212-214]

Suzuki coupling of iodoarene **162** with boronic acid **163** using $PdCl_2$(1,1'-bis(diphenylphosphino) ferrocene (dppf)) and K_3PO_4 in 2-MeTHF/H_2O at 73 °C afforded the biaryl intermediate **164** (Scheme 24). Iodoarene **162** can be obtained in a two-step sequence starting from readily available amine **167**. Subsequent Boc deprotection with TMSCl in MeOH furnished the corresponding piperidine **165** in 91% yield over the two-step sequence. Final *N*-acylation of **165** with intermediate **166** under propylphosphonic anhydride (T3P)/*N*-methylmorpholine (NMM) conditions in DCM/i-PrOH delivered rilzabrutinib in 89% yield.[215-217]

The synthetic campaign for rilzabrutinib leverages a palladium-mediated Suzuki endgame conducted in a sustainable 2-MeTHF/H_2O biphasic system, reflecting a contemporary focus on biorenewable solvent selection. The route is characterized by highly efficient downstream functionalizations, including a TMSCl-mediated Boc-cleavage (91% yield) and a robust final acylation utilizing T3P to afford the API in 89% yield. Qualitatively, the employment of T3P and 2-MeTHF highlights an emphasis on operational safety and streamlined workup procedures. However, the lack of a reported yield for the initial biaryl coupling stage introduces a minor transparency gap, a common feature in patent-derived sequences that limits a full quantitative assessment of the end-to-end mass intensity.

2.6. Neurology and pain management

2.6.1. Tradipitant

Tradipitant (Nereus) is a novel substance P/neurokinin-1 (NK-1) receptor antagonist developed

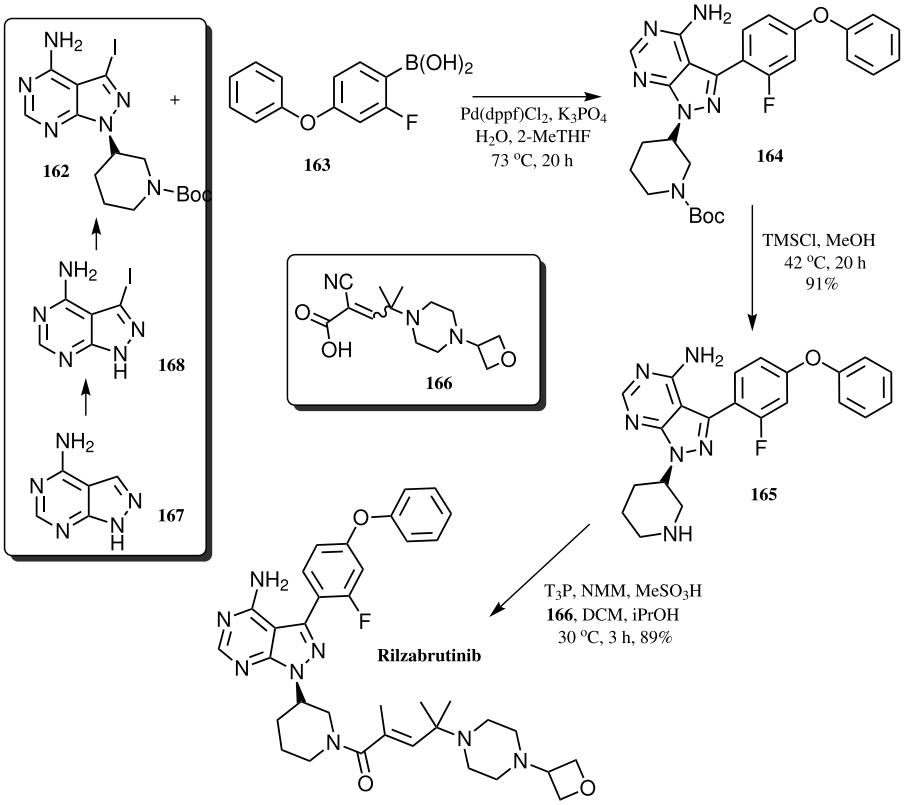

Scheme 24. Concise synthesis of rilzabrutinib.

by Vanda Pharmaceuticals targeting the management of sensory-related disorders, specifically motion sickness, where traditional therapies failed or led to central nervous system (CNS) adverse effects.[218] In December 2025, FDA granted initial approval for Nereus for the prevention of vomiting induced by motion in adults. Currently, it has also been investigated for other indications, as gastroparesis and atopic dermatitis.[219,220] The mechanism of action of tradipitant involves the high-affinity antagonism of the neurokinin-1 (NK-1) receptor which are largely expressed in the brainstem, blocking the binding of Substance P, a key neurotransmitter in emetogenic and nauseogenic pathways, disrupting signals that trigger the vomiting reflex observed in motion sickness. Furthermore, its peripheral action in the gastrointestinal tract may contribute to its efficacy by modulating gastric motility and enteric nervous system responses, providing a dual central and peripheral approach to preventing motion-induced emesis.[221-223] The clinical development of tradipitant was supported by MOTION clinical trials, which involved adult participants on boat trips under variable sea conditions, exhibiting significant reduction on the incidence of vomiting compared to placebo, even in rough sea conditions. Additionally, tradipitant has demonstrated potential in Phase II trials for gastroparesis, where it significantly improved average daily nausea scores over a 4-week period.[224]

A reported route to tradipitant (Scheme 25) starts from 4-bromopyridine hydrochloride (**169**) and proceeds through a Sonogashira/azide-alkyne cycloaddition sequence followed by iodination, zinc insertion, and a final Negishi cross-coupling. Specifically, Sonogashira coupling of **169** with trimethylsilylacetylene in THF (Et_3N, $ZnBr_2$, PPh_3, $PdCl_2$, 60 °C) affords 4-(trimethylsilylethynyl) pyridine (**170**), although no yield was disclosed. Subsequent cycloaddition with 1-azidomethyl-3,5-bis(trifluoromethyl) benzene (**171**) in heptane provides triazole **172** in 72% yield. Electrophilic iododesilylation of **172** using ICl in dichloroethane furnishes iodotriazole **174** (85%). Treatment of **174** with Zn/$ZnCl_2$/TMSCl and catalytic 1,2-dibromoethane in DMF at 65 °C generates the corresponding organozinc species in situ, which is used directly-without isolation-in a Negishi coupling with (2-bromopyridin-3-yl)(2-chlorophenyl)methanone (**174**) under $Pd(PPh_3)_4$ catalysis (60 °C) to deliver tradipitant.[225,226]

The coupling partner **174** can be prepared independently via acylation of morpholine (**176**) with 2-chlorobenzoyl chloride (**175**) in toluene/pyridine to give 4-(2-chlorobenzoyl)morpholine (**177**, 81%), followed by lithium diisopropylamide (LDA)-mediated reaction with 2-bromopyridine (**178**) at −78 °C to afford ketone **174**, reported in low yield.[227]

Synthesis of tradipitant is defined by a sophisticated transition from robust click chemistry to an organometallic-

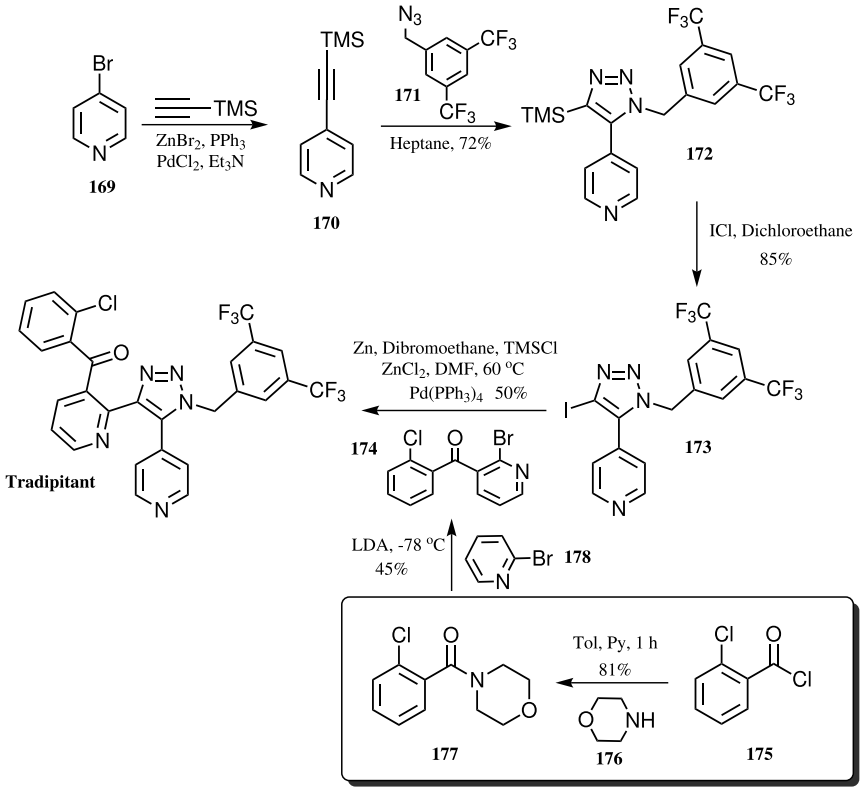

Scheme 25. Tradipitant synthesis.

driven endgame. While the azide-alkyne cycloaddition successfully constructs the triazole core in 72% yield, the subsequent reliance on iodine monochloride and *in situ* organozinc generation introduces substantial corrosive hazards and operational complexity. Furthermore, the cumulative efficiency is severely throttled by the independent preparation of the benzoylpyridine fragment, which necessitates cryogenic lithiation (–78 °C) and suffers from poorly disclosed 'low yields'. Qualitatively, the extensive use of noble metal catalysis and the requirement for multiple sacrificial handles highlight significant opportunities for process intensification, particularly through the development of more direct C–H functionalization strategies to circumvent the current silyl-iodo-zinc relay sequence.

2.6.2. Suzetrigine

Suzetrigine (Journavx, VX-548), developed by Vertex Pharmaceuticals, is a first-in-class non-opioid analgesics, highly selective inhibitor of the voltage-gated sodium channel, engineered to target the NaV1.8 channels located in the peripheral nervous system.[228,229] FDA granted approval for suzetrigine in January 2025 for the treatment of moderate-to-severe acute pain, following its previous designations as a Breakthrough Therapy and Fast Track candidate.[230] Unlike traditional opioids that act on the CNS and carry significant risks of respiratory depression and addiction common to opioid drugs, suzetrigine inhibits channels predominantly located in primary afferent nociceptors. By blocking these channels, the drug effectively halts the transmission of pain signals before they reach the spinal cord and brain, offering a targeted mechanism of action that avoids the systemic side effects typically associated with broad-spectrum sodium channel blockers or μ-opioid receptor agonists.[231-234] The clinical development of suzetrigine culminated in a robust Phase 3 program that demonstrated significant efficacy in managing moderate-to-severe acute pain. Furthermore, additional large-scale Phase 3 for assessment of safety and effectiveness across various surgical and non-surgical pain models confirmed a favorable safety profile and consistent analgesic performance to address the gap between over-the-counter non-steroidal anti-inflammatory drugs (NSAID) and potent opioids in clinical practice.[235-237]

The patent linear route to synthesize suzetrigine (Scheme 26) has been disclosed starting with the treatment of substituted phenylacetic acid **179** with CDI and then the ketone **180** was added, furnishing the phenylfuranone **181** in 85.2% yield. This compound was then subjected to a palladium catalyzed hydrogenation to give phenyldihydrofuranone (**182**) in 95.5% yield. The reduction of **182** was conducted smoothly with DIBAL-H affording phenyltetrahydrofuran-2-ol (**183**) in 99.7% yield. The acetal previously generated was activated by means of the reaction with 4-nitrobenzoyl chloride (**184**) giving the ester **185**. This crude material was utilized to a nucleophilic substitution reaction with trimethylsilyl cyanide (TMSCN) in presence of boron trifluoride to furnish the cyano-intermediate **186**. The cyano group of this intermediate was hydrolyzed in a methanolic solution of KOH, forming the correspondent carboxylic acid after reactional medium neutralization with HCl (**187**), which was cocrystallized with quinine in dichloromethane/2-propnanol/*n*-heptane solvent system to afford the enantiomeric pure salt in about 85% yield. Following the synthetic route sequence, this salt was broken with HCl, and the free acid was treated with oxalyl chloride to afford the equivalent acyl chloride **188** which was, then, reacted with methyl 4-aminopicolinate (**189**) to provide the amide **190** in about 85% yield (three steps). Last step involves the treatment of **190** with ammonia in tetrahydrofuran/methanol solution to give suzetrigine, the final product, in 92% yield.[238]

The synthetic trajectory toward suzetrigine is delineated by a highly efficient linear assembly that effectively navigates stereochemical complexity through the use of classical resolution. Starting from a substituted phenylacetic acid precursor, the roadmap achieves exceptional downstream yields, notably in the near-quantitative DIBAL-H reduction (99.7%) and the subsequent quinine-mediated cocrystallization, which establishes enantiopurity in 85% yield. Qualitatively, the preparative sequence is marked by the employment of hazardous reagents-specifically TMSCN and oxalyl chloride-and a reliance on problematic halogenated solvents like DCM for the resolution endgame. Nevertheless, the cumulative throughput remains robust, with the final functionalizations proceeding in high yields to deliver the API, highlighting a process that prioritizes chemical reliability and high stepwise recovery in a traditional medicinal chemistry framework.

2.7. Dermatology

2.7.1. Remibrutinib

Developed by Novartis, remibrutinib (Rhapsido) is a novel, highly selective, and potent covalent oral Bruton's tyrosine kinase (BTK) inhibitor, approved by FDA in September 2025. It was designed to treat chronic spontaneous urticaria (CSU) in adults, addressing the limitations of standard treatments whose symptoms remain inadequately controlled despite the use of second-generation H1 antihistamines.[239-242] Remibrutinib's granting was followed by robust Phase 3 clinical trials (REMIX-1 and REMIX-2

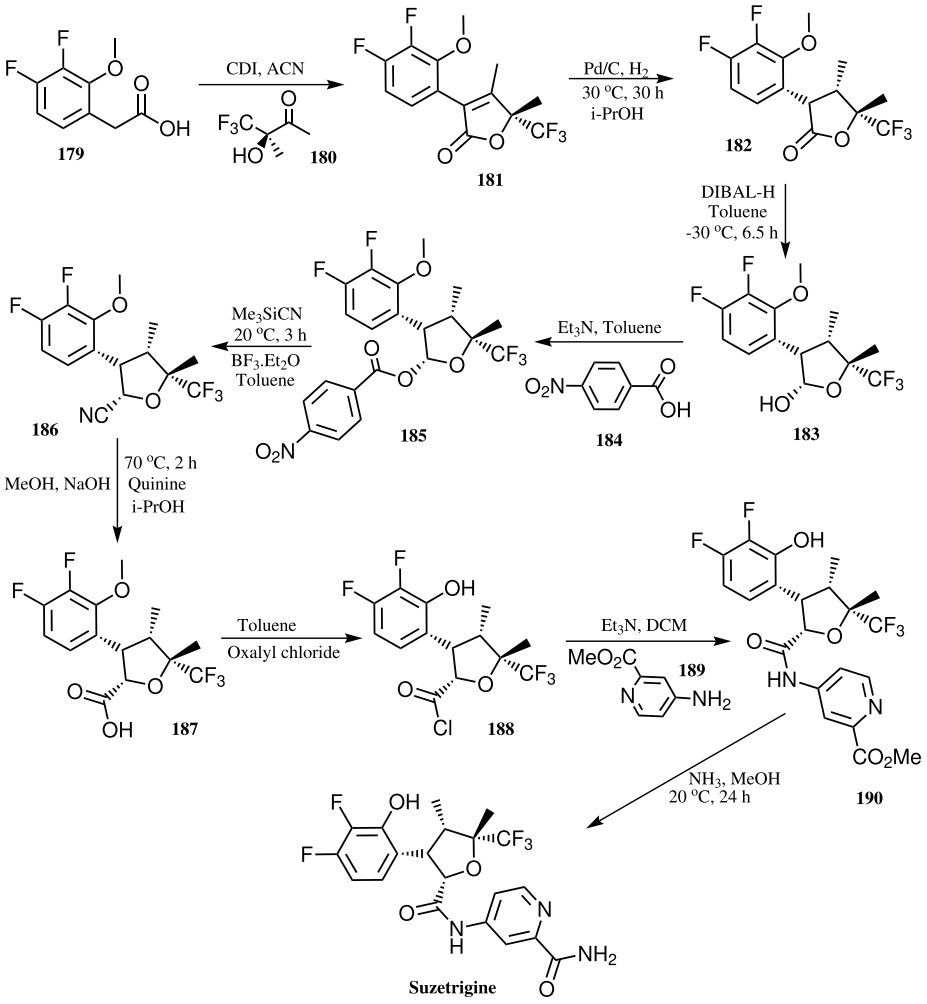

Scheme 26. Linear route to suzetrigine.

studies). It was demonstrated that oral remibrutinib (25 mg b.i.d.) achieved rapid and sustained improvements in CSU, as *per* measurement by the weekly Urticaria Activity Score (UAS7). Long-term studies also confirmed that remibrutinib was capable of maintaining CSU symptoms under control, as well as keeping satisfactory safety profile.[243-245] Its mechanism of action centers on its highly selective covalent inhibition of BTK, relevant for the FcεRI receptor pathway in mast cells and basophils, which are the primary effector cells in CSU pathogenesis. By covalently binding to BTK, remibrutinib blocks the signaling that leads to the degranulation of these cells and the subsequent release of histamine and other inflammatory mediators.[245-247]

Instead of building the heteroaryl-aryl bond at the very end, this remibrutinib route first assembles a functionalized anilide fragment and then forges the key biaryl linkage to a 6-chloropyrimidine partner before a short deprotection/acylation finish (Scheme 27). Thus, 4-cyclopropyl-2-fluorobenzoic acid (**191**) is converted to the corresponding acid chloride **192** with $SOCl_2$/pyridine in toluene (50 °C) and subsequently coupled with 3-bromo-5-fluoro-2-methylaniline (**193**) using DIPEA in i-PrOAc to afford benzamide **194**. Miyaura borylation of **194** with a diboron reagent under Pd catalysis (cataCXium®-3G precatalyst, DIPEA, MeOH, 50 °C) provides the boron coupling partner **195**, which undergoes Suzuki-Miyaura coupling with 6-chloropyrimidine derivative **196** (XPhos-Pd-G2, Et_3N, ethylene glycol, 60 °C) to deliver intermediate **197** in 77% yield.[248,249] The pyrimidine electrophile **196** can be prepared from 4,6-dichloropyrimidin-5-ol (**201**) via Mitsunobu *O*-alkylation with *N*-Boc-*N*-methyl-2-hydroxyethylamine (**200**) (accessible by Boc protection of *N*-methyl-2-hydroxyethylamine, **199**), followed by SN_{Ar} amination with ammonia (25% NH_3 in i-PrOH/H_2O, 70 °C) to give the 4-amino-6-chloropyrimidine derivative **196**.

An alternative entry to **197** relies on a reductive cross-coupling between bromide **194** and pyrimidine **196** ($NiCl_2$, Zn, MgI_2, PPh_3; DMAc, 40 °C), avoiding the discrete borylation step. Removal of the Boc group from **197** with TFA in DCM affords secondary amine **198**, and final

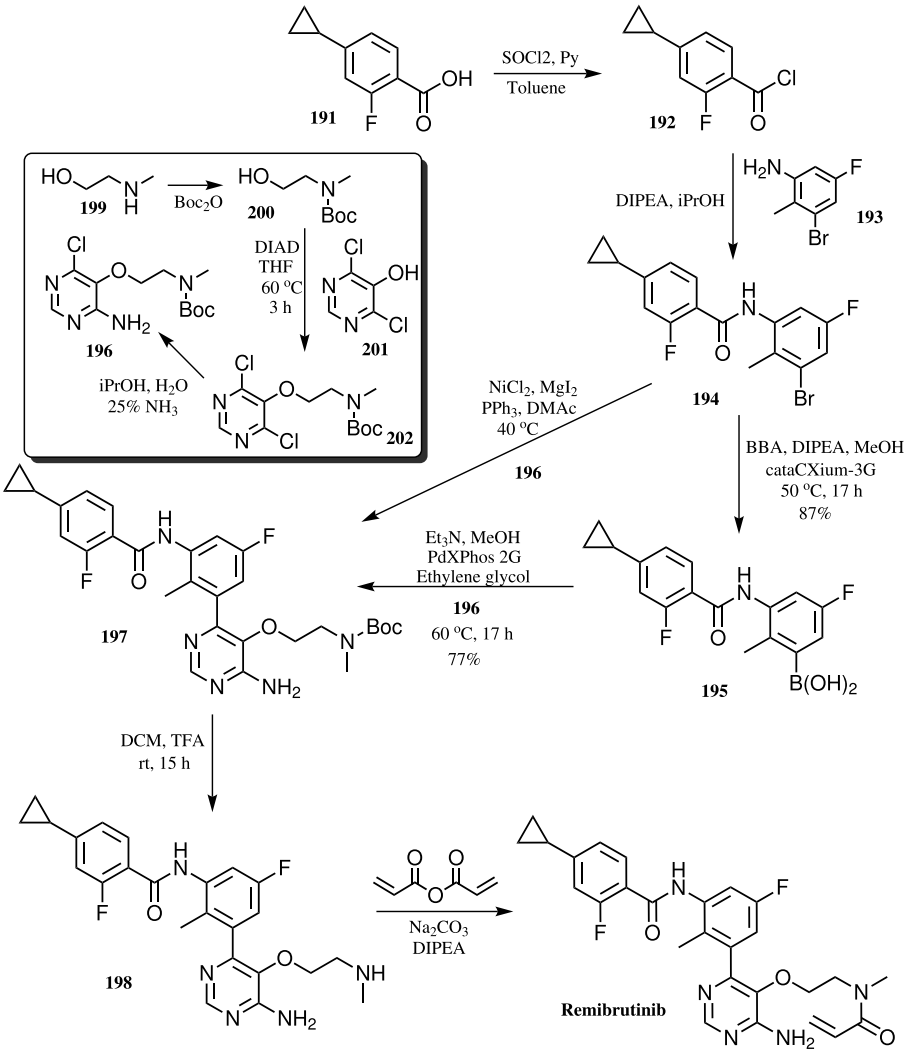

Scheme 27. Remibrutinib and its intermediate synthesis.

acylation with acrylic anhydride in the presence of Na_2CO_3 at 60 °C furnishes remibrutinib.

A notable feature of this strategy is the choice between a standard Suzuki-Miyaura protocol (77% yield) and a nickel-catalyzed reductive coupling, the latter offering a more streamlined pathway by avoiding a separate borylation stage. Qualitatively, the process is flagged by the employment of hazardous reagents like thionyl chloride and the stoichiometric waste generated during the Mitsunobu-mediated pyrimidine functionalization. However, the industrial assessment of this route is significantly hampered by extensive transparency gaps, as isolated yields for the majority of the sequence-including the final installation of the acryloyl motif-remain undisclosed in the current patent literature. This underscores the persistent challenge of benchmarking the absolute material efficiency of clinical candidates when only partial transformational data is available.

2.7.2. Delgocitinib

Delgocitinib was originally discovered and developed by Japan Tobacco Inc. as a potent inhibitor of the Janus kinase (JAK) family. In 2014, LEO Pharma entered into a licensing agreement for the development of a topical formulation for treatment of moderate-to-severe chronic hand eczema (CHE) in adults who have had an inadequate response to topical corticosteroids or for whom such treatments are not clinically advisable, making it the first topical JAK inhibitor specifically approved for this condition by FDA in July 2025.[250-253] Its regulatory approval was supported by clinical trials (DELTA 1, 2 and 3), including evaluations on long-term safety and efficacy. These trials demonstrated that delgocitinib cream (20 mg g^{-1} b.i.d.) significantly improved skin clearance and symptom relief compared to the vehicle after 16 weeks, with clinical response measured by the Investigator's Global Assessment for CHE (IGA-CHE) and the Hand Eczema Severity Index (HECSI) for up to 52 weeks of treatment.[254,255] Delgocitinib is a

pan-JAK inhibitor that non-selectively targets all four members of the JAK family: JAK1, JAK2, JAK3, and tyrosine kinase 2 (TYK2). By inhibiting these enzymes, the drug effectively blocks the JAK-STAT signaling pathway, which is a central mediator in the pathogenesis of inflammatory skin diseases, suppressing the biological effects of multiple pro-inflammatory cytokines which are typically elevated in eczematous conditions (gamma-interferon - IFN-γ, interleukines IL-4, IL-13, IL-17A, IL-22). This targeted approach modulates the overactive immune response and restores skin barrier function while minimizing the systemic risks often associated with oral JAK inhibitors.[256-259]

A convergent patent route to delgocitinib builds the azetidine-derived spirocyclic amine core from a chiral aminoalcohol precursor and then installs the heteroaryl fragment in the late stages (Scheme 28). *N*-Alkylation of 2(*S*)-(benzylamino)propan-1-ol (**203**) with *tert*-butyl bromoacetate (**204**) in the presence of K_2CO_3 (toluene) affords *tert*-butyl *N*-benzyl-*N*-[(2*S*)-1-hydroxypropan-2-yl]glycinate (**205**). Conversion of the alcohol into the corresponding chloride under MsCl/Et_3N conditions in THF, accompanied by rearrangement, gives *tert*-butyl *N*-benzyl-*N*-[(2*R*)-2-chloropropyl] glycinate (**206**). Base-mediated cyclization of **206** (LiHMDS, *N*,*N*'-dimethylpropyleneurea (DMPU), THF) furnishes *tert*-butyl 1-benzyl-3(*S*)-methylazetidine-2-carboxylate (**207**), and subsequent hydrogenolysis (H_2, Pd/C, MeOH) removes the benzyl group to deliver *tert*-butyl 3-(*S*)-methylazetidine-2-carboxylate (**208**). Protection of the azetidine nitrogen with CbzCl (DIPEA, THF) provides **209**.[260]

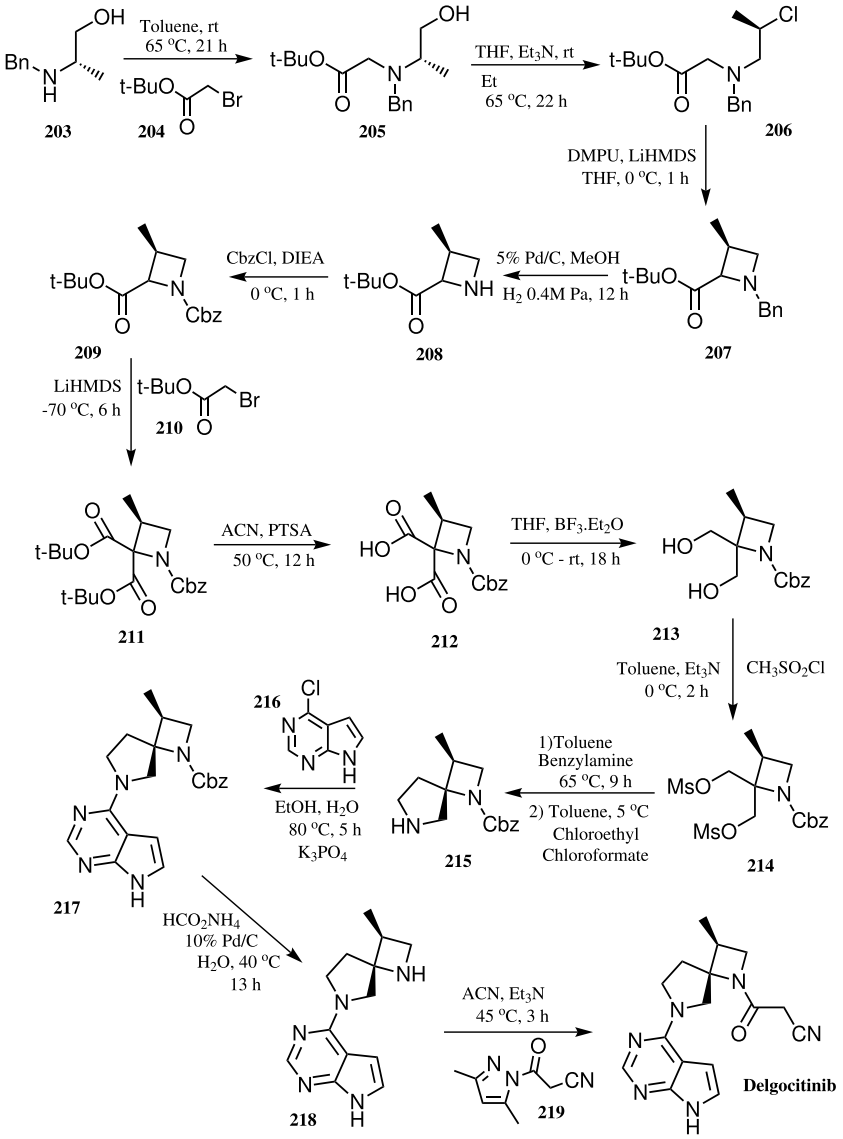

Scheme 28. Convergent route to delgocitinib.

Lithiation of **209** with LiHMDS at −65 °C, followed by alkylation with *tert*-butyl bromoacetate (**210**) at −70 °C, affords intermediate **211**. Acid-mediated ester cleavage (*p*-PTSA, ACN) gives the corresponding diacid **212**, which is reduced with $BF_3{\cdot}Et_2O$ in THF to diol **213**. Sulfonylation (MsCl, Et_3N, toluene) converts **213** into dimesylate **214**, and intramolecular cyclization in the presence of benzylamine delivers the 1,6-diazaspiro[3.4] octane framework **215**. The resulting *N*-benzyl substituent is removed using 2-chloroethyl chloroformate (toluene) to furnish 1-Cbz-(3*S*,4*R*)-3-methyl-1,6-diazaspiro[3.4] octane (**215**). With the spirocyclic amine in hand, coupling of **215** with 4-chloropyrrolo[2,3-*d*]pyrimidine (**216**) under basic conditions (K_3PO_4, EtOH/H_2O, 80 °C) affords the Cbz-protected adduct **217**. Final Cbz removal using ammonium formate in the presence of 10% Pd/C (H_2O) provides 4-[(3*S*,4*R*)-3-methyl-1,6-diazaspiro[3.4]oct-6-yl] pyrrolo[2,3-*d*]pyrimidine (**218**), which undergoes acylation with 1-(cyanoacetyl)-3,5-dimethylpyrazole (**219**) in the presence of Et_3N (ACN) to furnish delgocitinib.[261]

While the route demonstrates a high level of molecular complexity, it is delineated by substantial operational and scalability hurdles, notably the requirement for cryogenic lithiation (at −70 °C) and a heavy reliance on a multiple protecting group strategy. Qualitatively, the employment of corrosive mesyl chloride and the requirement for noble metal-catalyzed hydrogenolysis for deprotection further underscore a process with high mass intensity. In the absence of reported isolated yields or conversion metrics in the patent literature, the end-to-end material efficiency remains opaque, highlighting a synthetic strategy that currently prioritizes scaffold assembly over the qualitative sustainability metrics required for a robust industrial manufacturing paradigm.

2.8. Pulmonology

2.8.1. Nerandomilast

Nerandomilast (Jascayd), developed by Boehringer Ingelheim, is the first selective phosphodiesterase-4B (PDE4B) inhibitor approved for clinical use. FDA granted its approval for the treatment of idiopathic pulmonary fibrosis (IPF) in adult patients supported by breakthrough therapy designation due to the urgent medical need for more effective and better-tolerated treatments for this progressive and terminal lung disease. It was specifically engineered to address the limitations of non-selective PDE4 inhibitors, which are often hindered by gastrointestinal side effects.[262-265] The clinical efficacy of nerandomilast was demonstrated through the FIBRONEER clinical trials. Nerandomilast significantly reduced the annual rate of decline in forced vital capacity (FVC) compared to placebo, while showing benefit both as a monotherapy and when used concomitantly with existing antifibrotic agents like nintedanib or pirfenidone, with manageable issues regarding safety profile.[266-269] Its mechanism of action a based on preferential inhibition of the PDE4B enzyme isoform, exhibiting approximately 29-fold higher selectivity for PDE4B over other subtypes such as PDE4A, C, and D. By inhibiting PDE4B, the drug prevents the degradation of cyclic adenosine monophosphate (cAMP) in inflammatory and structural lung cells suppressing the production of pro-inflammatory cytokines and inhibits the activation of fibroblasts into myofibroblasts. This dual mechanism effectively targets both the inflammatory and fibrotic pathways of IPF, preserving epithelial integrity and slowing the irreversible remodeling of lung tissue.[270-273]

In the disclosed patent route to nerandomilast, a substituted thioester precursor is first assembled and cyclized to a thienopyrimidine core, which is then sequentially functionalized via chlorination and two late-stage aminations (Scheme 29). *S*-Alkylation of methyl thioglycolate (**220**) with methyl acrylate in the presence of piperidine, affords methyl 3-[(2-methoxy-2-oxoethyl)thio]propanoate (**221**). This intermediate is subjected to a Dieckmann-type cyclocondensation using $TiCl_3$(i-PrOH)-generated in situ from $TiCl_4$ and i-PrOH in DCM at −10 °C-in the presence of Et_3N (−10 °C), furnishes methyl 3-oxotetrahydrothiophene-2-carboxylate (**222**).[274,275]

Condensation of **222** with urea under acidic conditions (HCl, MeOH) provides 3-ureido-4,5-dihydrothiophene-2-carboxylic acid methyl ester (**223**, 95%), which undergoes intramolecular cyclization upon heating with NaOH in water to give 6,7-dihydrothieno[3,2-d]pyrimidine-2,4-dio (**224**). Chlorination with $POCl_3$ at 110 °C converts **224** into 2,4-dichloro-6,7-dihydrothieno[3,2-d]pyrimidine (**225**, 88%). Regioselective SN_{Ar} at C4 with (1-aminocyclobutyl) methanol tosylate (**226**) in the presence of Et_3N (ACN, 75 °C) affords (1-((2-chloro-6,7-dihydrothieno[3,2-*d*] pyrimidin-4-yl)amino)cyclobutyl)methanol (**227**, 57%). Asymmetric oxidation of **227** using t-BuOOH in the presence of (*S*)-1,1'-bi-2-naphthol ((*S*)-BINOL) (DCM/H_2O) provides the corresponding 5-oxide (**228**). Final nucleophilic amination of **228** with 5-chloro-2-(piperidin-4-yl)pyrimidine (**229**) in the presence of DIPEA (THF, 65 °C) delivers nerandomilast.[276]

The sequence initiates with a transition-metal-mediated Dieckmann-type cyclocondensation utilizing $TiCl_4$ at sub-ambient temperatures (−10 °C), a transformation that, while effective, introduces significant operational complexity

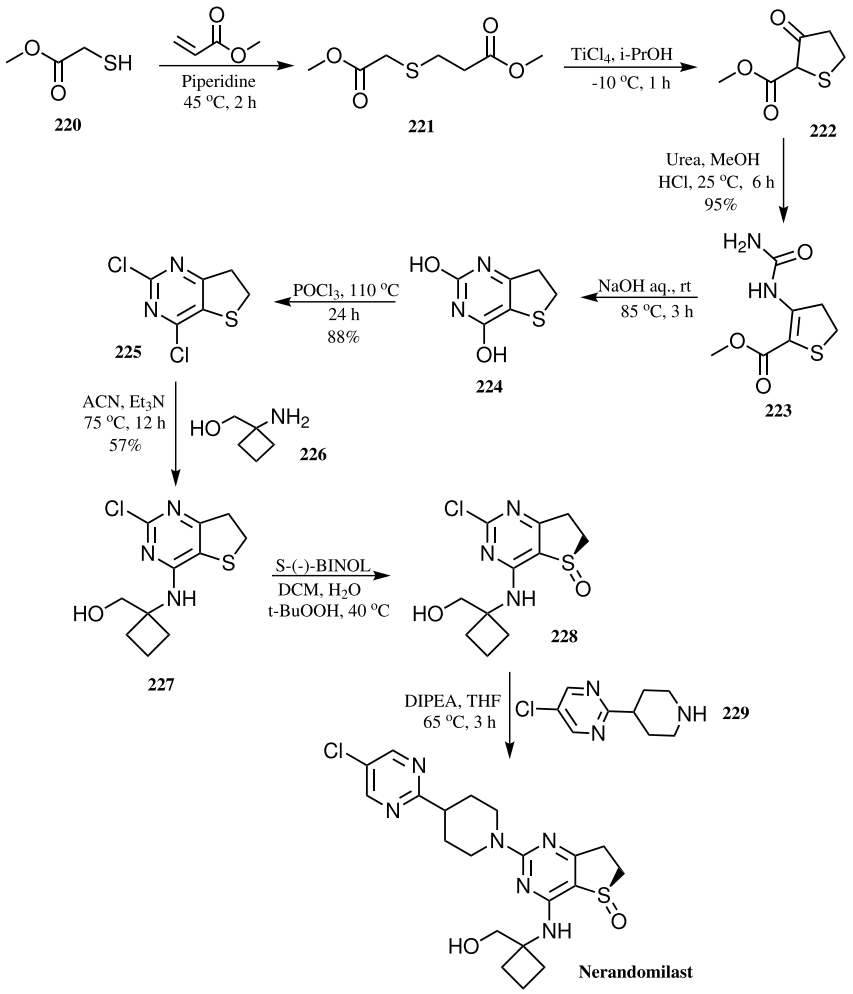

Scheme 29. Synthesis of nerandomilast.

and inorganic waste streams. Qualitatively, the synthesis is flagged by the employment of hazardous $POCl_3$ at 110 °C for the di-chlorination phase and a persistent reliance on chlorinated solvents like DCM. A notable methodological highlight is the asymmetric sulfoxidation mediated by *t*-BuOOH and (*S*)-BINOL, which installs the requisite chirality prior to the final nucleophilic amination. While the initial heterocyclic constructions are high-yielding (> 88%), the cumulative material throughput is restrained by the 57% yield observed during the first substitution and the lack of disclosed efficiency for the asymmetric oxidation endgame, highlighting opportunities for further process intensification in the biaryl coupling phase.

2.8.2. Brensocatib

Brensocatib (Brinsupri, AZD7986) was developed by Insmed Inc. as a first-in-class, selective, and second-generation reversible inhibitor of dipeptidyl peptidase 1 (DPP1) to modulate neutrophil-mediated inflammation. In August 2025, FDA granted approval for brensocatib for the treatment of non-cystic fibrosis bronchiectasis (NCFBE) in adult and pediatric patients aged 12 years and older.[277,278] The clinical development program for brensocatib demonstrated significant therapeutic potential. Phase I trial in healthy subjects established that the drug induces a sustained, exposure-dependent reduction in whole-blood neutrophil elastase (NE) activity, which were further validated in a Phase II randomized, placebo-controlled trial involving patients with NCFBE, where oral administration of 10 and 25 mg doses significantly reduced sputum NE activity and prolonged the time to the first pulmonary exacerbation, demonstrating a clear pharmacokinetic/pharmacodynamic relationship.[279-281] Its mechanism of action involves the inhibition of DPP1 (cathepsin C), a lysosomal cysteine protease responsible for the *N*-terminal processing and activation of neutrophil serine proteases (NSP), specifically neutrophil elastase, proteinase 3, and cathepsin G, during neutrophil maturation in the bone marrow. By preventing the activation of these pro-inflammatory enzymes before neutrophils enter systemic circulation, brensocatib reduces the neutrophil-dominant inflammatory cascade of bronchiectasis by

lowering the levels of active NSP responsible for that tissue damage and mucus hypersecretion in chronic airway diseases.[282-284]

One disclosed approach to brensocatib (Scheme 30) begins with rapid assembly of the benzoxazolinone fragment from 2-amino-4-chlorophenol (**230**), followed by late-stage arylation and installation of the oxazepane carboxamide side chain. Treatment of **230** with CDI at room temperature (2.5 h) affords chlorzoxazone **231** in 98% yield. Subsequent *N*-methylation with MeI and Cs_2CO_3 in DMF provides 5-chloro-3-methyl-1,3-benzoxazol-2-one (**232**) in quantitative yield. Miyaura borylation of **232** with bis(pinacolato)diboron using XPhos/XPhos-Pd-G2 and KOAc (80 °C) furnishes boronate ester **233** (66%), which is coupled with *N*-Boc-2(*S*)-amino-3-(4-iodophenyl)propanamide (**234**) under Suzuki-Miyaura conditions ($Pd(dppf)Cl_2 \cdot CH_2Cl_2$, K_2CO_3, dioxane, 75 °C) to give biaryl benzoxazolinone derivative **235**. Boc removal with HCl in DCM/dioxane affords the corresponding free amine **236**, which undergoes coupling with *N*-Boc-1,4-oxazepane-2(*S*)-carboxylic acid (**237**) under T3P/DIEA activation in DMF (50 °C), delivering *N*-protected brensocatib (**238**) in 98% yield. Final deprotection with formic acid at 37 °C provides brensocatib in 91% yield.[285,286]

The oxazepane acid **237** can be prepared from 1-(benzyl(3-hydroxypropyl)amino)-3-benzyloxy-2(*S*)-propanol (**239**) via mesylation (MsCl, DIPEA, DCM) to give **240**, followed by intramolecular cyclization with NaH in DMF to afford 4-benzyl-2(*S*)-((benzyloxy) methyl)-1,4-oxazepane (**241**). Subsequent *O*-debenzylation and oxidation (TEMPO, Bu_4NHSO_4, toluene) furnishes carboxylic acid **237**.

The molecular assembly of brensocatib underscores a robust transition from simple phenolic precursors to a highly functionalized oxazepane derivative, marked by a balance of classical and contemporary synthetic methodologies. The synthesis is characterized by high-yielding terminal stages, including a T3P-mediated coupling (98%) and a mild deprotection in formic acid.

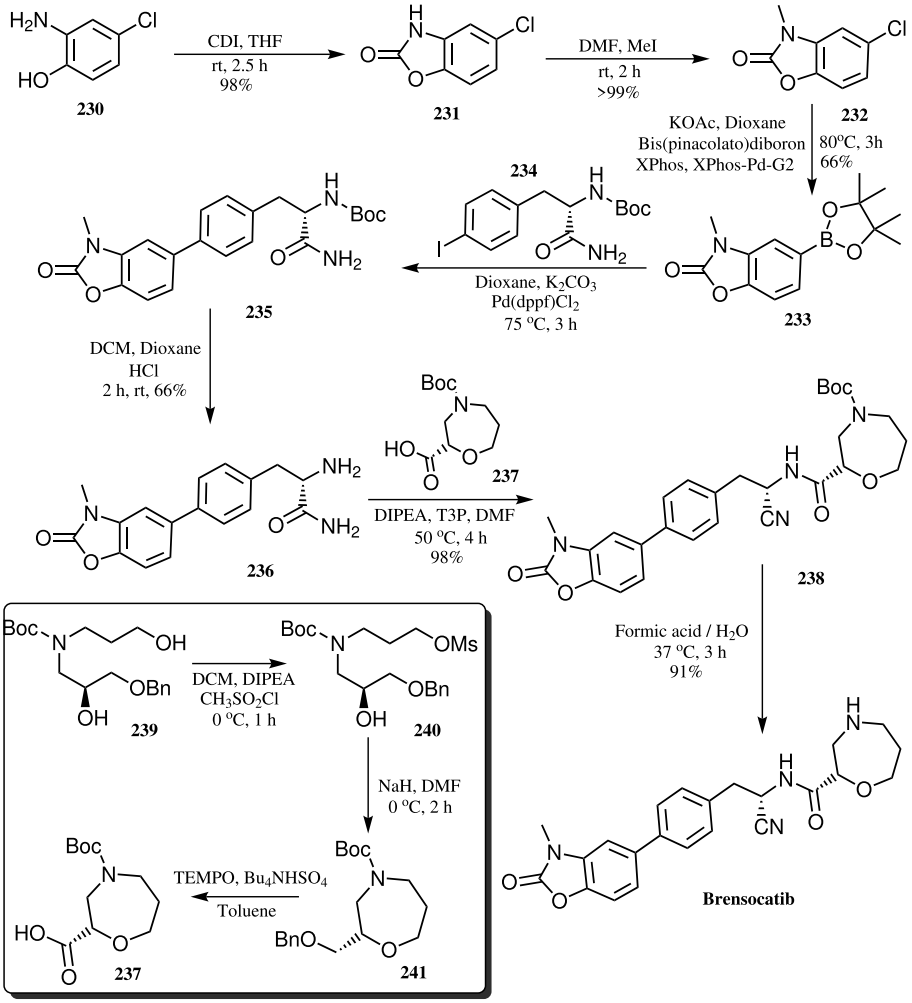

Scheme 30. Synthesis of brensocatib and its intermediates.

Qualitatively, the synthetic campaign is delineated by the employment of hazardous reagents, notably methyl iodide and sodium hydride, alongside the requirement for precious metal catalysis (Pd/XPhos) during the biaryl construction. While the borylation phase serves as a primary efficiency bottleneck (66% yield), the overall throughput is further obscured by transparency gaps in the preparation of the chiral oxazepane side chain. Addressing these quantitative deficiencies and exploring greener alkylation alternatives could significantly enhance the industrial scalability and environmental profile of this clinical candidate.

2.9. Ophthalmology

2.9.1. Aceclidine

Aceclidine (Vizz), developed by Lenz Therapeutics Inc. as an ophthalmic solution for treatment of presbyopia, an age-related condition characterized by a progressive loss of the eye's ability to focus on near objects due to decreased lens elasticity and ciliary muscle efficiency. FDA approval was granted in July 2025 as a cholinergic agonist indicated for adults, providing a non-surgical alternative to traditional corrective measures like glasses or surgery.[287-289] Aceclidine clinical development was supported by the CLARITY programs that demonstrated substantial evidence of effectiveness, achieving improvement in near vision without compromising distance vision clarity. The safety study also established a favorable profile, with common adverse reactions limited primarily to instillation site irritation, dim vision, and temporary headaches.[289-292] The mechanism of action for aceclidine is uniquely targeted, acting as a selective muscarinic acetylcholine receptor agonist. The quinuclin-3-ol moiety, interestingly, is also part of the toxic chemical quinuclidine-3-yl benzilate (BZ), a Schedule 2 incapacitant chemical warfare agent listed by Organisation for the Prohibition of Chemical Weapons (OPCW), antagonizing the same receptors. Unlike older therapies like pilocarpine, aceclidine primarily binds to receptors on the iris sphincter muscle to cause gentle pupillary constriction that increases depth of focus and sharpens near vision while minimizing stimulation of the ciliary muscle. This selectivity is crucial for maintaining distance vision and reducing side effects such as accommodative spasms or eye strain commonly associated with non-selective miotics.[292-296]

Access to aceclidine is described through a short sequence featuring reduction (Scheme 31), activation, epoxidation, and a final nucleophilic ring opening. Reduction of 2-cyclopentyl-2(*R*)-hydroxy-2-phenylacetic acid (**242**) with $LiAlH_4$ in THF at room temperature affords primary alcohol **243**. Conversion to the corresponding tosylate **244** is achieved using TsCl and Et_3N in DCM. Treatment of **244** with K_2CO_3 in MeOH promotes intramolecular cyclization to give epoxide **245**, which is subsequently opened by quinuclidin-3(*R*)-ol (**246**) under basic conditions (NaH, DMSO) to furnish aceclidine.[297] Qualitatively, the synthesis is marked by the employment of hazardous and pyrophoric reagents, notably $LiAlH_4$ and sodium hydride in DMSO, both of which introduce substantial operational risks into the manufacturing paradigm. Although the sequence effectively leverages the nucleophilicity of quinuclidin-3(*R*)-ol for the final assembly, the absence of isolated yields for any stage prevents a definitive assessment of the route's mass intensity or commercial scalability. These findings suggest that while the route is chemically logical, significant process intensification-targeting the replacement of high-risk reagents and a more atom-economical endgame-would be required for a sustainable industrial transition.

2.9.2. Acoltremon

Acoltremon (Tryptyr, AR15512, AVX012), is a first-in-class small molecule developed by Alcon, following its acquisition of Aerie Pharmaceuticals. It was specifically

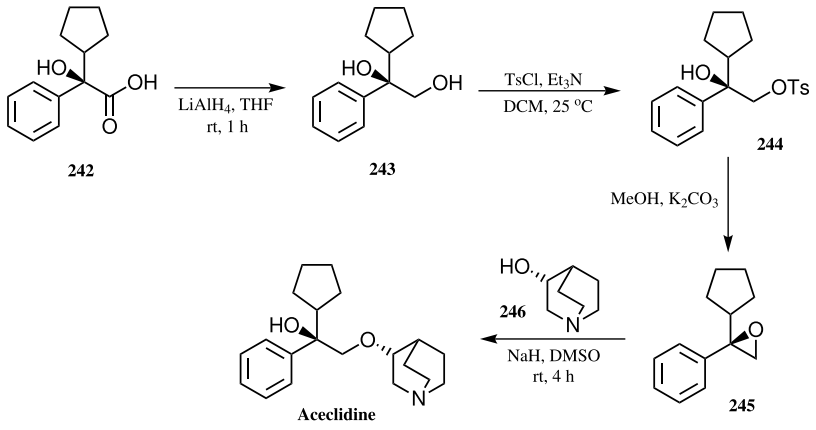

Scheme 31. (*S*)-Aceclidine synthesis.

designed for the treatment of dry eye disease (DED) as ophthalmic solution. Acoltremon is a potent and selective agonist of the transient receptor potential melastatin 8 receptor (TRPM8), receiving FDA approval in May 2025, marking the introduction of a novel therapeutic class that targets the neurosensory pathways of the ocular surface to restore tear film homeostasis.[298-300] Acoltremon clinical trials (COMET) demonstrated its safety and efficacy, showing early and sustained improvements in tear production and ocular surface staining, with a significantly higher proportion of patients achieving satisfactory scores in unanesthetized Schirmer test. The results also indicated meaningful reductions in adverse effects, such as ocular discomfort and dryness.[301,302] The mechanism of action of acoltremon is solely focused on the TRPM8 thermoreceptors located on the sensory nerve terminals of the cornea and eyelids. Unlike traditional DED therapies that primarily target inflammation, it acts as a TRPM8-mimetic agonist that activates these cold-sensitive ion channels. By simulating the natural cooling sensation that occurs during tear film evaporation, the drug triggers the trigeminal nerve pathway to initiate a parasympathetic efferent response. This physiological activation stimulates the lacrimal functional unit, leading to the natural secretion of all components of the basal tear film, enhancing ocular surface hydration.[303-305]

Acoltremon can be easily synthetized starting with the chlorination of (1*R*,2*S*,5*R*)-(–)-menthol (**247**) using zinc chloride and hydrochloric acid to give (1*S*,2*R*,4*R*)-2-chloro-1-isopropyl-4-methylcyclohexane (**248**) in 90% yield (Scheme 32). Preparation of Grignard reagent of **248** with magnesium in diethyl ether followed by addition of CO_2 furnishes the carboxylic acid **249** in 40% yield. As the last step, **249** is treated with the coupling reagent benzotriazol-1-yloxytripyrrolidinophosphonium hexafluorophosphate (PyBOP), base *N*,*N*-diisopropylethylamine (DIPEA), solvent dimethylacetamide (DMA) and *p*-anisidine (**250**) to give acoltremon in 79% yield.[306] While the route maintains a respectable ca. 28% global efficiency, the substantial material loss during the carbon dioxide insertion and the generation of stoichiometric phosphine oxide byproducts highlight typical process chemistry trade-offs. These findings suggest that future optimization of the Grignard formation-perhaps through the use of more sustainable ethereal alternatives or continuous flow carboxylation-could significantly enhance the industrial scalability and environmental profile of this molecule.

2.10. Gynecology

2.10.1. Elinzanetant

Elinzanetant (Lynkuet, NT-814) is an innovative non-hormonal, small-molecule antagonist of both neurokinin-1 (NK1) and neurokinin-3 (NK3) receptors. Developed by Bayer following its 2020 acquisition of KaNDy Therapeutics, it is directed to menopausal care. FDA approved Lynkuet in October 2025 for the treatment of moderate to severe vasomotor symptoms (VMS) associated with menopause, making it as first and only dual NK1 and NK3 receptor antagonist available in the market.[307-309] Elinzanetant clinical efficacy and safety were established through OASIS development program. These trials demonstrated that a daily dose (120 mg) significantly reduced the frequency and severity of moderate to severe VMS compared to placebo over 26 weeks, with a rapid onset of effect observed as early as the first week of treatment. Further evaluation of menopausal women over 52 weeks, confirming sustained efficacy in reducing hot flashes while also showing numerical improvements in sleep disturbances and menopause-related quality of life. It was also well-tolerated, with no associations found with hepatotoxicity, endometrial hyperplasia, or adverse changes in bone mineral density.[310-313] Its mechanism of action targets the underlying neurobiological causes of menopausal symptoms. The decline of estrogen levels in menopause leads to the hypertrophy and overactivity of kisspeptin/neurokinin B/dynorphin (KNDy) neurons in the thermoregulatory center of the hypothalamus. By antagonizing NK3 receptors, elinzanetant modulates the activity of these hyperactive neurons to stabilize thermoregulation and reduce hot flashes. Additionally, its antagonism of NK1 receptors contributes to reduce common VMS symptoms, as heat-sensing neuro-activity and sleep disturbances.[314-316]

A multistep patent sequence to elinzanetant assembles a 4-arylated, *N*-methylated aminopyridine fragment and couples it to a bicyclic amine via a late-stage Buchwald-Hartwig amination, with final desilylation delivering

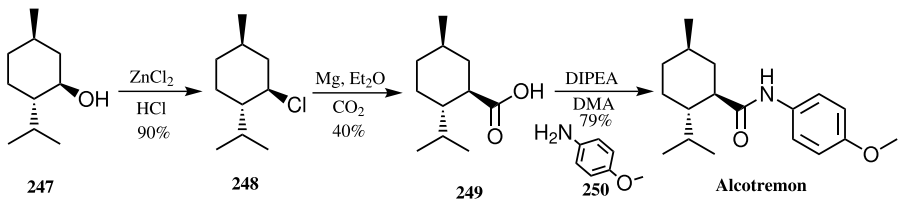

Scheme 32. Synthesis of acoltremon.

the API (Scheme 33). Boc protection of 3-amino-6-chloropyridine (**251**) using Boc_2O in refluxing dioxane affords carbamate **252**. Directed lithiation of **252** with BuLi/TMEDA (hexane/Et_2O, 0 °C), followed by iodination with I_2 in Et_2O, provides the 4-iodinated derivative **253**. Subsequent *N*-methylation with MeI under NaH/DMF conditions furnishes 6-chloro-4-iodo-*N*-methyl-*N*-Boc pyridin-3-amine (**254**), and Boc removal with TFA in DCM gives the corresponding free amine **255**. Suzuki-Miyaura coupling of **255** with 4-fluoro-2-methylphenylboronic acid (**256**) ($Pd(OAc)_2$, PPh_3, Na_2CO_3; DME, 80 °C) yields 6-chloro-4-(4-fluoro-2-methylphenyl)-*N*-methylpyridin-3-amine (**257**) in 83% yield. Acylation of **257** with 2-[3,5-bis(trifluoromethyl)phenyl]-2-methylpropanoyl chloride (**258**) using KHMDS affords amide **259**. The remaining aryl chloride is then displaced via Buchwald-Hartwig amination with bicyclic partner **260** under $Pd(t\text{-}Bu_3P)_2$ catalysis (cetrimonium chloride, NaOH; toluene, 90 °C, 24 h) to give *O*-TBDMS-protected elinzanetant (**261**), and final desilylation with HCl in MeOH furnishes elinzanetant.[317-319] While the Suzuki-Miyaura biaryl coupling proceeds with a commendable 83% yield, the qualitative sustainability of the process is hampered by a reliance on Class 2 solvents (dioxane, DME) and the requirement for chromatographic diastereomer separation to access the chiral bicyclic core. In the absence of disclosed yields for the pivotal amination and final deprotection stages, the end-to-end mass intensity remains opaque, highlighting significant opportunities for process intensification-specifically targeting the development of a more stereoselective assembly for the bicyclic fragment to minimize material attrition.

The bicyclic coupling partner **260** (Scheme 34) is prepared from 4-Boc-3-morpholinecarboxylic acid (**262**) and methyl D-serinate hydrochloride via amide bond formation (TBTU, DIPEA, DCM), followed by TFA-promoted deprotection/

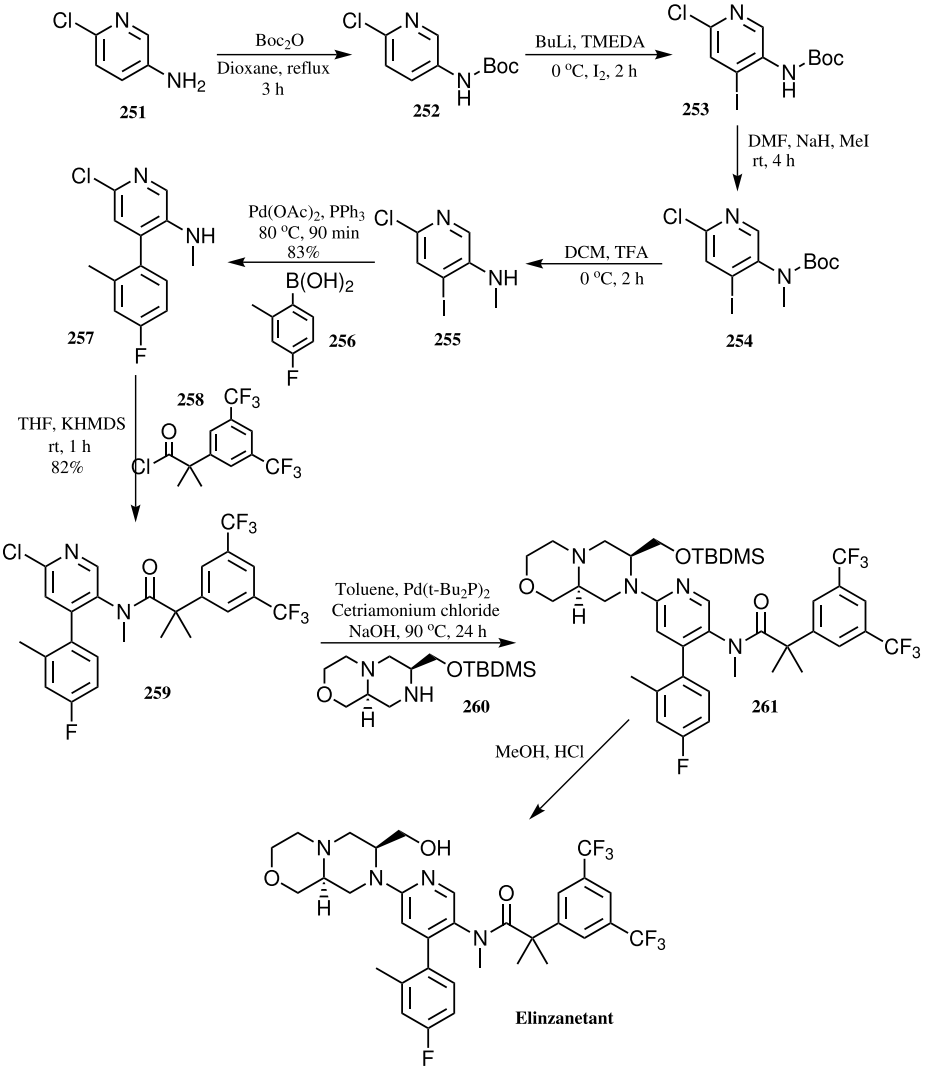

Scheme 33. Convergent synthesis of elizanetant.

cyclization to provide diketone **264** (7(*R*)-(hydroxymethyl)-1,3,4,7,8,9*a*-hexahydropyrazino[2,1-*c*][1,4]oxazine-6,9-dione). Reduction of the di-carbonyl functionality with BH_3·THF at room temperature affords the corresponding aminoalcohol **265**, which is *O*-silylated with TBDMSCl/Et_3N in DCM; separation of the resulting diastereomers by flash chromatography then delivers the (*S*,*S*)-configured bicyclic intermediate **260**.[317-319]

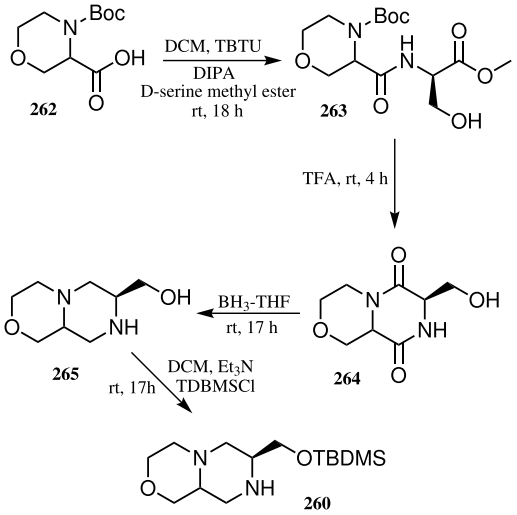

Scheme 34. Synthesis of intermediate **260**.

2.11. Endocrinology

2.11.1. Paltusotine

Paltusotine (Palsonify, CRN00808) was discovered by Crinetics Pharmaceuticals as a first-in-class, potent, and highly selective non-peptide agonist of the somatostatin receptor subtype 2 (SST2) for the long-term treatment of adults with acromegaly. Unlike traditional peptide-based somatostatin receptor ligands (SRL) such as octreotide and lanreotide, which require parenteral administration due to poor oral bioavailability, paltusotine was engineered as a small-molecule quinoline derivative specifically designed for once-daily oral consumption. FDA approval came in September 2025. It is indicated for acromegaly patients who have had an inadequate response to surgery or for whom surgery is not a viable option.[320-322] The clinical efficacy and safety of paltusotine were established through PATHFNDR (PATHFNDR-1, PATHFNDR-2) and ACROBAT clinical development programs trials. PATHFNDR enrolled patients with biochemically uncontrolled acromegaly, 55.6% of patients treated with paltusotine achieved IGF-1 normalization at 24 weeks compared to only 5.3% in the placebo group. ACROBAT, in turn, demonstrated that patients switching from injectable SRL could maintain stable insulin-like growth factor 1 (IGF-1) and growth hormone (GH) levels when transitioning to oral paltusotine. The drug was generally well-tolerated, with a safety profile consistent with the known effects of somatostatin analogs, as mild to moderate gastrointestinal symptoms and biliary complications.[323-326] Paltusotine acts by selectively binding to the SST2 receptor on the surface of growth hormone-secreting pituitary adenoma cells. This binding activates the Gi/o protein signaling pathway, leading to the inhibition of adenylate cyclase and a subsequent decrease in intracellular cyclic adenosine monophosphate (cAMP) levels. This signaling cascade effectively suppresses the hypersecretion of GH and reduces the liver production of IGF-1, thereby alleviating the systemic complications and symptoms of acromegaly. Its non-peptide structure allows for a good pharmacokinetics and a sustained pharmacodynamic effect, presenting a more convenient and less invasive alternative to current, life-long injectable therapies.[327-330]

A reported synthesis of paltusotine builds a halogenated quinoline electrophile and then introduces the aryl substituents through a late-stage, sequential Suzuki strategy (Scheme 35). Initial chlorination of 6-bromoquinolin-4(1*H*)-one (**266**) with NCS in AcOH (50 °C) affords 6-bromo-3-chloroquinolin-4-ol (**267**, 78%). Conversion to 4,6-dibromo-3-chloroquinoline (**267**) is achieved by treatment with PBr_3 in DMF (5 h), delivering **268** in 65% yield. Nucleophilic aromatic substitution at C4 with 4-(*N*-Boc-amino)piperidine (**40**) (DIPEA, DMSO, 140 °C, 6 h) furnishes *N*-Boc-1-(6-bromo-3-chloroquinolin-4-yl) piperidin-4-amine (**260**) in 70% yield.[331]

An alternative entry to the same intermediate avoids the PBr_3-mediated bromination of **267**. Coupling of **40** with 6-bromo-4-chloroquinoline (**274**) using K_2CO_3 in DMF (105 °C) provides *N*-Boc-1-(6-bromoquinolin-4-yl)piperidin-4-amine (**275**, 84%), which is then regioselectively chlorinated with NCS in the presence of DIPA (toluene, 70 °C, 4 h) to give **269** in 66% yield.

From **269**, Suzuki coupling with (3-cyano-2-hydroxyphenyl)boronic acid (**270**) ($PdCl_2$(dppf)·CH_2Cl_2, K_2CO_3; dioxane, 85 °C) affords intermediate **271**, which is carried forward without isolation into a second Suzuki coupling with 3,5-difluorophenylboronic acid (**272**) using $PdCl_2$(amphos)$_2$ (100 °C) to deliver **273** in 45% yield over the two-step, telescoped sequence. Final Boc deprotection with 6 M HCl in i-PrOH affords the dihydrochloride salt, which upon basification with NH_4OH in water provides paltusotine hydrochloride.[332]

For the principal approach to **269** (**266** → **267** → **268** → **269**), the overall yield is ca. 36% against ca. 55% to the alternative synthetic step, with the NCS chlorination (66%) representing the principal drawback. From intermediate **269**, the two-step Suzuki sequence from **260** to

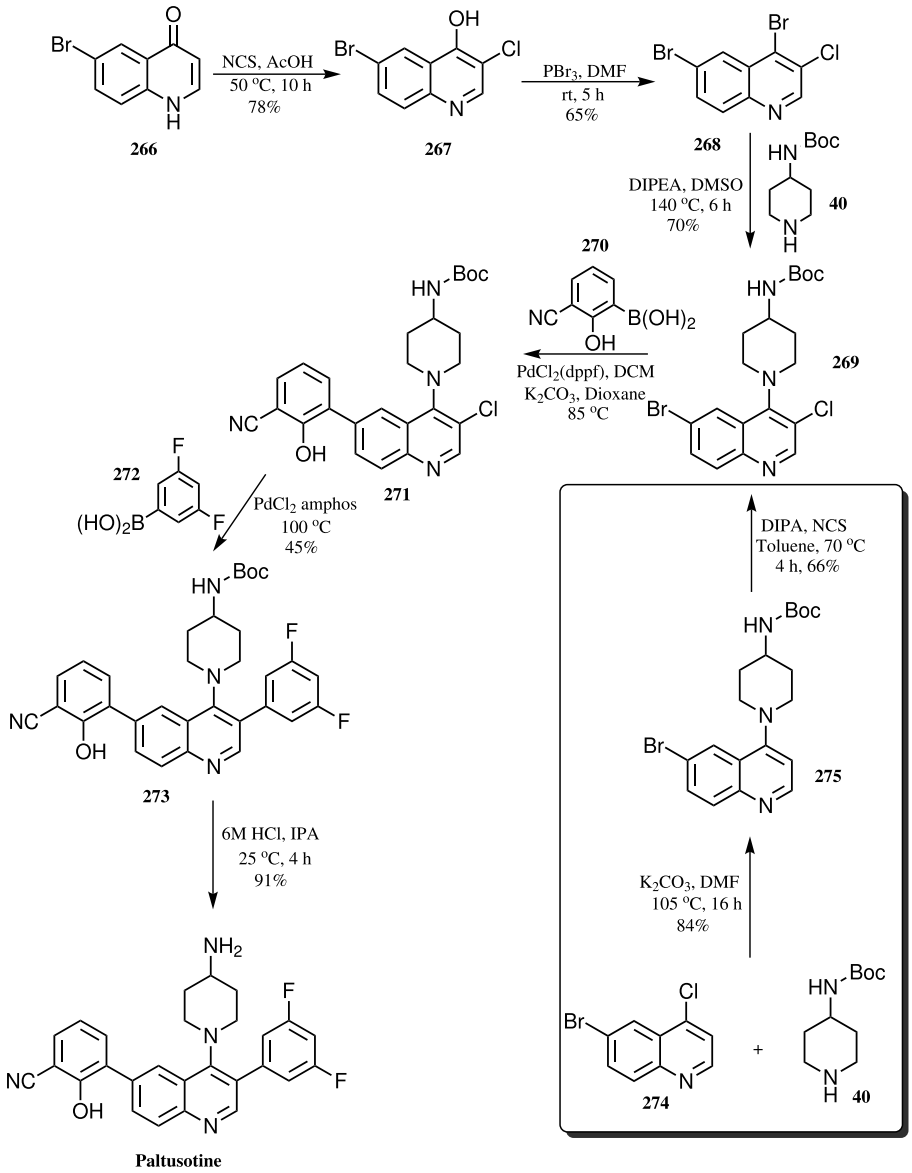

Scheme 35. Paltusotine synthesis.

273 is reported at 45% overall, this telescoped coupling is a dominant determinant of end-to-end efficiency. Combining the disclosed yields gives an approximate cumulative yield of ca. 16% from **266** to **273** via the main strategy *versus* ca. 25% from **274** to **273**.

The primary itinerary relies on a demanding PBr_3-mediated activation and a high-temperature SN_{Ar} (140 °C), an alternative assembly significantly improves the intermediate throughput from ca. 36 to ca. 55% by utilizing a more streamlined chlorination-coupling sequence. Qualitatively, the strategy is delineated by the employment of hazardous phosphorus-based reagents and the operational complexity of managing two successive palladium-catalyzed cross-couplings without intermediate isolation. Despite the efficiency gains of the alternative route, which elevates the cumulative yield to ca. 25%, the process remains constrained by the regioselective NCS chlorination phase. These findings suggest that while the telescoped endgame successfully manages molecular complexity, future process intensification should target the refinement of the halogenation stages to further enhance the commercial scalability and atom economy of this clinical candidate.

2.12. Nephrology

2.12.1. Atrasentan

Atrasentan (Vanrafia) developed by Novartis for the treatment of primary immunoglobulin A nephropathy (IgAN). Originally explored by AbbVie for

diabetic nephropathy and later, FDA granted atrasentan accelerated approval in April 2025 specifically to reduce proteinuria in adults with primary IgAN at risk of rapid disease progression, as clinical data showed significant reduction in the urine protein-to-creatinine ratio (UPCR), indicator for kidneys' conditions.[333-335] Its clinical efficacy and safety were primarily established different clinical development programs (ALIGN, SONAR, ALARM). In these trials, a daily dose atrasentan (0.75 mg) reduced the risk of major renal events, as end-stage kidney disease, while clinical benefit in slowing the decline of kidney function is still under ongoing trials. Safety profiles across these studies indicate that while the drug is generally well-tolerated at low doses, with common adverse reactions including peripheral edema and anemia.[336-339] Atrasentan mechanism of action is based on a potent and highly selective endothelin A (ET-A) receptor antagonist. In the pathogenesis of IgAN, the endothelin system is overactivated, leading to glomerular hypertension, inflammation, and fibrosis. By selectively blocking the receptor, it counteracts the deleterious effects of ET-1, such as mesangial cell proliferation and podocyte injury, thereby reducing the leakage of proteins into the urine. This targeted approach aims to lower residual albuminuria that persists even under maximum tolerated doses of renin-angiotensin system (RAS) inhibitors, addressing a critical factor linked to long-term renal failure.[340,341]

A representative synthesis of atrasentan begins with construction of a nitrostyrene from piperonal (**276**) and subsequently forges the pyrrolidine core via reductive cyclization (Scheme 36). Condensation of **276** with nitromethane in AcOH, promoted by ammonium acetate, affords nitrostyrene **277**. Base-mediated coupling of **277** with ethyl 2-(4-methoxybenzoyl)acetate (**278**) using DBU in toluene (90 min) provides the corresponding 4-nitrobutyrate **279**. Reductive cyclization of **279** under hydrogenation conditions (H_2, Raney-Ni, EtOH) furnishes the (*cis*,*cis*)-pyrrolidine **280**, which is epimerized to the (*trans*,*trans*) isomer **281** upon treatment with NaOEt in refluxing EtOH. The resulting racemic ester **281** is then alkylated with 2-bromo-*N*,*N*-dibutylacetamide (**282**) and subjected to optical resolution using (*S*)-(+)-mandelic acid to afford enantioenriched ester **283**. Final saponification with NaOH in hot water delivers atrasentan.[342,343]

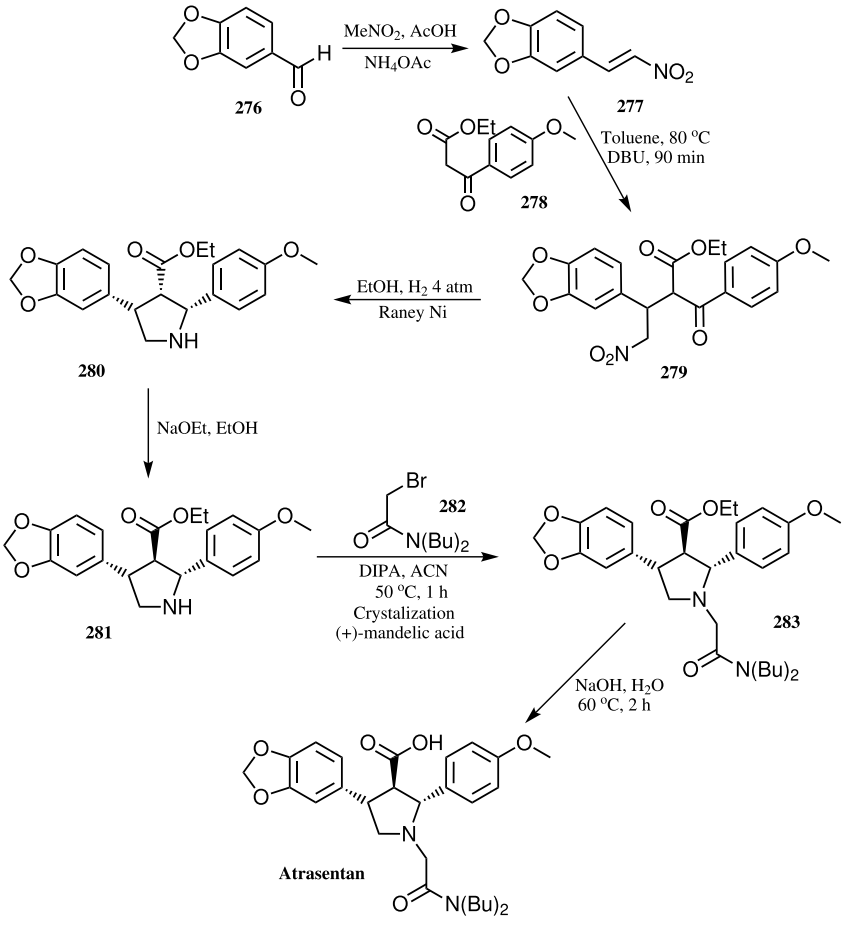

Scheme 36. Atrasentan synthesis.

A notable technical feature is the employment of Raney-nickel catalysis for the heterocyclic ring closure, a transformation that necessitates a subsequent NaOEt-mediated epimerization to correct the relative stereochemistry of the scaffold. Synthetic strategy is delineated by a reliance on classical optical resolution with (*S*)-(+)-mandelic acid to establish enantiopurity. While reliable, inherently limits the global material throughput compared to contemporary asymmetric inductions. The sequence concludes with a robust aqueous saponification to deliver the final API. Overall, this preparative framework illustrates a traditional yet effective approach to complex pyrrolidines, though it presents clear opportunities for process intensification, particularly regarding the development of a more stereoselective cyclization to circumvent the current epimerization-resolution relay.

3. Conclusions and Perspectives

The 2025 FDA approval landscape reinforces the continued centrality of small molecules as a source of first-in-class or best-in-class therapies, even as biologics expand their footprint. In 2025, the FDA approved 46 new drugs comprising 31 small-molecule entities, reflecting sustained innovation in privileged scaffolds and mechanism-driven design. At the therapeutic level, the portfolio remains strongly shaped by oncology-16 oncology approvals (34% of all approvals)-while also highlighting a broader diversification into cardiology, dermatology, hematology, and rare diseases. Importantly, the market signal accompanying these approvals suggests a shift toward therapeutic niches and smaller patient populations, with implications for how synthetic routes must be designed for agility, robustness, and cost-of-goods under tighter commercial volumes. From a synthetic chemistry standpoint, the routes analyzed throughout this review converge on a consistent message: end-to-end efficiency is disproportionately governed by a small number of yield-limiting operations, often late in the sequence, and frequently associated with high complexity, stereochemical requirements, or functionalization of densely substituted heteroaromatics. This is evident across multiple case studies where cumulative yields range from highly efficient sequences-e.g., zongertinib (ca. 46.1% overall yield, limited mainly by an *N*-acylation step)-to markedly eroded throughput driven by single low-yield steps, as in sunvozertinib (ca. 5.3% overall yield dominated by a 14% coupling), or peptide assembly bottlenecks such as elamipretide, where a key coupling at 22% constrains the overall efficiency to ca. 13%. In parallel, convergent planning can mitigate linear attrition but does not eliminate it, ziftomenib illustrates how fragment yields and a highly efficient final union still translate into a modest global yield when one branch remains inefficient.

Collectively, these examples underscore that future route innovation will be decided less by "can we make it?" and more by where we lose material, time, and sustainability margin-and how rapidly those losses can be engineered out. Looking forward, three directions appear particularly enabling for the next cycle of small-molecule innovation. First, data-driven retrosynthesis and AI-assisted route selection will increasingly influence decisions earlier in development, accelerating identification of step-economical and scalable disconnections-an evolution already aligned with the broader trajectory of AI adoption across pharma. Second, sustainability is moving from a "nice-to-have" to a design constraint, pushing the field toward greener solvents, higher catalyst efficiency, telescoping, and alternative activation modes that reduce waste and energy demand. Third, the community would benefit from a stronger norm of quantitative transparency (isolated yields, conversions, impurity profiles) in public disclosures-particularly patents-because incomplete reporting limits the ability to benchmark routes, identify true bottlenecks, and translate medicinal chemistry into manufacturable processes. In this sense, the 2025 portfolio is not only a snapshot of therapeutic innovation, but also a roadmap for where synthetic strategy, process intensification, and sustainability must co-evolve to deliver the next generation of medicines reliably and at scale.

Supplementary Information

Supplementary information is available free of charge at http://jbcs.sbq.org.br as PDF file.

Data Availability Statement

All data obtained in this research is available in the text.

Acknowledgments

The authors gratefully acknowledge the financial support provided by CNPq. We also thank UFRJ for providing research infrastructure.

Author Contributions

Authors contributed equally to this manuscript.

Rodrigo Octavio M. A. de Souza *is an Associate Professor at the Institute of Chemistry, Federal University of Rio de Janeiro (UFRJ), where he heads the Biocatalysis and Organic Synthesis Group. He holds a PhD in Natural Products Chemistry from UFRJ and has a distinguished international background as a visiting researcher at the University of Graz (Prof Oliver Kappe) and as a Humboldt Research Fellow (Prof Uwe Bornscheuer). A pioneer in establishing continuous-flow chemo-enzymatic processes in Brazil, his research focuses on sustainable and scalable methodologies for the pharmaceutical, cosmetics, and food industries. Beyond academia, he is the co-founder of Novasynth Tecnologia, a startup dedicated to automated continuous synthesis solutions and FlowPrint Innovations focused on automation and 3D printing. Dr. de Souza serves as the South American Editor for the Journal of Flow Chemistry, Associate Editor for RSC Advances (Royal Society of Chemistry) and Organic Chemistry Editor of Quimica Nova. He is a CNPq Productivity Fellow and has published extensively in the fields of flow chemistry, biocatalysis, and organic synthesis.*

Samir Cavalcante *obtained his PhD (2018) and MSc (2006) in Chemistry of Natural Products from the Walter Mors Institute for Natural Products Research (IPPN) at the Universidade Federal do Rio de Janeiro. As Organisation for the Prohibition of Chemical Weapons Fellow (OPCW), he was visiting researcher at Spiez Laboratory (Switzerland, 2012) and Finnish Institute for Verification of the Chemical Weapons Convention (VERIFIN, Finland, 2016). Currently, Cavalcante is the Organic Chemistry Researcher at Brazilian Army Institute of CBRN (OPCW Designated Laboratory, 2024-2025), United Nations Secretary-General's Mechanism (UNSGM) Qualified Expert, Patent Advisor at Licks Attorneys and Scientific Consultant at Asymmetra.*

Edgar Schaeffer *graduated in Chemistry at Federal Rural University of Rio de Janeiro (2015) and concluded his PhD in Natural Products Chemistry at Federal University of Rio de Janeiro in 2023. Schaeffer has expertise in Chemistry, with emphasis in Organic Chemistry - Organic Synthesis, working primarily on the following topics: Cross-coupling Reactions and structural modifications of flavonoids and quinones. Since 2022, Schaeffer has been contributing to the scientific endeavors of pharmaceutical companies. Currently, Schaeffer is the Founding Partner and Scientific Director of Asymmetra.*

Raquel Ana Capela Leão *is a researcher at the Biocatalysis and Organic Synthesis Group (BOSS) at the Institute of Chemistry, UFRJ. She holds a PhD in Organic Chemistry from Fluminense Federal University (UFF) and completed postdoctoral fellowships at the University of Aveiro (Portugal), UFRJ, and the University of Alicante (Spain). Her expertise lies in organic synthesis and biocatalysis, specifically in the application of lipases and the development of innovative synthetic methodologies. Her current work focuses on the implementation of chemoenzymatic processes in continuous flow systems for the efficient and sustainable production of Active Pharmaceutical Ingredients (APIs).*

Felipe Lopes Nunes da Silva *holds a degree in Chemistry from the Federal Institute of Education, Science and Technology of Rio de Janeiro (2017). He earned his MSc in Natural Products Chemistry (2021) and PhD in Chemistry (2025) from the Federal University of Rio de Janeiro, including a sandwich period at Karl-Franzens-Universität Graz, Austria, under the supervision of Prof Dr Christian Oliver Kappe. His current research focuses on the development of continuous-flow synthesis processes for active pharmaceutical ingredients (APIs), as well as the continuous synthesis of cannabinoids. He works as a chemical process development researcher at the startup Novasynth and as a postdoctoral researcher in the Biocatalysis and Organic Synthesis Group (BOSS Group) in Federal University of Rio de Janeiro under the supervision of Prof Dr Rodrigo O. M. A. de Souza.*

References

1. Fierce Biotech; *IMS Health Forecasts Global Pharmaceutical Market Growth of 4 - 6 Percent in 2010; Predicts 4 - 7 Percent Expansion Through 2013*. [Link] accessed in January 2026
2. IQVIA Institute for Human Data Science; *Global Medicine Spending to Reach $2.3 Trillion by 2028 as More Patients Get Access to Better Therapies, Says IQVIA Institute Report.* [Link] accessed in January 2026
3. Vélez, D. E.; Torres, B. L.; Hernández, G.; *Genes* **2025**, *16*, 376. [Crossref]

4. Song, C. H.; Han, J.-W.; *SpringerPlus* **2016**, *23*, 692. [Crossref]
5. Serrano, D. R.; Luciano, F. C.; Anaya, B. J.; Ongoren, B.; Kara, A.; Molina, G.; Ramirez, B. I.; Sánchez-Guirales, S. A.; Simon, J. A.; Tomietto, G.; Rapti, C.; Ruiz, H. K.; Rawat, S.; Kumar, D.; Lalatsa, A.; *Pharmaceutics* **2024**, *14*, 1328. [Crossref]
6. Wang, Q.; Sun, B.; Yi, Y.; Velkov, T.; Shen, J.; Dai, C.; Jiang, H.; *Int. J. Mol. Sci.* **2025**, *26*, 10037. [Crossref]
7. Abdelsayed, M.; *Int. J. Mol. Sci.* **2025**, *26*, 6996. [Crossref]
8. United States Food and Drug Administration (FDA); *Novel Drug Approvals for 2025*. [Link] accessed in January 2026
9. United States Food and Drug Administration (FDA); *Novel Drug Approvals at FDA*. [Link] accessed in January 2026
10. Baedeker, M.; Möller, C. C.; *Nat. Rev. Drug Discovery* **2026**, *25*, 91. [Crossref]
11. United States Food and Drug Administration (FDA); *FDA Grants Accelerated Approval to Sevabertinib for Non-Squamous Non-Small Cell Lung Cancer*. [Link] accessed in January 2026
12. Trillo Aliaga, P.; Spitaleri, G.; Attili, I.; Corvaja, C.; Battaiotto, E.; Angelopoulos, P. A.; Del Signore, E.; Passaro, A.; de Marinis, F.; *Molecules* **2025**, *30*, 2645. [Crossref]
13. Siegel, F.; Siegel, S.; Kotynkova, K.; Karsli Uzunbas, G.; Korr, D.; Tomono, H.; Andersen, S.; Denney, D.; Berger, M.; Schulze, V. K.; Lewis, T. A.; Kaplan, B.; Golfier, S.; Mortier, J.; Hillig, R. C.; Boemer, U.; Petersen, K.; Eis, K.; Williams, S.; Ruttinger, D.; Cherniack, A. D.; Loong, H. H.; Goto, K.; Grassi, P.; Meyerson, M.; Greulich, H.; *Cancer Discovery* **2026**, *16*, 81. [Crossref]
14. Le, X.; Kim, T. M.; Loong, H. H.; Prelaj, A.; Goh, B. C.; Li, L.; Fang, Y.; Lu, S.; Dong, X.; Wu, L.; Shinno, Y.; Daniele, G.; Yang, T. Y.; Kim, H. R.; Ruiter, G.; Zhao, J.; Novello, S.; Miao, L.; Janne, P. A.; Goto, K.; Ruttinger, D.; Descamps, T.; Brase, J. C.; Bao, W.; Li, R.; Brega, N.; Grassi, P.; Girard, N.; Tan, D. S.; *N. Engl. J. Med.* **2025**, *393*, 1819. [Crossref]
15. United States Food and Drug Administration (FDA); *FDA Approved Drug Products: HYRNUO® (Sevabertinib) Tablets, for Oral Use (label, November 2025).* [Link] accessed in January 2026
16. Siegel, S.; Siegel, F.; Schulze, V.; Graham, K.; Sülzle, D.; Bömer, U.; Korr, D.; Schröder, J.; Mönning, U.; Niehues, M.; Meyerson, M.; Greulich, H.; Kaplan, B.; *WO2020216781A1*, **2020**.
17. Kura Oncology, Inc.; Kyowa Kirin Co., Ltd.; *Kura Oncology and Kyowa Kirin announce FDA approval of KOMZIFTI™ (ziftomenib).* [Link] accessed in January 2026
18. Dali, S. A.; Al-Mashdali, A. F.; Kalfah, A.; Mohamed, S. F.; *Crit. Rev. Oncol. Hematol.* **2025**, *213*, 104783. [Crossref]
19. Mitra, A.; Ahsan, J. M.; Tabachri, M.; El-Shahat, T.; Leoni, M.; Dale, S.; *Clin. Transl. Sci.* **2025**, *18*, e70153. [Crossref]
20. Kura Oncology, Inc.; FDA Approved Drug Products: *KOMZIFTI (ziftomenib) Capsules, for Oral Use (Prescribing Information)*. [Link] accessed in January 2026
21. Rausch, J.; Dzama, M. M.; Dolgikh, N.; Stiller, H. L.; Bohl, S. R.; Lahrmann, C.; Kunz, K.; Kessler, L.; Echchannaoui, H.; Chen, C.-W.; Kindler, T.; Döhner, K.; Burrows, F.; Theobald, M.; Sasca, D.; Kühn, M. W. M.; *Haematologica* **2023**, *108*, 2837. [Crossref]
22. Wang, E. S.; Issa, G. C.; Erba, H. P.; Altman, J. K.; Montesinos, P.; DeBotton, S.; Walter, R. B.; Pettit, K.; Savona, M. R.; Shah, M. V.; Kremyanskaya, M.; Baer, M. R.; Foran, J. M.; Schiller, G.; Ades, L.; Heiblig, M.; Berthon, C.; Peterlin, P.; Rodriguez-Arboli, E.; Salamero, O.; Patnaik, M. M.; Papayannidis, C.; Grembecka, J.; Cierpicki, T.; Clegg, B.; Ray, J.; Linhares, B. M.; Nie, K.; Mitra, A.; Ahsan, J. M.; Tabachri, M.; Soifer, H. S.; Corum, D.; Leoni, M.; Dale, S.; Fathi, A. T.; *Lancet Oncol.* **2024**, *25*, 1310. [Crossref]
23. Wang, E. S.; Montesinos, P.; Foran, J.; Erba, H.; Rodriguez-Arboli, E.; Fedorov, K.; Heiblig, M.; Heidel, F. H.; Altman, J. K.; Baer, M. R.; Ades, L.; Pettit, K.; Peterlin, P.; Papayannidis, C.; Berthon, C.; Walter, R. B.; Shah, M. V.; Balasubramanian, S.; Khawandanah, M.; Salamero Garcia, O.; Bergeron, J.; Madanat, Y. F.; Roboz, G. J.; Ulrickson, M.; Redner, R. L.; McCloskey, J.; Pigneux, A.; de la Fuente Burguera, A.; Mitra, A.; Soifer, H. S.; Tabachri, M.; Zhang, Z.; Riches, M.; Corum, D.; Leoni, M.; Issa, G. C.; Fathi, A. T.; *J. Clin. Oncol.* **2025**, *43*, 3381. [Crossref]
24. Bakale, R. P.; Sengupta, D.; Sun, X.; Zhang, J.; Deng, X.; Cai, K.; Guo, L.; Li, C.; Zhu, L.; Haldar, A.; Kovvuri, V. R. R.; Naini, S. R.; Pappula, U.; Roy, S.; Senanayake, C. H.; Sirasani, G.; Yadaw, A.; *WO2025232874A1*, **2025**.
25. Keam, S. J.; *Drugs* **2026**, *86*, 135. [Crossref]
26. Lloyd, M. R.; Wander, S. A.; Hamilton, E.; Razavi, P.; Bardia, A.; *Ther. Adv. Med. Oncol.* **2022**, *14*, 17588359221113694. [Crossref]
27. Bhagwat, S. V.; Mur, C.; Vandekopple, M.; Zhao, B.; Shen, W.; Marugan, C.; Capen, A.; Kindler, L.; Stephens, J. R.; Huber, L.; Castanares, M. A.; Garcia-Tapia, D.; Cohen, J. D.; Bastian, J.; Mattioni, B.; Yuen, E.; Baker, T. K.; Rodriguez Cruz, V.; Fei, D.; Manro, J. R.; Pulliam, N.; Dowless, M. S.; Ortiz Ruiz, M. J.; Yu, C.; Puca, L.; Klippel, A.; Bacchion, F.; Ismail-Khan, R.; Rodrik-Outmezguine, V.; Peng, S. B.; Lallena, M. J.; Gong, X.; de Dios, A.; *Cancer Res.* **2025**, *85*, 777. [Crossref]
28. Jhaveri, K. L.; Lim, E.; Jeselsohn, R.; Ma, C. X.; Hamilton, E. P.; Osborne, C.; Bhave, M.; Kaufman, P. A.; Beck, J. T.; Manso Sanchez, L.; Parajuli, R.; Wang, H. C.; Tao, J. J.; Im, S. A.; Harnden, K.; Yonemori, K.; Dhakal, A.; Neven, P.; Aftimos, P.; Pierga, J. Y.; Lu, Y. S.; Larson, T.; Jerez, Y.; Sideras, K.; Sohn, J.; Kim, S. B.; Saura, C.; Bardia, A.; Sammons, S. L.; Bacchion, F.; Li, Y.; Yuen, E.; Estrem, S. T.; Rodrik-Outmezguine, V.; Nguyen, B.; Ismail-Khan, R.; Smyth, L.; Beeram, M.; *J. Clin. Oncol.* **2024**, *42*, 4173. [Crossref]
29. Jhaveri, K. L.; Jeselsohn, R.; Lim, E.; Hamilton, E. P.; Yonemori, K.; Beck, J. T.; Harnden, K.; Neven, P.; Aftimos, P.; Lu, Y. S.;

Sohn, J.; Kim, S. B.; Saura, C.; Bardia, A.; Bacchion, F.; Yuen, E.; Estrem, S. T.; Rodrik-Outmezguine, V.; Ismail-Khan, R.; Beeram, M.; *J. Clin. Oncol.* **2022**, *40*, 1021. [Crossref]

30. Jhaveri, K.; O'Shaughnessy, J.; Andre, F.; Goetz, M. P.; Harbeck, N.; Martín, M.; Bidard, F.-C.; Thomas, Z. M.; Young, S.; Ismail-Khan, R.; Smyth, L. M.; Gnant, M.; *Cancer Res.* **2023**, *83*, OT1-01-02. [Crossref]
31. Neven, P.; Stahl, N.; Losada, M. J. V.; Jimenez, M. M.; Kaufman, P. A.; Harbeck, N.; Hunt, K.; Carter, S. A.; Bidard, F. C.; Fasching, P.; Aftimos, P.G.; Wheatley, D.; Hamilton, E. P.; Aft, R.; Kulkarni, S.; Ismail-Khan, R.; Karacsonyi, C.; Estrem, S. T.; Ozbek, U.; Ciruelos, E. M.; *Ann. Oncol.* **2023**, *34*, S292. [Crossref]
32. Datta-Mannan, A.; Czeskis, B.; Shanks, E.; Yuen, E.; Hall, S.; Rodriguez Cruz, V.; Cassidy, K.; *Clin. Pharmacol. Drug Dev.* **2025**, *14*, 764. [Crossref]
33. United States Food and Drug Administration (FDA); *FDA Approved Drug Products: INLURIYO (Imlunestrant) Tablets, for Oral Use (label).* [Link] accessed in January 2026
34. United States Food and Drug Administration (FDA); *FDA Approves Imlunestrant for ER-Positive, HER2-Negative, ESR1-Mutated Advanced or Metastatic Breast Cancer*. [Link] accessed in January 2026
35. Cohen, J. D.; Sall, D. J.; *US2023242545A1*, **2020**.
36. Bastian, J. A.; Cohen, J. D.; Rubio, A.; Sall, D. J.; *WO2020014435A1*, **2020**.
37. Heymach, J. V.; Ruiter, G.; Ahn, M. J.; Girard, N.; Smit, E. F.; Planchard, D.; Wu, Y. L.; Cho, B. C.; Yamamoto, N.; Sabari, J. K.; Zhao, Y.; Tu, H. Y.; Yoh, K.; Nadal, E.; Sadrolhefazi, B.; Rohrbacher, M.; von Wangenheim, U.; Eigenbrod-Giese, S.; Zugazagoitia, J.; *N. Engl. J. Med.* **2025**, *392*, 2321. [Crossref]
38. Brazel, D.; Park, C. J.; Nagasaka, M.; *Crit. Rev. Oncol. Hematol.* **2025**, *215*, 104896. [Crossref]
39. United States Food and Drug Administration (FDA); *FDA Grants Accelerated Approval to Zongertinib for Non-Squamous NSCLC with HER2 TKD Activating Mutations*. [Link] accessed in January 2026
40. United States Food and Drug Administration (FDA); *FDA Approved Drug Products: Hernexeos (zongertinib) Tablets, for Oral Use (label, August 2025).* [Link] accessed in January 2026
41. Ismail, A.; Desai, A.; Boumber, Y.; *Front. Oncol.* **2025**, *15*, 1624124. [Crossref]
42. Wilding, B.; Woelflingseder, L.; Baum, A.; Chylinski, K.; Vainorius, G.; Gibson, N.; Waizenegger, I. C.; Gerlach, D.; Augsten, M.; Spreitzer, F.; Shirai, Y.; Ikegami, M.; Tilandyova, S.; Scharn, D.; Pearson, M. A.; Popow, J.; Obenauf, A. C.; Yamamoto, N.; Kondo, S.; Opdam, F. L.; Bruining, A.; Kohsaka, S.; Kraut, N.; Heymach, J. V.; Solca, F.; Neumuller, R. A.; *Cancer Discovery* **2025**, *15*, 119. [Crossref]
43. Chong, E.; Dong, W.; Li, R.; Mulder, J. A.; Trofimov, A.; *WO2025026901A1*, **2025**.
44. Werthmann, U.; Gao, J. J.; Li, H.; Mulder, J. A.; Omar, T. M.; *WO2024133302A1*, **2024**.
45. Li, Z.; Zhong, W.; Wang, J.; Zeng, Q.; Tsui, H.; Yang, Z.; Zhang, X.; *WO2019214634A1*, **2019**.
46. Lyssikatos, J. P.; Marmsater, F. P.; Zhao, Q.; Greschuk, J. M.; *WO2007059257A2*, **2007**.
47. Mantoulidis, A.; Dahmann, G.; Ettmayer, P.; Klein, C.; Steurer, S.; Waizenegger, I.; Zahn, S. K.; *WO2010026262A1*, **2010**.
48. Arrillaga-Romany, I.; Gardner, S. L.; Odia, Y.; Aguilera, D.; Allen, J. E.; Batchelor, T.; Butowski, N.; Chen, C.; Cloughesy, T.; Cluster, A.; de Groot, J.; Dixit, K. S.; Graber, J. J.; Haggiagi, A. M.; Harrison, R. A.; Kheradpour, A.; Kilburn, L. B.; Kurz, S. C.; Lu, G.; MacDonald, T. J.; Mehta, M.; Melemed, A. S.; Nghiemphu, P. L.; Ramage, S. C.; Shonka, N.; Sumrall, A.; Tarapore, R. S.; Taylor, L.; Umemura, Y.; Wen, P. Y.; *J. Clin. Oncol*. **2024**, *42*, 1542. [Crossref]
49. United States Food and Drug Administration (FDA); *FDA Grants Accelerated Approval to Dordaviprone for Diffuse Midline Glioma*. [Link] accessed in January 2026
50. Pathak, S. O.; Manohar, S. M.; *Biomolecules* **2025**, *15*, 463. [Crossref]
51. Prabhu, V. V.; Morrow, S.; Rahman Kawakibi, A.; Zhou, L.; Ralff, M. D.; Ray, J.; Jhaveri, A.; Ferrarini, I.; Lee, Y. S.; Parker, C.; Zhang, Y.; Borsuk, R.; Chang, W.-I.; Honeyman, J. N.; Tavora, F.; Carneiro, B.; Raufi, A. G.; Huntington, K. E.; Carlsen, L.; Louie, A.; Safran, H.; Seyhan, A.; Tarapore, R. S.; Schalop, L.; Stogniew, M.; Allen, J. E.; Oster, W.; El-Deiry, W. S.; *Neoplasia* **2020**, *22*, 725. [Crossref]
52. Teffera, Y.; Tippin, T.; Bartkus, A.; de Castro, F. A.; Faison, S. L.; Morrison, M.; Mullin, M. J.; Naderer, O.; *Clin. Pharmacol. Drug Dev.* **2025**, *14*, 549. [Crossref]
53. Odia, Y.; Koschmann, C.; Vitanza, N. A.; de Blank, P.; Aguilera, D.; Allen, J.; Daghistani, D.; Hall, M.; Khatib, Z.; Kline, C.; MacDonald, T.; Mueller, S.; Faison, S. L.; Allen, J. E.; Naderer, O. J.; Ramage, S. C.; Tarapore, R. S.; McGovern, S. L.; Khatua, S.; Zaky, W.; Gardner, S. L.; *Neuro Oncol.* **2024**, *26*, S155. [Crossref]
54. United States Food and Drug Administration (FDA); *FDA Approved Drug Products: MODEYSO (Dordaviprone) Capsules, for Oral Use (Label).* [Link] accessed in January 2026
55. Stogniew, M.; Allen, J. E.; *US2025241920A1*, **2025**.
56. Huang, Z.; Wang, K.; Cai, J.; Li, S.; *CN115477613A*, **2022**.
57. Hayashi, H.; *Lancet Respir. Med.* **2024**, *12*, 185. [Crossref]
58. Wang, M.; Yang, J. C.; Mitchell, P. L.; Fang, J.; Camidge, D. R.; Nian, W.; Chiu, C. H.; Zhou, J.; Zhao, Y.; Su, W. C.; Yang, T. Y.; Zhu, V. W.; Millward, M.; Fan, Y.; Huang, W. T.; Cheng, Y.; Jiang, L.; Brungs, D.; Bazhenova, L.; Lee, C. K.; Gao, B.; Xu, Y.; Hsu, W. H.; Zheng, L.; Janne, P. A.; *Cancer Discovery* **2022**, *12*, 1676. [Crossref]
59. Mitsudomi, T.; *Transl. Lung Cancer Res.* **2025**, *14*, 334. [Crossref]

60. Wang, M.; Fan, Y.; Sun, M.; Wang, Y.; Zhao, Y.; Jin, B.; Hu, Y.; Han, Z.; Song, X.; Liu, A.; Tang, K.; Ding, C.; Liang, L.; Wu, L.; Gao, J.; Wang, J.; Cheng, Y.; Zhou, J.; He, Y.; Dong, X.; Yao, Y.; Yu, Y.; Wang, H.; Sun, S.; Huang, J.; Fang, J.; Li, W.; Wang, L.; Ren, X.; Zhou, C.; Hu, Y.; Zhao, D.; Yang, R.; Xu, F.; Huang, Y.; Pan, Y.; Cui, J.; Xu, Y.; Yang, Z.; Shi, Y.; *Lancet Respir. Med.* **2024**, *12*, 217. [Crossref]
61. United States Food and Drug Administration (FDA); *FDA Grants Accelerated Approval to Sunvozertinib for Metastatic Non-Small Cell Lung Cancer with EGFR Exon 20 Insertion Mutations*. [Link] accessed in January 2026
62. Dhillon, S.; *Drugs* **2023**, *83*, 1629. [Crossref]
63. United States Food and Drug Administration (FDA); *FDA Approved Drug Products: ZEGFROVY (Sunvozertinib) Tablets, for Oral Use (label).* [Link] accessed in January 2026
64. Wang, M.; Xu, Y.; Huang, W. T.; Su, W. C.; Gao, B.; Lee, C. K.; Fang, J.; Zhu, X.; Yang, Z.; Jänne, P. A.; Yang, J. C.; *Lung Cancer* **2025**, *199*, 108053. [Crossref]
65. Xu, Y.; Chen, M.; Gao, X.; Liu, X.; Zhao, J.; Zhong, W.; Wang, M.; Lang, H.; Yip, C.; Wang, M.; *Cancer Lett.* **2025**, *630*, 217904. [Crossref]
66. Yang, Z.; Zhang, X.; *US11896597B2*, **2024**.
67. Wang, Y.-T.; Yang, P.-C.; Zhang, J.-Y.; Sun, J.-F. *Molecules* **2024**, *29*, 1448. [Crossref]
68. Li, Z.; Zou, H.; Zhu, W.; Shen, C.; Wang, R.; Liu, W.; Chen, X.; Tsui, H.; Yang, Z.; Zhang, X.; *WO2019149164A1*, **2019**.
69. Khan, I.; Sahar, A.; Numra, S.; Saha, N.; Nidhi; Parveen, R.; *Expert Opin. Pharmacother.* **2025**, *26*, 765. [Crossref]
70. United States Food and Drug Administration (FDA); *FDA Approves Taletrectinib for ROS1-Positive Non-Small Cell Lung Cancer*. [Link] accessed in January 2026
71. Waliany, S.; Lin, J. J.; *J. Clin. Oncol.* **2024**, *42*, 2622. [Crossref]
72. Nagasaka, M.; Brazel, D.; Ou, S. I.; *Expert Opin. Investig. Drugs* **2024**, *33*, 79. [Crossref]
73. Pérol, M.; Li, W.; Pennell, N. A.; Liu, G.; Ohe, Y.; De Braud, F.; Nagasaka, M.; Felip, E.; Xiong, A.; Zhang, Y.; Fan, H.; Wang, X.; Li, S.; Lai, R. K.; Ran, F.; Zhang, X.; Chen, W.; Bazhenova, L.; Zhou, C.; *J. Clin. Oncol.* **2025**, *43*, 1920. [Crossref]
74. United States Food and Drug Administration (FDA); *FDA Approved Drug Products: Ibtrozi (taletrectinib) capsules, for oral administration (label, June 2025)*. [Link] accessed in January 2026
75. Takeda, Y.; Yoshikawa, K.; Kagoshima, Y.; Yamamoto, Y.; Tanaka, R.; Tominaga, Y.; Kiga, M.; Hamada, Y.; *WO2013183578A1*, **2013**.
76. Zhou, F.; Chen, D. D.; Guo, F.; Ren, Z.; Shang, L.; Wang, H.; *WO2023220967A1*, **2023**.
77. Caldwell, T. M.; Ahn, Y. M.; Bulfer, S. L.; Leary, C. B.; Hood, M. M.; Lu, W. P.; Vogeti, L.; Vogeti, S.; Kaufman, M. D.; Wise, S. C.; Le Bourdonnec, B.; Smith, B. D.; Flynn, D. L.; *Bioorg. Med. Chem. Lett.* **2022**, *74*, 128928. [Crossref]
78. Smith, B. D.; Kaufman, M. D.; Wise, S. C.; Ahn, Y. M.; Caldwell, T. M.; Leary, C. B.; Lu, W. P.; Tan, G.; Vogeti, L.; Vogeti, S.; Wilky, B. A.; Davis, L. E.; Sharma, M.; Ruiz-Soto, R.; Flynn, D. L.; *Mol. Cancer Ther.* **2021**, *20*, 2098. [Crossref]
79. United States Food and Drug Administration (FDA); *FDA approves vimseltinib for symptomatic tenosynovial giant cell tumor*. [Link] accessed in January 2026
80. United States Food and Drug Administration (FDA); *FDA Approved Drug Products: Romvimza (Vimseltinib) Capsules, for Oral Use (Label, February 2025)*. [Link] accessed in January 2026
81. Dou, F.; Lu, D.; Gao, J.; *Intractable Rare Dis. Res.* **2025**, *14*, 143. [Crossref]
82. Gelderblom, H.; Bhadri, V.; Stacchiotti, S.; Bauer, S.; Wagner, A. J.; van de Sande, M.; Bernthal, N. M.; López Pousa, A.; Razak, A. A.; Italiano, A.; Ahmed, M.; Le Cesne, A.; Tinoco, G.; Boye, K.; Martín-Broto, J.; Palmerini, E.; Tafuto, S.; Pratap, S.; Powers, B. C.; Reichardt, P.; Casado Herráez, A.; Rutkowski, P.; Tait, C.; Zarins, F.; Harrow, B.; Sharma, M. G.; Ruiz-Soto, R.; Sherman, M. L.; Blay, J. Y.; Tap, W. D.; *Lancet* **2024**, *403*, 2709. [Crossref]
83. Kostik, E.; Gelormini, A.; Kaufman, M. D.; *WO2025231105A1*, **2025**.
84. Flynn, D.; Smith, B.; Soto, R.; Kuida, K.; *WO2020139828A1*, **2020**.
85. Ahn, Y.; Vogeti, L.; Caldwell, T. M.; Kaufman, M. D.; Flynn, D. L.; *WO2014145025A2*, **2014**.
86. Hoy, S. M.; *Drugs* **2025**, *85*, 977. [Crossref]
87. United States Food and Drug Administration (FDA); *FDA Approves Mirdametinib for Adult and Pediatric Patients with Neurofibromatosis Type 1 who have Symptomatic Plexiform Neurofibromas not Amenable to Complete Resection*. [Link] accessed in January 2026
88. Oztosun, G.; Armstrong, A.; Hirbe, A. C.; *Expert Opin. Investig. Drugs* **2025**, *34*, 665. [Crossref]
89. Ioannou, M.; Lalwani, K.; Ayanlaja, A. A.; Chinnasamy, V.; Pratilas, C. A.; Schreck, K. C.; *Mol. Cancer Ther.* **2024**, *23*, 1261. [Crossref]
90. Moertel, C. L.; Hirbe, A. C.; Shuhaiber, H. H.; Bielamowicz, K.; Sidhu, A.; Viskochil, D.; Weber, M. D.; Lokku, A.; Smith, L. M.; Foreman, N. K.; Hajjar, F. M.; McNall-Knapp, R. Y.; Weintraub, L.; Antony, R.; Franson, A. T.; Meade, J.; Schiff, D.; Walbert, T.; Ambady, P.; Bota, D. A.; Campen, C. J.; Kaur, G.; Klesse, L. J.; Maraka, S.; Moots, P. L.; Nevel, K.; Bornhorst, M.; Aguilar-Bonilla, A.; Chagnon, S.; Dalvi, N.; Gupta, P.; Khatib, Z.; Metrock, L. K.; Nghiemphu, P. L.; Roberts, R. D.; Robison, N. J.; Sadighi, Z.; Stapleton, S.; Babovic-Vuksanovic, D.; Gershon, T. R.; *J. Clin. Oncol.* **2025**, *43*, 716. [Crossref]
91. Weiss, B. D.; Wolters, P. L.; Plotkin, S. R.; Widemann, B. C.; Tonsgard, J. H.; Blakeley, J.; Allen, J. C.; Schorry, E.; Korf, B.; Robison, N. J.; Goldman, S.; Vinks, A. A.; Emoto, C.; Fukuda,

T.; Robinson, C. T.; Cutter, G.; Edwards, L.; Dombi, E.; Ratner, N.; Packer, R.; Fisher, M. J.; *J. Clin. Oncol.* **2021**, *39*, 797. [Crossref]

92. United States Food and Drug Administration (FDA); *FDA Approved Drug Products: GOMEKLI (Mirdametinib) Capsules and Tablets, for Oral and Oral Suspension Use (Label).* [Link] accessed in January 2026
93. Armstrong, A. E.; Belzberg, A. J.; Crawford, J. R.; Hirbe, A. C.; Wang, Z. J.; *BMC Cancer* **2023**, *23*, 553. [Crossref]
94. Barrett, S. D.; Biwersi, C.; Kaufman, M.; Tecle, H.; Warmus, J. S.; *WO0206213A2*, **2002**.
95. Irdam, E. A.; Nanninga, T. N.; Davis, E. M.; Tjiong, H. I.; Weaver, J. K.; Winkle, D. D.; *WO2006134469A1*, **2006**.
96. Gavriilaki, E.; Dolgyras, P.; Konstantinidis, I.; Mallouri, D.; Salvaras, G.; Demosthenous, C.; Batsis, I.; Vardi, A.; Papadopoulos, I.; Tsokkou, S.; Bousiou, Z.; Karavalakis, G.; Varelas, C.; Panteliadou, A.; Spyridis, N.; Syrigou, A.; Marvaki, A.; Papathanasiou, M.; Papalexandri, A.; Lalayanni, C.; Vadikoliou, C.; Athanasiadou, A.; Sakellari, I.; *Pharmaceuticals* **2025**, *18*, 1631. [Crossref]
97. United States Food and Drug Administration (FDA); *FDA Approves Treosulfan with Fludarabine as a Preparative Regimen for alloHSCT in Adult and Pediatric Patients with AML or MDS*. [Link] accessed in January 2026
98. Uzay, A.; Gündoğdu, Y.; Koşan, B.; Yetiş, T.; Kartı, S. S.; *Cancer Med.* **2024**, *13*, e7292. [Crossref]
99. Pasic, I.; Moya, T. A.; Remberger, M.; Chen, C.; Gerbitz, A.; Kim, D. D. H.; Kumar, R.; Lam, W.; Law, A. D.; Lipton, J. H.; Michelis, F. V.; Novitzky-Basso, I.; Viswabandya, A.; Mattsson, J.; *Transplant. Cell Ther.* **2024**, *30*, 681.e1. [Crossref]
100. Beelen, D. W.; Stelljes, M.; Reményi, P.; Wagner-Drouet, E. M.; Dreger, P.; Bethge, W.; Ciceri, F.; Stölzel, F.; Junghanß, C.; Labussiere-Wallet, H.; Schaefer-Eckart, K.; Grigoleit, G. U.; Scheid, C.; Patriarca, F.; Rambaldi, A.; Niederwieser, D.; Hilgendorf, I.; Russo, D.; Socié, G.; Holler, E.; Glass, B.; Casper, J.; Wulf, G.; Basara, N.; Bieniaszewska, M.; Stuhler, G.; Verbeek, M.; La Rocca, U.; Finke, J.; Benedetti, F.; Pichlmeier, U.; Klein, A.; Baumgart, J.; Markiewicz, M.; *Am. J. Hematol.* **2022**, *97*, 1023. [Crossref]
101. United States Food and Drug Administration (FDA); *FDA Approved Drug Products: GRAFAPEX (Treosulfan) for Injection, for Intravenous Use (label)*. [Link] accessed in January 2026
102. Sharma, A. K.; Upadhyay, S.; Dua, H.; Musmade, S.; Singh, G.; Lahiri, S.; Cabri, W.; *WO2019043587A2*, **2019**.
103. Blair, H. A.; *Drugs* **2025**, *85*, 1319. [Crossref]
104. United States Food and Drug Administration (FDA); *FDA Grants Accelerated Approval to the Combination of Avutometinib and Defactinib for KRAS-Mutated Recurrent Low-Grade Serous Ovarian Cancer*. [Link] accessed in January 2026
105. Verastem Oncology; *FDA Approved Drug Products: Avmapki Fakzynja Co-Pack (avutometinib capsules; defactinib tablets), for oral use (Prescribing Information).* [Link] accessed in January 2026
106. Martinez-Garcia, M.; Banerji, U.; Albanell, J.; Bahleda, R.; Dolly, S.; Kraeber-Bodere, F.; Rojo, F.; Routier, E.; Guarin, E.; Xu, Z. X.; Rueger, R.; Tessier, J. J.; Shochat, E.; Blotner, S.; Naegelen, V. M.; Soria, J. C.; *Clin. Cancer Res.* **2012**, *18*, 4806. [Crossref]
107. Wang, H.; Chi, L.; Yu, F.; Dai, H.; Si, X.; Gao, C.; Wang, Z.; Liu, L.; Zheng, J.; Ke, Y.; Liu, H.; Zhang, Q.; *Bioorg. Med. Chem.* **2022**, *70*, 116922. [Crossref]
108. Banerjee, S. N.; Van Nieuwenhuysen, E.; Aghajanian, C.; D'Hondt, V.; Monk, B. J.; Clamp, A.; Prendergast, E.; Oaknin, A.; Ring, K.; Colombo, N.; Holloway, R. W.; Rodrigues, M.; Chon, H. S.; Gourley, C.; Santin, A. D.; Thaker, P. H.; Gennigens, C.; Newman, G.; Salinas, E.; Youssoufian, H.; Moore, K. N.; Lustgarten, S.; O'Malley, D. M.; Van Gorp, T.; Grisham, R. N.; *Future Oncol.* **2025**, *21*, 3859. [Crossref]
109. Banerjee, S.; Krebs, M. G.; Greystoke, A.; Garces, A. I.; Perez, V. S.; Terbuch, A.; Shinde, R.; Caldwell, R.; Grochot, R.; Rouhifard, M.; Ruddle, R.; Gurel, B.; Swales, K.; Tunariu, N.; Prout, T.; Parmar, M.; Symeonides, S.; Rekowski, J.; Yap, C.; Sharp, A.; Paschalis, A.; Lopez, J.; Minchom, A.; de Bono, J. S.; Banerji, U.; *Nat. Med.* **2025**, *31*, 3074. [Crossref]
110. Hartwich, T. M. P.; Mansolf, M.; Demirkiran, C.; Greenman, M.; Bellone, S.; McNamara, B.; Nandi, S. P.; Alexandrov, L. B.; Yang-Hartwich, Y.; Coma, S.; Pachter, J.; Santin, A. D.; *Cancer Med.* **2024**, *13*, e70210. [Crossref]
111. Murakata, M.; Ikeda, T.; Ichige, T.; *WO2013035754A1*, **2013**.
112. Iikura, H.; Hyoudoh, I.; Aoki, T.; Furuichi, N.; Matsushita, M.; Watanabe, F.; Ozawa, S.; Sakaitani, M.; Ho, P.-S.; Tomii, Y.; Takanashi, K.; Harada, N.; *WO2007091736A1*, **2007**.
113. Qin, Q.; Wang, R.; Fu, Q.; Zhang, G.; Wu, T.; Liu, N.; Lv, R.; Yin, W.; Sun, Y.; Sun, Y.; Zhao, D.; Cheng, M.; *J. Enzyme Inhib. Med. Chem.* **2022**, *37*, 2241. [Crossref]
114. Hartman, J. J.; Hwee, D. T.; Robert-Paganin, J.; Chuang, C.; Chin, E. R.; Edell, S.; Lee, K. H.; Madhvani, R.; Paliwal, P.; Pernier, J.; Sarkar, S. S.; Schaletzky, J.; Schauer, K.; Taheri, K. D.; Wang, J.; Wehri, E.; Wu, Y.; Houdusse, A.; Morgan, B. P.; Malik, F. I.; *Nat. Cardiovasc. Res.* **2024**, *3*, 1003. [Crossref]
115. Saleh, D.; Eskandari, M.; Choudhury, L.; *Future Cardiol.* **2025**, *21*, 685. [Crossref]
116. Sebastian, S. A.; Padda, I.; Lehr, E. J.; Johal, G.; *Am. J. Cardiovasc. Drugs* **2023**, *23*, 519. [Crossref]
117. Maron, M. S.; Masri, A.; Nassif, M. E.; Barriales-Villa, R.; Arad, M.; Cardim, N.; Choudhury, L.; Claggett, B.; Coats, C. J.; Dungen, H. D.; Garcia-Pavia, P.; Hagege, A. A.; Januzzi, J. L.; Lee, M. M. Y.; Lewis, G. D.; Ma, C. S.; Michels, M.; Olivotto, I.; Oreziak, A.; Owens, A. T.; Spertus, J. A.; Solomon, S. D.; Tfelt-Hansen, J.; van Sinttruije, M.; Veselka, J.; Watkins, H.;

Jacoby, D. L.; Heitner, S. B.; Kupfer, S.; Malik, F. I.; Meng, L.; Wohltman, A.; Abraham, T. P.; *N. Engl. J. Med.* **2024**, *390*, 1849. [Crossref]

118. Xu, D.; Divanji, P.; Griffith, A.; Sukhun, R.; Cheplo, K.; Li, J.; German, P.; *Pharmacol. Res. Perspect.* **2024**, *12*, e70006. [Crossref]
119. United States Food and Drug Administration (FDA); *FDA Approved Drug Products: MYQORZO (aficamten) Tablets, for Oral Use (label, December 2025)*. [Link] accessed in January 2026
120. United States Food and Drug Administration (FDA); *FDA Approves Drug to Improve Functional Capacity and Symptoms in Adults with Rare Inherited Heart Condition*. [Link] accessed in January 2026
121. Zhao, X.; Liu, H.; Tian, W.; Fang, L.; Yu, M.; Wu, X.; Liu, A.; Wan, R.; Li, L.; Luo, J.; Li, Y.; Liu, B.; He, Y.; Chen, X.; Li, Y.; Xu, D.; Wang, H.; Han, X.; *Front. Pharmacol.* **2023**, *14*, 1227470. [Crossref]
122. Maron, M. S.; Masri, A.; Choudhury, L.; Olivotto, I.; Saberi, S.; Wang, A.; Garcia-Pavia, P.; Lakdawala, N. K.; Nagueh, S. F.; Rader, F.; Tower-Rader, A.; Turer, A.T.; Coats, C.; Fifer, M. A.; Owens, A.; Solomon, S. D.; Watkins, H.; Barriales-Villa, R.; Kramer, C. M.; Wong, T. C.; Paige, S. L.; Heitner, S. B.; Kupfer, S.; Malik, F. I.; Meng, L.; Wohltman, A.; Abraham, T.; *J. Am. Coll. Cardiol.* **2023**, *81*, 34. [Crossref]
123. Garcia-Pavia, P.; Maron, M. S.; Masri, A.; Merkely, B.; Nassif, M. E.; Peña-Peña, M. L.; Barriales-Villa, R.; Bilen, O.; Burroughs, M.; Claggett, B.; Costabel, J. P.; Correia, E. B.; Dybro, A. M.; Elliott, P.; Hegde, S. M.; Lakdawala, N. K.; Lewis, G. D.; Mann, A.; Miao, Z. M.; Nair, A.; Poulsen, S. H.; Reant, P.; Schulze, P. C.; Solomon, S. D.; Wang, A.; Sohn, R.; Berhane, I.; Heitner, S. B.; Jacoby, D. L.; Kupfer, S.; Malik, F. I.; Wohltman, A.; Fifer, M. A.; *N. Engl. J. Med.* **2025**, *393*, 949. [Crossref]
124. Chuang, C.; Morgan, B. P.; Vanderwal, M.; Wang, W.; Ashcraft, L. W.; *WO2019144041A1*, **2019**.
125. Tom, N.; Pfeiffer, M.; Andersen, D.; Gao, Q.; *WO2021011807A1*, **2021**.
126. Calvert, P.; Gupta, D.; *Future Cardiol.* **2024**, *20*, 163. [Crossref]
127. United States Food and Drug Administration (FDA); *FDA Approves Drug for Type of Abnormally Fast Heart Rhythm*. [Link] accessed in January 2026
128. Jha, M.; Song, D.; Kung, A.; Lo, S.; Sacher, A.; Ang, S. P.; Akthar, A.; Jain, H.; Ahmed, R.; Bates, M.; Lee, S.; Goldbarg, S.; *J. Clin. Med.* **2025**, *14*, 3720. [Crossref]
129. Macech, A.; Bragazzi, N. L.; Chirico, F.; Cander, B.; Pruc, M.; Rafique, Z.; Peacock, W. F.; Ziapour, A.; Szarpak, L.; Salak, A.; Jaguszewski, M. J.; *Cardiol. J.* **2024**, *31*, 640. [Crossref]
130. Abuelazm, M.; Kambalapalli, S.; Saleh, O.; Elzeftawy, M. A.; Albakri, K.; Gowaily, I.; Abdelazeem, B.; *Am. J. Cardiovasc. Drugs* **2023**, *23*, 379. [Crossref]
131. Ip, J. E.; Wight, D.; Yue, C. S.; Nguyen, D.; Plat, F.; Stambler, B. S.; *Clin. Pharmacol. Drug Dev.* **2024**, *13*, 367. [Crossref]
132. Milestone Pharmaceuticals Inc.; *FDA Approved Drug Products: CARDAMYST™ (etripamil) Nasal Spray (Prescribing Information, December 2025)*. [Link] accessed in January 2026
133. Ip, J. E.; Coutu, B.; Bennett, M. T.; Pandey, A. S.; Stambler, B. S.; Sager, P.; Chen, M.; Shardonofsky, S.; Plat, F.; Camm, A. J.; *J. Am. Heart Assoc.* **2023**, *12*, e028227. [Crossref]
134. Martin, P. M.; *WO2016165014A1*, **2016**.
135. Maguire, M. P.; Rioux, E.; Leighton, H. J.; *WO2008156820A1*, **2008**.
136. Bibi, L.; Azam, H.; Yaseen, F.; *Ir. J. Med. Sci.* **2025**. [Crossref]
137. Blair, H. A.; *Drugs* **2025**, *85*, 1499. [Crossref]
138. KalVista Pharmaceuticals, Inc.; *KalVista Pharmaceuticals Announces FDA Approval of EKTERLY® (sebetralstat), First and Only Oral On-demand Treatment for Hereditary Angioedema*. [Link] accessed in January 2026
139. Farkas, H.; Balla, Z.; *Expert Opin. Pharmacother.* **2025**, *26*, 685. [Crossref]
140. KalVista Pharmaceuticals, Inc.; *FDA Approved Drug Products: EKTERLY (sebetralstat) Tablets, for Oral Use (Prescribing Information, July 2025)*. [Link] accessed in January 2026
141. Farkas, H.; Anderson, J.; Bouillet, L.; Caballero, T.; Cancian, M.; Craig, T.; Fukunaga, A.; Grivcheva-Panovska, V.; Guilarte, M.; Honda, D.; Kanarek, H.; Kiani-Alikhan, S.; Kinaciyan, T.; Leguevaques, D.; Longhurst, H. J.; Magerl, M.; Manning, M. E.; Martinez-Saguer, I.; Melamed, I.; O'Connor, M. E.; Peter, J.; Savic, S.; Soteres, D. F.; Staevska, M.; Staubach-Renz, P.; Stobiecki, M.; Tachdjian, R.; Valerieva, A.; Yong, P. F. K.; Hao, J.; Iverson, M.; Smith, M. D.; Yea, C. M.; Audhya, P. K.; Aygoren-Pursun, E.; Bernstein, J. A.; Cohn, D. M.; Lumry, W. R.; Riedl, M. A.; Zanichelli, A.; Maurer, M.; *J. Allergy Clin. Immunol. Pract.* **2025**, *13*, P3094. [Crossref]
142. Qadri, M.; Iqbal, M. U.; Hajj, F.; *Ann. Med. Surg.* **2025**, *87*, 9141. [Crossref]
143. Davie, R. L.; Edwards, H. J.; Evans, D. M.; Hodgson, S. T.; Stocks, M. J.; Smith, A. J.; Rushbrooke, L. J.; Pethen, S. J.; Roe, M. B.; Clark, D. E.; McEwan, P. A.; Hampton, S. L.; *J. Med. Chem.* **2022**, *65*, 13629. [Crossref]
144. United States Food and Drug Administration (FDA); *FDA Approves 1st Drug for Thymidine Kinase 2 Deficiency, a very Rare Mitochondrial Disease*. [Link] accessed in January 2026
145. Chow, E.; Miller, L.; Clearman, A.; Arnold, P.; Koenig, M. K.; Russo, S. N.; *Mol. Genet. Metab.* **2025**, *145*, 109159. [Crossref]
146. Domínguez-González, C.; Hernández-Laín, A.; Rivas, E.; Hernández-Voth, A.; Sayas Catalán, J.; Fernández-Torrón, R.; Fuiza-Luces, C.; García García, J.; Morís, G.; Olivé, M.; Miralles, F.; Díaz-Manera, J.; Caballero, C.; Méndez-Ferrer, B.; Martí, R.; García Arumi, E.; Badosa, M. C.; Esteban, J.; Jimenez-Mallebrera, C.; Encinar, A. B.; Arenas, J.; Hirano,

M.; Martin, M. Á.; Paradas, C.; *Orphanet J. Rare Dis.* **2019**, *14*, 100. [Crossref]
147. Domínguez-González, C.; Madruga-Garrido, M.; Hirano, M.; Martí, I.; Martín, M. A.; Munell, F.; Nascimento, A.; Olivé, M.; Quan, J.; Sardina, M. D.; Martí, R.; Paradas, C.; *Orphanet J. Rare Dis.* **2021**, *16*, 407. [Crossref]
148. ClinicalTrials.gov; *NCT03701568*. [Link] accessed in January 2026
149. ClinicalTrials.gov; *NCT03845712*. [Link] accessed in January 2026
150. ClinicalTrials.gov; *NCT05017818*. [Link] accessed in January 2026
151. ClinicalTrials.gov; *NCT06590493*. [Link] accessed in January 2026
152. Hirano, M.; Osorio, A. N.; Ma, Y.; Boudiaf, N.; Kim, R.; VanMeter, S.; Brunnert, M.; Domínguez-González, C.; *Neurology* **2025**, *104*, 3690. [Crossref]
153. United States Food and Drug Administration (FDA); *Kygevvi Prescribing Information*. [Link] accessed in January 2026
154. Lopez-Gomez, C.; Levy, R. J.; Sanchez-Quintero, M. J.; Juanola-Falgarona, M.; Barca, E.; Garcia-Diaz, B.; Tadesse, S.; Garone, C.; Hirano, M.; *Ann. Neurol.* **2017**, *81*, 641. [Crossref]
155. Stealth BioTherapeutics Inc.; *Stealth BioTherapeutics Announces FDA Accelerated Approval of FORZINITY™ (elamipretide) injection, the First Therapy for Progressive and Life-limiting Ultra-rare Genetic Disease Barth Syndrome*. [Link] accessed in January 2026
156. United States Food and Drug Administration (FDA); *FDA Grants Accelerated Approval to First Treatment for Barth Syndrome*. [Link] accessed in January 2026
157. Patel, P. S.; Pabla, N. S.; Bajwa, A.; *Semin. Nephrol.* **2026**, *46*, 151676. [Crossref]
158. Radovic, M.; Gartzke, L. P.; Wink, S. E.; van der Kleij, J. A.; Politiek, F. A.; Krenning, G.; *Biomolecules* **2025**, *15*, 614. [Crossref]
159. Sabbah, H. N.; Alder, N. N.; Sparagna, G. C.; Bruce, J. E.; Stauffer, B. L.; Chao, L. H.; Pitceathly, R. D. S.; Maack, C.; Marcinek, D. J.; *Biomed. Pharmacother.* **2025**, *187*, 118056. [Crossref]
160. ClinicalTrials.gov; *NCT05162768*. [Link] accessed in January 2026
161. ClinicalTrials.gov; *NCT03098797*. [Link] accessed in January 2026
162. ClinicalTrials.gov; *NCT03323749*. [Link] accessed in January 2026
163. Tung, C.; Varzideh, F.; Farroni, E.; Mone, P.; Kansakar, U.; Jankauskas, S. S.; Santulli, G.; *Int. J. Mol. Sci.* **2025**, *26*, 944. [Crossref]
164. Nhu, N. T.; Xiao, S. Y.; Liu, Y.; Kumar, V. B.; Cui, Z. Y.; Lee, S. D.; *Front. Integr. Neurosci.* **2022**, *15*, 747901. [Crossref]
165. Duncan, S.; Wilson, D. T.; *WO2016144905A1*, **2016**.
166. Zhao, X.; Zheng, M.; Yu, X.; Gao, H.; Cornille, F.; *WO2015197723A*1, **2015**.
167. PTC Therapeutics, Inc.; *Sephience*. [Link] accessed in January 2026
168. PTC Therapeutics, Inc.; *PTC Therapeutics Announces FDA Approval of Sephience™ (sepiapterin) for the Treatment of Children and Adults Living with Phenylketonuria (PKU)*. [Link] accessed in January 2026
169. European Medicines Agency (EMA); Sephience (EPAR). [Link] accessed in January 2026
170. United States Food and Drug Administration (FDA); *Search Orphan Drug Designations and Approvals - Sephience*. [Link] accessed in January 2026
171. Muntau, A. C.; Longo, N.; Ezgu, F.; Schwartz, I. V. D.; Lah, M.; Bratkovic, D.; Margvelashvili, L.; Kiykim, E.; Zori, R.; Campistol Plana, J.; Bélanger-Quintana, A.; Lund, A.; Guilder, L.; Chakrapani, A.; Mungan, H. N.; Guimas, A.; Cabrales Guerra, I. D. C.; MacDonald, A.; Ingalls, K.; Smith, N.; *Lancet* **2024**, *404*, 1333. [Crossref]
172. Smith, N.; Longo, N.; Levert, K.; Hyland, K.; Blau, N.; *Mol. Genet. Metab.* **2019**, *126*, 406. [Crossref]
173. ClinicalTrials.gov; *NCT06302348*. [Link] accessed in January 2026
174. Muntau, A. C.; Gallagher, S.; Lah, M.; Belanger-Quintana, A.; Longo, N.; *J. Comp. Eff. Res.* **2026**, *15*, e250116. [Crossref]
175. Harding, C. O.; *Lancet* **2024**, *404*, 1284. [Crossref]
176. Vásquez-Vivar, J.; Duquaine, D.; Whitsett, J.; Kalyanaraman, B.; Rajagopalan, S.; *Arterioscler. Thromb. Vasc. Biol.* **2002**, *22*, 1655. [Crossref]
177. Shiro, Y.; Murata, S.; Iwamatsu, F.; *WO2009047902A1*, **2009**.
178. Innoviva Specialty Therapeutics, Inc.; *U.S. FDA Approves NUZOLVENCE® (zoliflodacin), a First-in-Class, Single-dose, Oral Antibiotic for the Treatment of Uncomplicated Urogenital Gonorrhea in Adults and Adolescents*. [Link] accessed in January 2026
179. Global Antibiotic Research & Development Partnership (GARDP); [Link] accessed in January 2026
180. Innoviva Specialty Therapeutics, Inc.; *Nuzolvence*. [Link] accessed in January 2026
181. United States Food and Drug Administration (FDA); *FDA Approves Two Oral Therapies to Treat Gonorrhea*. [Link] accessed in January 2026
182. Luckey, A.; Balasegaram, M.; Barbee, L. A.; Batteiger, T. A.; Broadhurst, H.; Cohen, S. E.; Delany-Moretlwe, S.; de Vries, H. J. C.; Dionne, J. A.; Gill, K.; Kenyon, C.; Kittiyaowamarn, R.; Lewis, D.; Mueller, J. P.; Naicker, V.; O'Brien, S.; O'Donnell, J. P.; Phanuphak, N.; Spooner, E.; Srinivasan, S.; Taylor, S. N.; Unemo, M.; Zwane, Z.; Hook, E. W. 3rd.; *Lancet* **2026**, *407*, 147. [Crossref]
183. Taylor, S. N.; Marrazzo, J.; Batteiger, B. E.; Hook, E. W. 3rd.; Seña, A. C.; Long, J.; Wierzbicki, M. R.; Kwak, H.; Johnson,

S. M.; Lawrence, K.; Mueller, J.; *N. Engl. J. Med.* **2018**, *379*, 1835. [Crossref]
184. Pisano, L.; Giovannuzzi, S.; Supuran, C. T.; *Expert Opin. Ther. Pat.* **2024**, *34*, 511. [Crossref]
185. Reichert, E.; Yaesoubi, R.; Rönn, M. M.; Gift, T. L.; Salomon, J. A.; Grad, Y. H.; *Lancet Microbe* **2023**, *4*, e781. [Crossref]
186. Lang, K.; *BMJ* **2026**, *392*, s31. [Crossref]
187. Bradford, P. A.; Miller, A. A.; O'Donnell, J.; Mueller, J. P.; *ACS Infect. Dis.* **2020**, *6*, 1332. [Crossref]
188. Barvian, K.; Basarab, G. S.; Gowravaram, M. R.; Hauck, S. I.; Zhou, F.; *WO2010043893A1*, **2010**.
189. GlaxoSmithKline (GSK); *Blujepa (gepotidacin) approved by US FDA as oral option for treatment of uncomplicated urogenital gonorrhoea (uGC).* [Link] accessed in January 2026
190. GlaxoSmithKline (GSK); *Blujepa (gepotidacin), patient information*. [Link] accessed in January 2026
191. United States Food and Drug Administration (FDA); *Blujepa (gepotidacin) prescribing information.* [Link] accessed in January 2026
192. ClinicalTrials.gov; *NCT04020341*. [Link] accessed in January 2026
193. Wagenlehner, F.; Perry, C. R.; Hooton, T. M.; Scangarella-Oman, N. E.; Millns, H.; Janmohamed, S.; Kramer, M.; Kushner, P.; Powell, M.; Jarvis, E.; Dennison, J.; Sheets, A.; Butler, D.; Breton, J.; *Future Microbiol.* **2025**, *20*, 265. [Crossref]
194. Scangarella-Oman, N. E.; Hossain, M.; Dixon, P. B.; Ingraham, K.; Min, S.; Tiffany, C. A.; Perry, C. R.; Raychaudhuri, A.; Dumont, E. F.; Huang, J.; Hook, E. W. 3rd.; Miller, L. A.; *Antimicrob. Agents Chemother.* **2018**, *62*, e01221-18. [Crossref]
195. Scangarella-Oman, N. E.; Hossain, M.; Hoover, J. L.; Perry, C. R.; Tiffany, C.; Brath, A.; Dumont, E. F.; *Antimicrob. Agents Chemother.* **2022**, *66*, e0149221. [Crossref]
196. Watkins, R. R.; Thapaliya, D.; Lemonovich, T. L.; Bonomo, R. A.; *J. Antimicrob. Chemother.* **2023**, *78*, 1137. [Crossref]
197. Oviatt, A. A.; Collins, J. A.; Mann, C. A.; Huang, J.; Mattern, K.; Chan, P. F.; Osheroff, N.; *ACS Infect. Dis.* **2025**, *11*, 3093. [Crossref]
198. Nawrot, D.; Ambrożkiewicz-Mosler, W.; Doležal, M.; Bouz, G.; *Eur. J. Med. Chem.* **2024**, *266*, 116077. [Crossref]
199. Ruggieri, F.; Compagne, N.; Antraygues, K.; Eveque, M.; Flipo, M.; Willand, N.; *Eur. J. Med. Chem.* **2023**, *256*, 115413. [Crossref]
200. Ali, A. S. M.; Anderson, C. S.; *Lancet* **2024**, *403*, 702. [Crossref]
201. Axten, J. M.; Brooks, G.; Brown, P.; Davies, D.; Gallagher, T. F.; Markwell, R. E.; Miller, W. H.; Pearson, N. D.; Seefeld, M.; *WO2004058144A2*, **2004**.
202. Widdowson, K. L.; *WO2016027249A1*, **2016**.
203. Sanofi; *Wayrilz prescribing information*. [Link] accessed in January 2026
204. United States Food and Drug Administration (FDA); *FDA Approves Drug to Treat Adults with Persistent or Chronic Immune Thrombocytopenia*. [Link] accessed in January 2026
205. Sanofi; *Study to Evaluate Rilzabrutinib in Adults and Adolescents with Persistent or Chronic Immune Thrombocytopenia (ITP).* [Link] accessed in January 2026
206. Kuter, D. J.; Efraim, M.; Mayer, J.; Trněný, M.; McDonald, V.; Bird, R.; Regenbogen, T.; Garg, M.; Kaplan, Z.; Tzvetkov, N.; Choi, P. Y.; Jansen, A. J. G.; Kostal, M.; Baker, R.; Gumulec, J.; Lee, E. J.; Cunningham, I.; Goncalves, I.; Warner, M.; Boccia, R.; Gernsheimer, T.; Ghanima, W.; Bandman, O.; Burns, R.; Neale, A.; Thomas, D.; Arora, P.; Zheng, B.; Cooper, N.; *N. Engl. J. Med.* **2022**, *386*, 1421. [Crossref]
207. Hujjat, S. F. Z.; Chandani, H. K.; Khan, M. S.; Chandani, D. K.; Mahmoud, A.; *Ann. Med. Surg.* **2025**, *87*, 7907. [Crossref]
208. Liu, L.; Xiao, Y.; Jia, Y.; Shao, Z.; Shi, J.; Cui, C.; *Drug Des. Devel. Ther.* **2025**, *19*, 8161. [Crossref]
209. Langrish, C. L.; Bradshaw, J. M.; Francesco, M. R.; Owens, T. D.; Xing, Y.; Shu, J.; LaStant, J.; Bisconte, A.; Outerbridge, C.; White, S. D.; Hill, R. J.; Brameld, K. A.; Goldstein, D. M.; Nunn, P. A.; *J. Immunol.* **2021**, *206*, 1454. [Crossref]
210. Moore, D. C.; Parish, P. C.; Arnall, J. R.; Elmes, J. B.; *Expert Opin. Pharmacother.* **2025**, *26*, 1583. [Crossref]
211. Labanca, C.; Martino, E. A.; Vigna, E.; Bruzzese, A.; Mendicino, F.; Caridà, G.; Lucia, E.; Olivito, V.; Manicardi, V.; Amodio, N.; Neri, A.; Morabito, F.; Gentile, M.; *Eur. J. Haematol.* **2025**, *115*, 4. [Crossref]
212. ClinicalTrials.gov; *NCT04562766*. [Link] accessed in January 2026
213. ClinicalTrials.gov; *NCT03395210*. [Link] accessed in January 2026
214. Kuter, D. J.; Ghanima, W.; Cooper, N.; Liebman, H. A.; Zhang, L.; Hu, Y.; Miyakawa, Y.; Homenda, W.; Galindo, L. E. M.; Basquiera, A. L.; Tan, C. W.; Saydam, G.; Hütter-Krönke, M. L.; Chai-Adisaksopha, C.; Gómez-Almaguer, D.; Tran, H.; Shin, H. J.; Dantas da Cunha Jr., A.; Lazar, Z.; Izquierdo, C. P.; Kirgner, I.; Lucchini, E.; Kuzmina, G.; Fillitz, M.; Audia, S.; Taparia, M.; Cordoba, M.; Diab, R.; Yao, M.; Gouia, I.; Lee, M.; Daak, A.; *Blood* **2025**, *145*, 2914. [Crossref]
215. Ahmad, N.; Boyall, D.; Charrier, J.-D.; Davis, C.; Davis, R.; Durrant, S.; Etxebarria, I. J. G.; Fraysse, D.; Jimenez, J.-M.; Kay, D.; Knegtel, R.; Middleton, D.; Odonnell, M.; Panesar, M.; Pierard, F.; Pinder, J.; Shaw, D.; Storck, P.-H.; Studley, J.; Twin, H.; *WO2014089379A1*, **2014**.
216. Comte, M.; Cruciani, P.; Larquetoux, L.; Latremoliere, O.; Lemaitre, C.; Ochsenbein, P.; Versproumy, P.; *WO2025029842A2*, **2025**.
217. Owens, T.; Verner, E.; *WO2014039899A1*, **2014**.
218. Vanda Pharmaceuticals Inc.; *Vanda Pharmaceuticals Announces FDA Approval of NEREUS™ (tradipitant) for the Prevention of*

Vomiting Induced by Motion: A Historic Scientific Milestone in the Prevention of Motion Sickness. [Link] accessed in January 2026
219. Vanda Pharmaceuticals Inc.; *Nereus prescribing information*. [Link] accessed in January 2026
220. Pojawa-Gołąb, M.; Jaworecka, K.; Reich, A.; *Dermatol. Ther.* **2019**, *9*, 391. [Crossref]
221. Carlin, J. L.; Lieberman, V. R.; Dahal, A.; Keefe, M. S.; Xiao, C.; Birznieks, G.; Abell, T. L.; Lembo, A.; Parkman, H. P.; Polymeropoulos, M. H.; *Gastroenterology* **2021**, *160*, 76. [Crossref]
222. Polymeropoulos, V. M.; Kiely, L.; Bushman, M. L.; Sutherland, E. B.; Goldberg, A. R.; Pham, A. X.; Miller, C. R.; Mourad, R.; Davis, T. R.; Pham, N. V.; Morgan, D. B.; Giles, A. K.; Xiao, C.; Polymeropoulos, C. M.; Birznieks, G.; Polymeropoulos, M. H.; *Front. Neurol.* **2025**, *16*, 1550670. [Crossref]
223. Polymeropoulos, V. M.; Czeisler, M. É.; Gibson, M. M.; Anderson, A. A.; Miglo, J.; Wang, J.; Xiao, C.; Polymeropoulos, C. M.; Birznieks, G.; Polymeropoulos, M. H.; *Front. Neurol.* **2020**, *11*, 563373. [Crossref]
224. ClinicalTrials.gov; *NCT04327661*. [Link] accessed in January 2026
225. Kobierski, M. E.; Kopach, M. E.; Chen, P.; *WO2008079600A1*, **2008**.
226. Amegadzie, A. K.; Gardinier, K. M.; Hembre, E. J.; Hong, J. E.; Jungheim, L. N.; Muehl, B. S.; Remick, D. M.; Robertson, M. A.; Savin, K. A.; *WO03091226A1*, **2003**.
227. Kopach, M. E.; Wilson, T. M.; Kobierski, M. E.; *WO2017031215A1*, **2017**.
228. Vertex Pharmaceuticals Inc.; *Journavx*. [Link] accessed in January 2026
229. Bertoch, T.; D'Aunno, D.; McCoun, J.; Solanki, D.; Taber, L.; Urban, J.; Oswald, J.; Swisher, M. W.; Tian, S.; Miao, X.; Correll, D. J.; Negulescu, P.; Bozic, C.; Weiner, S. G.; *Anesthesiology* **2025**, *142*, 1085. [Crossref]
230. United States Food and Drug Administration (FDA); *FDA Approves Novel Non-Opioid Treatment for Moderate to Severe Acute Pain*. [Link] accessed in January 2026
231. Hang Kong, A. Y.; Tan, H. S.; Habib, A. S.; *Pain Manage.* **2024**, *14*, 477. [Crossref]
232. Osteen, J. D.; Immani, S.; Tapley, T. L.; Indersmitten, T.; Hurst, N. W.; Healey, T.; Aertgeerts, K.; Negulescu, P. A.; Lechner, S. M.; *Pain Ther.* **2025**, *14*, 655. [Crossref]
233. Jones, J.; Correll, D. J.; Lechner, S. M.; Jazic, I.; Miao, X.; Shaw, D.; Simard, C.; Osteen, J. D.; Hare, B.; Beaton, A.; Bertoch, T.; Buvanendran, A.; Habib, A. S.; Pizzi, L. J.; Pollak, R. A.; Weiner, S. G.; Bozic, C.; Negulescu, P.; White, P. F.; *N. Engl. J. Med.* **2023**, *389*, 393. [Crossref]
234. Wu, Z.; Lu, D.; *Eur. J. Med. Chem.* **2026**, *302*, 118326. [Crossref]
235. Vertex Pharmaceuticals Inc.; *Vertex Announces Positive Results From the VX-548 Phase 3 Program for the Treatment of Moderate-to-Severe Acute Pain*. [Link] accessed in January 2026
236. Jones, M.; Demery, A.; Al-Horani, R. A.; *Drugs Drug Candidates* **2025**, *4*, 32. [Crossref]
237. Robinson, C. L.; Schatman, M. E.; Hasoon, J.; Chung, M.; Emerick, T.; Lo Bianco, G.; Ashina, S.; Yong, R. J.; *J. Pain Res.* **2025**, *18*, 2047. [Crossref]
238. Harrison, C.; *WO2022256660A1*, **2022**.
239. United States Food and Drug Administration (FDA); *Rhapsido-Highlights of Prescribing Information*. [Link] accessed in January 2026
240. Novartis; Rhapsido. [Link] accessed in January 2026
241. Novartis; *Novartis Receives FDA Approval for Rhapsido (remibrutinib), the only Oral Targeted BTKi Treatment for Chronic Spontaneous Urticaria (CSU)*. [Link] accessed in January 2026
242. Kolkhir, P.; Giménez-Arnau, A. M.; Kulthanan, K.; Peter, J.; Metz, M.; Maurer, M.; *Nat. Rev. Dis. Primers* **2022**, *8*, 61. [Crossref]
243. Metz, M.; Giménez-Arnau, A.; Hide, M.; Lebwohl, M.; Mosnaim, G.; Saini, S.; Sussman, G.; Szalewski, R.; Haemmerle, S.; Lheritier, K.; Martzloff, E. D.; Seko, N.; Wang, P.; Zharkov, A.; Maurer, M.; *N. Engl. J. Med.* **2025**, *392*, 984. [Crossref]
244. Giménez-Arnau, A. M.; Szalewski, R.; Hide, M.; Jain, V.; Khemis, A.; Lebwohl, M.; Metz, M.; Mosnaim, G.; Palumbo, M.; Şavk, E.; Sussman, G.; Walecka-Herniczek, I.; Yang, B.; Field, C.; Haemmerle, S.; Lheritier, K.; Machado, P. G. P.; Martzloff, E. D.; Seko, N.; Wang, P.; Zharkov, A.; Saini, S.; *J. Allergy Clin. Immunol.* **2026**, *157*, 143. [Crossref]
245. Maurer, M.; Berger, W.; Giménez-Arnau, A.; Hayama, K.; Jain, V.; Reich, A.; Haemmerle, S.; Lheritier, K.; Walsh, P.; Xia, S.; Storim, J.; *J. Allergy Clin. Immunol.* **2022**, *150*, 1498. [Crossref]
246. Maurer, M.; Giménez-Arnau, A.; Jain, V.; Tillinghast, J.; Tolcachier, A.; Ningen, S.; Hayam, K.; Lheritier, K.; Walsh, P.; Haemmerle, S.; *J. Allergy Clin. Immunol.* **2022**, *149*, AB179. [Crossref]
247. Burhan, M.; Ashraf, S.; Ali, A.; Shahid, I.; Ahmed, J.; Shah, M. S. U.; Das, N. B.; Nashwan, A. J.; *Int. Arch. Allergy Immunol.***2025**, 40911497. [Crossref]
248. Angst, D.; Gessier, F.; Vulpetti, A.; *WO2015079417A1*, **2015**.
249. Figuccia, A.; Lovelle, L.; Parmentier, M.; *WO2024069507A1*, **2024**.
250. LEO Pharma; *Anzupgo*. [Link] accessed in January 2026
251. Jawaid, Z.; Khalid, M.; Waafira, A.; *Ann. Med. Surg.* **2025**, *87*, 6916. [Crossref]
252. LEO Pharma; *LEO Pharma Announces FDA Approval of ANZUPGO® (delgocitinib) Cream in the U.S.* [Link] accessed in January 2026
253. Dhillon, S.; *Drugs* **2020**, *80*, 609. [Crossref]

254. Giménez-Arnau, A. M.; Pinter, A.; Sondermann, W.; Reguiai, Z.; Woolf, R.; Lynde, C.; Legat, F. J.; Costanzo, A.; Silvestre, J. F.; Mellerup, N.; Østerdal, M. L.; Plohberger, U.; Ryttig, L.; Bauer, A.; *Lancet* **2025**, *405*, 1676. [Crossref]
255. Gooderham, M.; Molin, S.; Bissonnette, R.; Worm, M.; Crépy, M. N.; Stingeni, L.; Warren, R. B.; Schliemann, S.; Schuttelaar, M. L.; Ferrucci, S.; Serra-Baldrich, E.; Silverberg, J. I.; Balita-Crisostomo, C. L.; Østerdal, M. L.; Plohberger, U.; Agner, T.; *J. Am. Acad. Dermatol.* **2025**, *93*, 95. [Crossref]
256. Yamamoto, Y.; Otsuka, A.; Nakashima, C.; Ishida, Y.; Honda, T.; Egawa, G.; Amano, W.; Usui, K.; Hamada, Y.; Wada, M.; Tanimoto, A.; Konishi, N.; Hayashi, M.; Matsushita, M.; Kabashima, K.; *J. Dermatol. Sci.* **2020**, *97*, 161. [Crossref]
257. Meledathu, S.; Naidu, M. P.; Brunner, P. M.; *J. Allergy Clin. Immunol.* **2025**, *155*, 1124. [Crossref]
258. Szalus, K.; Trzeciak, M.; Nowicki, R. J.; *Microorganisms* **2020**, *8*, 1743. [Crossref]
259. Abe, M.; Igarashi, A.; Kitajima, H.; Toyama, H.; Kabashima, K.; Saeki, H.; *J. Dermatol.* **2025**, *52*, 1232. [Crossref]
260. Figuccia, A.; Lovelle, L.; Parmentier, M.; *WO2018117151A1*, **2024**.
261. 19. Yamasaki, T.; Hara, Y.; Sakai, T.; Murakami, K.; Hara, K.; Manta, N.; *WO2017006968A1*, **2017**.
262. Boehringer Ingelheim; FDA Approved Jascayd. [Link] accessed in January 2026
263. Ibrahim, M.; Piazza, G. A.; Ahsan, F.; *Trends Pharmacol. Sci.* **2026**, *47*, 120. [Crossref]
264. Maher, T. M.; Assassi, S.; Azuma, A.; Cottin, V.; Hoffmann-Vold, A. M.; Kreuter, M.; Oldham, J. M.; Richeldi, L.; Valenzuela, C.; Wijsenbeek, M. S.; Clerisme-Beaty, E.; Coeck, C.; Gu, H.; Ritter, I.; Schlosser, A.; Stowasser, S.; Voss, F.; Weimann, G.; Zoz, D. F.; Martinez, F. J.; *N. Engl. J. Med.* **2025**, *392*, 2203. [Crossref]
265. Hujjat, S. F. Z.; Chandani, H. K.; Chandani, D. K.; Khan, M. S.; Mahmoud, A.; *Ann. Med. Surg.* **2025**, *88*, 1. [Crossref]
266. ClinicalTrials.gov; *NCT05321069*. [Link] accessed in January 2026
267. ClinicalTrials.gov; *NCT04419506*. [Link] accessed in January 2026
268. ClinicalTrials.gov; *NCT05321082*. [Link] accessed in January 2026
269. Wuyts, W. A.; Richeldi, L.; Assassi, S.; Azuma, A.; Cottin, V.; Hoffmann-Vold, A. M.; Kreuter, M.; Oldham, J. M.; Martinez, F. J.; Valenzuela, C.; Wijsenbeek, M. S.; Kanakapura, M.; James, A.; Weimann, G.; Drzewuski, C.; Coeck, C.; Maher, T. M.; *BMC Pulm. Med.* **2025**, *26*, 10. [Crossref]
270. Herrmann, F. E.; Hesslinger, C.; Wollin, L.; Nickolaus, P.; *Front. Pharmacol.* **2022**, *13*, 838449. [Crossref]
271. Richeldi, L.; Azuma, A.; Cottin, V.; Kreuter, M.; Maher, T. M.; Martinez, F. J.; Oldham, J. M.; Valenzuela, C.; Clerisme-Beaty, E.; Gordat, M.; Wachtlin, D.; Liu, Y.; Schlecker, C.; Stowasser, S.; Zoz, D. F.; Wijsenbeek, M. S.; *N. Engl. J. Med.* **2025**, *392*, 2193. [Crossref]
272. Reininger, D.; Wolf, F.; Mayr, C. H.; Wespel, S. L.; Laufhaeger, N.; Geillinger-Kästle, K.; Dick, A.; Gantner, F.; Nickolaus, P.; Herrmann, F. E.; *Am. J. Respir. Cell Mol. Biol.* **2025**, *73*, 700. [Crossref]
273. Boehringer Ingelheim; *Nerandomilast mechanism of action*. [Link] accessed in January 2026
274. Frutos, R. P.; Tampone, T. G.; Mulder, J. A.; Krishnamurthy, D.; Senanayake, C. H.; *WO2009140127A2*, **2009**.
275. Pouzet, P. a J.; Nickolaus, P.; Werthmann, U.; Frutos, R. P.; Yang, B.-S.; Kim, S.; Mulder, J. A.; Patel, N.; Senanayake, C. H.; Tampone, T. G.; Wei, X.; *WO2013026797A1*, **2013**.
276. Abella, J. M.; Brodmann, T.; Chen, D.; Dang, M. T. Q.; Frutos, R. P.; Gao, J. J.; Gerstmann, F.; Hagenkoetter, R.; Li, R.; Marckart, D. J.; Mulder, J. A.; Orben, J.; Stange, C.; Tampone, T. G.; Weber, D.; *WO2025131986A1*, **2025**.
277. Insmed, Inc.; *FDA Approves BRINSUPRI™ (brensocatib) as the First and Only Treatment for Non-Cystic Fibrosis Bronchiectasis, a Serious, Chronic Lung Disease*. [Link] accessed in January 2026
278. Doyle, K.; Lönn, H.; Käck, H.; Van de Poël, A.; Swallow, S.; Gardiner, P.; Connolly, S.; Root, J.; Wikell, C.; Dahl, G.; Stenvall, K.; Johannesson, P.; *J. Med. Chem.* **2016**, *59*, 9457. [Crossref]
279. Palmér, R.; Mäenpää, J.; Jauhiainen, A.; Larsson, B.; Mo, J.; Russell, M.; Root, J.; Prothon, S.; Chialda, L.; Forte, P.; Egelrud, T.; Stenvall, K.; Gardiner, P.; *Clin. Pharmacol. Ther.* **2018**, *104*, 1155. [Crossref]
280. Chalmers, J. D.; Usansky, H.; Rubino, C. M.; Teper, A.; Fernandez, C.; Zou, J.; Mange, K. C.; *Clin. Pharmacokinet.* **2022**, *61*, 1457. [Crossref]
281. Chalmers, J. D.; Burgel, P. R.; Daley, C. L.; De Soyza, A.; Haworth, C. S.; Mauger, D.; Loebinger, M. R.; McShane, P. J.; Ringshausen, F. C.; Blasi, F.; Shteinberg, M.; Mange, K.; Teper, A.; Fernandez, C.; Zambrano, M.; Fan, C.; Zhang, X.; Metersky, M. L.; *N. Engl. J. Med.* **2025**, *392*, 1569. [Crossref]
282. Wu, X.; Liu, H.; Qin, Q.; Yuan, L.; Yao, Y.; Du, X.; Qin, Q.; Wang, L.; Zhao, Q.; Qin, L.; Xiang, Y.; Yang, M.; Qin, X.; Liu, C.; *iScience* **2025**, *28*, 113928. [Crossref]
283. Makaryan, V.; Kelley, M.; Bolyard, A. A.; Chugh, G.; Dale, D. C.; *J. Cell Immunol.* **2024**, *6*, 211. [Crossref]
284. Klöhn, M.; Burkard, T.; Janzen, J.; Haase, J. A.; Gömer, A.; Fu, R.; Ssebyatika, G.; Nocke, M. K.; Brown, R. J. P.; Krey, T.; Dao Thi, V. L.; Kinast, V.; Brüggemann, Y.; Todt, D.; Steinmann, E.; *Hepatology* **2024**, *80*, 1239. [Crossref]
285. Lönn, H. R.; Connolly, S.; Swallow, S.; Karlsson, S. P.; Aurell, C.-J.; Pontén, J. F.; Doyle, K. J.; Van, D. P. A. J.; Jones, G. P.; Watson, D. W.; Macritchie, J. A.; Palmer, N. J.; *WO2015110826A1*, **2015**.
286. Cage, P. A.; Furber, M.; Luckhurst, C. A.; Sanganee, H. J.; Stein, L. A.; *WO2009074829A1*, **2009**.

287. Bukhari, S. M. R.; Mehdi, H.; Abdullah, G.; Ans, M.; Raza, M.; *Ann. Med. Surg.* **2025**, *88*, 61. [Crossref]
288. United States Food and Drug Administration (FDA); *Center for Drug Evaluation and Research-Application number: 218585Orig1s000: VIZZ (aceclidine ophthalmic solution) 1.44%*. [Link] accessed in January 2026
289. Mullard, A.; *Nat. Rev. Drug Discovery* **2025**, *24*, 655. [Crossref]
290. ClinicalTrials.gov; *NCT05753189*. [Link] accessed in January 2026
291. ClinicalTrials.gov; *NCT05656027*. [Link] accessed in January 2026
292. ClinicalTrials.gov; *NCT05728944*. [Link] accessed in January 2026
293. Organisation for the Prohibition of Chemical Weapons (OPCW); *Chemical Weapons Convention (CWC)-Annex on Chemicals: Schedule 2*. [Link] accessed in January 2026
294. Lieberman, T. W.; Leopold, I. H.; *Am. J. Ophthalmol.* **1967**, *64*, 405. [Crossref]
295. Grzybowski, A.; Kapitanovaite, L.; Zemaitiene, R.; *Adv. Ophthalmol. Pract. Res.* **2024**, *4*, 220. [Crossref]
296. Agrahari, V.; Mandal, A.; Agrahari, V.; Trinh, H. M.; Joseph, M.; Ray, A.; Hadji, H.; Mitra, R.; Pal, D.; Mitra, A. K.; *Drug Delivery Transl. Res.* **2016**, *6*, 735. [Crossref]
297. Gardinier, K. M.; Audia, J. E.; Monn, J.; Myers, J.; Ahmad, N. M.; Gancia, E.; Skidmore, E. A.; Wagstaff, N.; Evans, D. G.; *WO2024130065A1*, **2024**.
298. Lee, A.; *Drugs* **2025**, *85*, 1307. [Crossref]
299. Alcon; *Tryptyr (acoltremon ophthalmic solution) 0.003%*. [Link] accessed in January 2026
300. Alcon; *Alcon Announces FDA Approval of TRYPTYR (acoltremon ophthalmic solution) 0.003% for the Treatment of the Signs and Symptoms of Dry Eye Disease*. [Link] accessed in January 2026
301. Wirta, D. L.; Senchyna, M.; Lewis, A. E.; Evans, D. G.; McLaurin, E. B.; Ousler, G. W.; Hollander, D. A.; *Ocul. Surf.* **2022**, *26*, 166. [Crossref]
302. Pattar, G. R.; Wirta, D.; Jerkins, G.; Paauw, J.; McLaurin, E. B.; Liu, A.; Evans, D. G.; Kenyon, K.; Cline, N.; Gupta, P. K.; Meng, I.; Senchyna, M.; *Ophthalmology* **2025**, *Sep 30*, S0161-6420(25)00605-0. [Crossref]
303. Khalid, M.; Zahid, E.; Shaheer, M.; *Ann. Med. Surg.* **2025**, *87*, 9121. [Crossref]
304. Malik, F. S.; Naveed, F.; Khan, A.; Fatima, M.; *Ann. Med. Surg.* **2025**, *87*, 6256. [Crossref]
305. Kühn, F. J.; Kühn, C.; Lückhoff, A.; *J. Biol. Chem.* **2009**, *284*, 4102. [Crossref]
306. Rodríguez-Arévalo, S.; Pujol, E.; Abás, S.; Galdeano, C.; Escolano, C.; Vázquez, S.; *Molecules* **2021**, *26*, 906. [Crossref]
307. Lee, A.; *Drugs* **2026**, *86*, 121. [Crossref]
308. Hager, M.; Goldstein, T.; Fitz, V.; Ott, J.; *Expert Opin. Pharmacother.* **2024**, *25*, 783. [Crossref]
309. Bayer; *Bayer's Lynkuet® (elinzanetant), the First and Only Neurokinin 1 and Neurokinin 3 Receptor Antagonist, Receives FDA Approval for Moderate to Severe Hot Flashes Due to Menopause*. [Link] accessed in January 2026
310. Bayer; *Elinzanetant Significantly Reduces Frequency of Moderate to Severe Vasomotor Symptoms Associated with Endocrine Therapy for Breast Cancer in Phase III OASIS-4 study*. [Link] accessed in January 2026
311. United States Food and Drug Administration (FDA); *Lynkuet-Highlights of Prescribing Information*. [Link] accessed in January 2026
312. ClinicalTrials.gov; *NCT05042362*. [Link] accessed in January 2026
313. ClinicalTrials.gov; *NCT05099159*. [Link] accessed in January 2026
314. Patel, A. H.; Pierret, A.; Mills, E. G.; Comninos, A. N.; Dhillo, W. S.; Abbara, A.; *BJOG* **2025**. [Crossref]
315. Pawsey, S.; Mills, E. G.; Ballantyne, E.; Donaldson, K.; Kerr, M.; Trower, M.; Dhilo, W. S.; *J. Clin. Endocrinol. Metab.* **2021**, *106*, e3221. [Crossref]
316. Panay, N.; Joffe, H.; Maki, P. M.; Nappi, R. E.; Pinkerton, J. V.; Simon, J. A.; Soares, C. N.; Thurston, R. C.; Francuski, M.; Caetano, C.; Genga, K.; Haberland, C.; Haseli Mashhadi, N.; Laapas, K.; Parke, S.; Seitz, C.; Schwarz, J.; Zuurman, L.; *JAMA Intern. Med.* **2025**, *185*, 1319. [Crossref]
317. Dinnell, K.; Elliott, J. M.; Hollingworth, G. J.; Shaw, D. E.; *US6476045B2*, **2002**.
318. Hoffmann, T.; Koblet, A.; Peters, J.-U.; Schnider, P.; Sleight, A.; Stadler, H.; *WO2005002577A1*, **2005**.
319. Alvaro, G.; Andreotti, D.; Belvedere, S.; Di, F. R.; Falchi, A.; Giovannini, R.; *WO2007028654A1*, **2007**.
320. Crinetics Pharmaceuticals, Inc.; *Palsonify*. [Link] accessed in January 2026
321. Zhao, J.; Wang, S.; Markison, S.; Kim, S. H.; Han, S.; Chen, M.; Kusnetzow, A. K.; Rico-Bautista, E.; Johns, M.; Luo, R.; Struthers, R. S.; Madan, A.; Zhu, Y.; Betz, S. F.; *ACS Med. Chem. Lett.* **2022**, *14*, 66. [Crossref]
322. United States Food and Drug Administration (FDA); *FDA Approves New Treatment for Acromegaly, a Rare Endocrine Disorder*. [Link] accessed in January 2026
323. Gadelha, M. R.; Gordon, M. B.; Doknic, M.; Mezősi, E.; Tóth, M.; Randeva, H.; Marmon, T.; Jochelson, T.; Luo, R.; Monahan, M.; Madan, A.; Ferrara-Cook, C.; Struthers, R. S.; Krasner, A.; *J. Clin. Endocrinol. Metab.* **2023**, *108*, e148. [Crossref]
324. ClinicalTrials.gov; *NCT05192382*. [Link] accessed in January 2026
325. ClinicalTrials.gov; *NCT04837040*. [Link] accessed in January 2026
326. Madan, A.; Markison, S.; Betz, S. F.; Krasner, A.; Luo, R.; Jochelson, T.; Lickliter, J.; Scott Struthers, R.; *Pituitary* **2022**, *25*, 328. [Crossref]

327. Ahmed, S.; Asghar, H.; Khalid, M.; *Ann. Med. Surg.* **2025**, *88*, 1068. [Crossref]
328. Biller, B. M. K.; Casagrande, A.; Elenkova, A.; Boguszewski, C. L.; Jallad, R. S.; Hu, B.; Hubina, E.; Fazeli, P. K.; Fleseriu, M.; Snyder, P. J.; Strasburger, C. J.; Bidlingmaier, M.; Zhao, Y.; Soares, B.; Trainer, P. J.; Struthers, R. S.; Krasner, A.; Gadelha, M. R.; *J. Clin. Endocrinol. Metab.* **2025**, dgaf579. [Crossref]
329. Wildemberg, L. E.; Fialho, C.; Gadelha, M. R.; *Best Pract. Res., Clin. Endocrinol. Metab.* **2024**, *38*, 101906. [Crossref]
330. Zhao, J.; Fu, H.; Yu, J.; Hong, W.; Tian, X.; Qi, J.; Sun, S.; Zhao, C.; Wu, C.; Xu, Z.; Cheng, L.; Chai, R.; Yan, W.; Wei, X.; Shao, Z.; *Nat. Commun.* **2023**, *14*, 962. [Crossref]
331. Zhao, J.; Han, S.; Kim, S. H.; Wang, S.; Zhu, Y.; *US2019382367A1*, **2019**.
332. Reddy, J. P.; Mirmehrabi, M.; Kota, M.; Dash, U.; Zhao, J.; Zhu, Y.; *US2019218202A1*, **2019**.
333. Novartis; *Novartis Receives FDA Accelerated Approval for Vanrafia® (atrasentan), the First and only Selective Endothelin A Receptor Antagonist for Proteinuria Reduction in Primary IgA Nephropathy (IgAN).* [Link] accessed in January 2026
334. Heerspink, H. J. L.; Jardine, M.; Kohan, D. E.; Lafayette, R A.; Levin, A.; Liew, A.; Zhang, H.; Lodha, A.; Gray, T.; Wang, Y.; Renfurm, R.; Barratt, J.; *N. Engl. J. Med.* **2025**, *392*, 544. [Crossref]
335. Rodrigues, J. C.; Haas, M.; Reich, H. N.; *Clin. J. Am. Soc. Nephrol.* **2017**, *12*, 677. [Crossref]
336. ClinicalTrials.gov; *NCT04573478*. [Link] accessed in January 2026
337. ClinicalTrials.gov; *NCT05852938*. [Link] accessed in January 2026
338. Heerspink, H. J. L.; Parving, H. H.; Andress, D. L.; Bakris, G.; Correa-Rotter, R.; Hou, F. F.; Kitzman, D. W.; Kohan, D.; Makino, H.; McMurray, J. J. V.; Melnick, J. Z.; Miller, M. G.; Pergola, P. E.; Perkovic, V.; Tobe, S.; Yi, T.; Wigderson, M.; de Zeeuw, D.; *Lancet* **2019**, *393*, 1937. [Crossref]
339. Quinn, D. I.; Tangen, C. M.; Hussain, M.; Lara Jr., P. N.; Goldkorn, A.; Moinpour, C. M.; Garzotto, M. G.; Mack, P. C.; Carducci, M. A.; Monk, J. P.; Twardowski, P. W.; Van Veldhuizen, P. J.; Agarwal, N.; Higano, C. S.; Vogelzang, N. J.; Thompson Jr., I. M.; *Lancet Oncol.* **2013**, *14*, 893. [Crossref]
340. de Zeeuw, D.; Coll, B.; Andress, D.; Brennan, J. J.; Tang, H.; Houser, M.; Correa-Rotter, R.; Kohan, D.; Lambers Heerspink, H. J.; Makino, H.; Perkovic, V.; Pritchett, Y.; Remuzzi, G.; Tobe, S. W.; Toto, R.; Viberti, G.; Parving, H. H.; *J. Am. Soc. Nephrol.* **2014**, *25*, 1083. [Crossref]
341. Pitcher, D.; Braddon, F.; Hendry, B.; Mercer, A.; Osmaston, K.; Saleem, M. A.; Steenkamp, R.; Wong, K.; Turner, A. N.; Wang, K.; Gale, D. P.; Barratt, J.; *Clin. J. Am. Soc. Nephrol.* **2023**, *18*, 727. [Crossref]
342. Winn, M.; Boyd, S. a; Hutchins, C. W.; Jae, H.-S.; Tasker, A. S.; Geldern, T. W. V.; Kester, J. a; Sorensen, B. K.; Szczepankiewicz, B. G.; Henry, K. J.; Liu, G.; Wittenberger, S. J.; King, S. A.; *WO9906397A2*, **1999**.
343. Winn, M.; Boyd, S. a; Hutchins, C. W.; Jae, H.-S.; Tasker, A. S.; Von, G. T. W.; Kester, J. a; Sorensen, B. K.; Szczepankiewicz, B. G.; Henry, K. J. J.; Liu, G.; Wittenberger, S. J.; King, S. A.; *WO9730045A1*, **1997**.

Submitted: February 6, 2026
Final version online: March 10, 2026